Technische Universität München, Fakultät für Medizin

Relevance of blood-based biomarkers for prediction of response to chemotherapy and prognosis in lung cancer patients

Kimberly Krüger

Vollständiger Abdruck der von der
Fakultät für Medizin
der Technischen Universität München zur Erlangung des akademischen Grades
eines Doktors der Naturwissenschaften (Dr. rer. nat.)
genehmigten Dissertation.

Vorsitzende/-r: Prof. Dr. Wilko Weichert

Prüfende/-r der Dissertation:

1. apl. Prof. Dr. Peter B. Luppa

2. Prof. Dr. Dietmar Zehn

Die Dissertation wurde am 01.10.2020 bei der Technischen Universität München
eingereicht und durch die
Fakultät für Medizin am 13.04.2021 angenommen.

Somewhere, something incredible is waiting to be known.

Carl Sagan

Acknowledgements

Zum Erfolg dieser Arbeit haben viele Menschen beigetragen, bei denen ich mich im Folgenden bedanken möchte.

Ein herzlicher Dank gilt meinen beiden Dissertationsbetreuern Prof. Dr. Luppa und Prof. Dr. Zehn für Ihre Begleitung durch den Promotionsprozess.

Ein besonderer Dank gilt meinem Mentor Prof. Dr. Holdenrieder in dessen Labor ich meine Versuche durchgeführt habe. Danke für die zahlreichen Stunden die du in Besprechungen und Diskussionen investiert hast und die diese Arbeit maßgeblich geprägt haben.

Wesentlich zu dieser Arbeit hat die Zusammenarbeit mit der Central European Society for Anticancer Research (CESAR) beigetragen. An dieser Stelle möchte ich Prof. Dr. Jörger als Studienleitung stellvertretend für alle Studiensites sowie Dr. Rössler vom CESAR Central Office für die Studienorganisation danken. Für die Organisation der Biomarker Substudie danke ich Dr. Hettwer von der Cebio. Außerdem danke ich der Roche Diagnostics GmbH für die zur Verfügungstellung der Reagenzien zur Messung der Tumormarker. Ein großer Dank gilt der Kooperation mit der QuoData Statistics GmbH, die mich wesentlich bei der Auswertung der Messergebnisse unterstützt hat, insbesondere Dr. Hettwer und Dr. Uhlig.

Bei den Mitarbeitern der Forschungsabteilung im Institut für Laboratoriumsmedizin möchte ich mich für angeregte Diskussionen und ständige Hilfsbereitschaft bedanken.

Vielen Dank an meine Familie die mich immer mit viel Verständnis in meinen Plänen unterstützt und begleitet hat. Insbesondere meinen Bruder Konstantin möchte ich für seine Hilfe bei der Korrektur danken.

Zum Abschluss möchte ich mich noch bei meinem Partner Johannes bedanken. Danke für die langjährige Unterstützung und Ermutigung meinem Weg zu folgen.

Content

Abbreviations ..... **IV**

Summary **1**

1 Introduction **2**

2 Theoretical background **3**

2.1 Lung cancer 3

2.1.1 Types of lung cancer 3

2.1.2 Epidemiology 5

2.1.3 Risk factors 5

2.1.4 Treatment of NSCLC 5

2.2 Immune checkpoint inhibitors 8

2.2.1 Physiological background 9

2.2.2 Application as biomarkers 13

2.2.3 Drugs 14

2.2.3 Side effects 16

2.2.4 Developments in the field of immune checkpoint inhibitors 16

2.3 Biomarkers 17

2.3.1 Definition 17

2.3.2 Tissue biomarkers in lung cancer 18

2.3.3 Blood biomarkers in lung cancer 19

3 Aim **25**

4 Patients, methods and materials 26

4.1 Patients 26

4.1.1 CESAR Biomarker Substudy 26

4.1.2 Healthy cohort 28

4.1.3 Ethics 29

4.2 Tumor markers ECLIA 29

4.2.1 ECLIA method 29

4.2.2 ECLIA quality control 29

4.2.3 ECLIA materials 29

4.3 PD-markers ELISA 31

4.3.1 ELISA method 31

4.3.2 ELISA validation 36

4.3.3 ELISA quality control 36

4.3.4 ELISA materials 37

4.4 Statistic tools clinical evaluation 41

5 Results 43

5.1 Tumor markers CESAR Biomarker Substudy 43

5.2 Prediction of therapy response 46

5.2.1 Prediction of poor response to therapy 48

5.2.2 Prediction of good response to therapy 55

5.3 Prognosis of survival probability 61

5.3.1 Progression free survival 65

5.3.2 Overall survival 73

5.4 Programmed cell death markers 81
5.4.1 Analytical validation 81
5.4.2 Preanalytical validation 81
5.4.3 CESAR Biomarker substudy 82
5.4.4 Healthy cohort 90
5.4.5 Comparison NSCLC and healthy 91

6 Discussion 94

7 Conclusion 102

8 Outlook 103

9 References 104

10 Table index 115

11 Figure index 116

Abbreviations

APC	Antigen-presenting cell
AUC	Area under the curve
AWMF	Association of the Scientific Medical Societies (Arbeitsgemeinschaft der Wissenschaftlichen Medizinischen Fachgesellschaften e.V.)
BSA	Bovine serum albumine
CA 125	Cancer antigen 125
CA 15-3	Cancer antigen 15-3
CEA	Carcinoembryonic antigen
CEPAC	CESAR Study of Paclitaxel Therapeutic Drug Monitoring
CESAR	Central European Society of Anticancer Research
ChT	Chemotherapy
CT	Computed tomography
ctDNA	Circulating tumor DNA
CTLA4	Cytotoxic T-lymphocyte-associated protein4
CV	Coefficient of variation
CYFRA 21-1	Soluble cytokeratin 19 fragment
ECL	Electrochemiluminescence
ECLIA	Electrochemiluminescence immune assay
ECOG	Eastern Cooperative Oncology Group
ELISA	Enzyme linked immunosorbent assay

EMA	European Medicines Agency
EOT	End of treatment
FDA	Food and Drug Administration
HR	Hazard ratio
HE4	Human epididymis protein 4
IASLC	International Association for the Study of Lung Cancer
ICI	Immune checkpoint inhibitor
ITIM	Immunoreceptor tyrosine-based inhibitory motif
ITSM	Immunoreceptor tyrosine-based switch motif
LLOQ	Lower limit of quantification
NCCN	National Comprehensive Cancer Network
NGS	Next generation sequencing
NSCLC	Non-small cell lung cancer
NSE	Neuron-specific enolase
OS	Overall survival
PBS	Phosphate buffered saline
PD	Progressive disease
PD-1	Programmed cell death protein 1
PD-L1	Programmed cell death 1 ligand 1
PD-L2	Programmed cell death 1 ligand 2
PFS	Progression free survival
PK	Pharmacokinetically

PR	Partial remission
ProGRP	Preliminary form of the gastrin-releasing protein
RaT	Radiotherapy
RGMb	Repulsive guidance molecule b
ROC	Receiver operating characteristics
SCCA	Squamous cell carcinoma antigen
SCLC	Small-cell lung cancer
SD	Stable disease
TDM	Therapeutic drug monitoring
TIL	Tumor infiltrating lymphocyte
TMD	Transmembrane domain
TME	Tumor microenvironment
TPS	Tumor proportion score
UICC	Union for International Cancer Control
ULOQ	Upper limit of quantification
WHO	World Health Organization

Summary

Lung cancer belongs to the most abundant and deadly cancer types in the German population. Although the variety of available medication including targeted drugs increased over the years even for advanced disease stages, there is still a lack for informative biomarkers for accompanying diagnostics. These will contribute to early treatment response assessments and individualized therapy management.

The aim of this study is to investigate the potential of eight tumor markers and new developed immunological biomarkers regarding prediction of therapy response and prognosis of survival in a cohort of 266 patients with advanced non-small cell lung cancer receiving chemotherapy.

Serial blood samples were collected in the CESAR Biomarker Substudy, a part of the clinical CEPAC-TDM trial. Commercial assays were applied to measure the eight tumor markers CYFRA 21-1, CEA, SCCA, NSE, ProGRP, CA 15-3, CA 125 and HE4. Novel ELISAs for the quantification of the soluble programmed cell death markers based on chemiluminescence detection technology were developed and established. Comprehensively analytical and preanalytical validation assured high quality sample assessments. Independent data analysis was performed in cooperation with a statistics company.

Before start of therapy tumor markers were not predictive for poor response to therapy objectified by computed tomography prior to cycle 3 , though marker changes between cycle 1 and 3 (C1, C3) indicated predictive value for CYFRA 21-1, CA 125 and NSE for poor and CYFRA 21-1 and CA 125 for good response. Prognostic potential for progression free survival was seen for pre-therapeutic levels of CA 15-3 and CA 125 and before start of C3 also for CYFRA 21-1, CEA, SCCA, CA 15-3 and CA 125. Prognostic value concerning overall survival was found for pre-therapeutic levels of CA 15-3 and at cycle 3 for CYFRA 21-1, CA 15-3 and CA 125. The programmed cell death markers were not predictive for response to therapy.

The comprehensive clinical characterization, validated assay procedures and an independent data analysis build a meaningful investigation of the predictive and prognostic potential of application of tumor markers and new immunological biomarkers.

Conclusively, the tumor markers CYFRA 21-1, CA 15-3 and CA 125 revealed predictive and prognostic potential and should be included in future biomarker trials in advanced lung cancer patients.

1 Introduction

Lung cancer is one of the most abundant cancer types in human kind. In 2016 the Robert Koch Institute estimated 492000 new cancer diagnoses in Germany. Lung cancer rates on position four accounting for nearly 9% of all cancer diagnoses (Rober Koch-Institut, 2019). Due to unspecific symptoms most of these carcinomas remain undetected until the disease reached its late stages. This results in short overall survival although a variety of treatment options is available. The class of tyrosine kinase inhibitors introduced the first targeted therapy option and showed great improvements in progression free and overall survival. Nevertheless many patients still did not benefit from the new approaches. In 2011, the immune checkpoint inhibitors (ICIs) introduced a new class of anti-cancer therapeutics convincing with unexpected therapy success in former untreatable patients. The approach relies on supporting immune response against the tumor cells. The development of targeted medication is accompanied by the need of target identification diagnostics.

Different approaches follow the path to realize a more and more individualized therapy. Not only the drugs themselves but the diagnostic markers play an important role in personalized medicine. Diagnostic tools which enable early differentiation between therapy responders and non-responders will enable an early shift of therapy. This not only spares the patient from the risk to suffer from adverse events but also can also lead to an effective treatment in the second place.

Biomarkers to reliably predict therapy response and forecast progression free survival and overall survival are still needed for all treatments in lung cancer. The majority of patients is still and will be for the next year, treated with a conventional chemotherapy which presents as the gold standard in lung cancer therapy. This work investigated eight tumor markers in an interventional study using a paclitaxel/platinum therapy regimen in NSCLC patients. Additionally, new biomarkers were investigated in the cohort. Three assays were developed to quantify the immune response modulating molecules, soluble programmed cell death markers PD-1, PD-L1 and PD-L2 in blood.

2 Theoretical background

2.1 Lung cancer

Lung cancer is currently one of the most abundant cancer types worldwide. First predominantly observed in men, cases in women are constantly rising due to adjustment of smoking habits and rising risk of environmental causes, like air pollution.

2.1.1 Types of lung cancer

According to histology lung tumors can be divided into several subtypes (Table 1). A major revision on earlier classification was published by the World Health Organization in 2015 (Travis et al., 2015). It is still valid and thus followed by the latest Manual published by the Tumorzentrum Munich in 2020 (Tumorzentrum München, 2020).

Commonly it is also distinguished between Non-small-cell lung cancer (NSCLC) and Small-cell lung cancer (SCLC). Whereas NSCLC encompassed the majority of diagnoses (85%), SCLC accounts for the remaining 15%. A further subdivision of NSCLC into the three main histological carcinomas adenocarcinoma, squamous-cell carcinoma and large-cell carcinoma can be performed according to the observed morphology. Under one percent of NSCLC belong to the rare subtypes adenosquamous carcinoma, sarcomatoid tumors, carcinoid tumors and bronchial gland tumors (Herold, 2018; Reck & Rabe, 2017) (Figure 1). The classification plays an important role in the therapy decision process as the choice of medication is based on the histology.

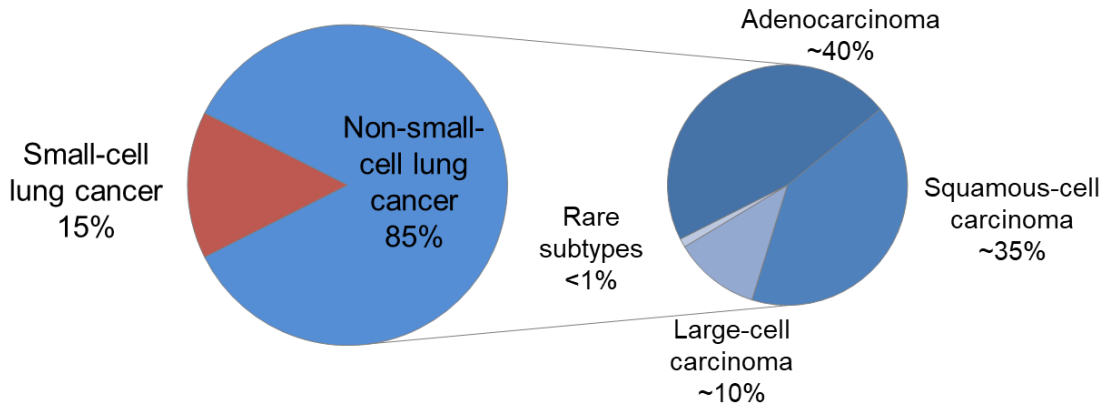

Figure 1: Lung carcinoma subtypes

The pie chart on the right side shows the two main subtypes small-cell lung cancer (red) and non-small-cell lung cancer (blue). The pie chart on the left side displays the subtypes of NSCLC and their proportions in different shades of blue. (Herold, 2018, p. 401).

Table 1: Differentiation of lung cancer subtypes

Histologic type and primary subtypification	
Epithelial tumors	**Mesenchymal tumors**
Adenocarcinoma	Pulmonary harmatoma
Squamous cell carcinoma	Chondroma
Neuroendocrine tumors	PEComatous tumors
Small cell carcinoma	Congenital peribronchial
Large cell neuroendocrine carcinoma	myofibroblastic tumor
Carcinoid tumors	Diffuse pulmonary lymphangiomatosis
Preinvasive lesion	Inflammatory myofibroblastic tumor
Large cell carcinoma	Epithelioid hemangioendothelioma
Adenosquamous carcinoma	Pleuropulmonary blastoma
Sarcomatoid carcinomas	Synovial sarcoma
Other and Unclassified carcinomas	Pulmonary artery intimal sarcoma
Salivary gland-type tumors	Pulmonary myxoid sarcoma
Papillomas	with EWSR1–CREB1 translocation
Adenomas	Myoepithelial tumors
Lymphohistiocytic tumors	**Tumors of ectopic origin**
Extranodal marginal zone lymphomas of	Germ cell tumors
mucosa-associated lympohoid tissue	Intrapulmonary thymoma
Diffuse large cell lymphoma	Melanoma
Lymphomatoid granulomatosis	Meningioma, NOS
Intravascular large B cell lymphoma	**Metastatic tumors**
Pulmonary Langerhans cell histiocytosis	
Erdheim–Chester disease	

NOS: not otherwise specified

Classification after the World Health Organizations' (WHO) specification in 2015 (Travis et al., 2015)

2.1.2 Epidemiology

Lung cancer is the second most abundant cancer type observed in men following after prostate cancer in Germany. Ranging behind breast and colorectal cancer it evolves at the third position of cancer diagnoses in women (Tumorzentrum München, 2020). Still, the numbers for woman suffering from lung cancer increase constantly due to a rising incidence in female smoking habits. About one quarter of male cancer patients suffers from lung cancer, whereas it is only 16% for women. Meanwhile men lead in all other subtypes, women outnumber men in the ratio for adenocarcinoma by a calculated relation of 1:6=m:f (Herold, 2018, p.400).

Regardless, lung cancer causes the most cancer deaths in men and the second most in women (Tumorzentrum München, 2020).

2.1.3 Risk factors

Since a lot of patients suffer from lung cancer, many risk factors have already been identified. Those include exposure to tobacco smoke (active and passive), marijuana, hookah, nutrition, radon-222, ionizing radiation, general air pollution (mostly by fine particles), diesel exhaust (ultrafine particles), asbestos, man-made mineral fibers, polycyclic aromatic hydrocarbons, chromates, silicon dioxide, arsenic, nickel, beryllium, cadmium, hard metal dusts containing wolfram/cobalt, halogenated ethers, mustard gas and lung scars for example caused by tuberculosis or thoracic perfusion traumata (Deutsche Krebsgesellschaft, 2018; Herold, 2018; Reck & Rabe, 2017). A genetic predisposition towards lung cancer development of two- to threefold when one parent is suffering from the disease was also found (Herold, 2018).

2.1.4 Treatment of NSCLC

Before start of treatment tumor subclassification is performed according to the histology (Table 1). After that, patients are staged into different categories following the observed clinical appearance (see Table 2). Therapy decision bases on different schemes, depending on tumor histology and stage.

The first treatment option considered in stage I-IIIA is tumor resection. Since it represents a curative method, resection is always applied in the absence of contraindications. Different factors, including maximal resilience, comorbidities (especially cardiovascular diseases), performance status defined by the Eastern Cooperation Oncology Group (ECOC-status) and others are assessed before treatment decision. Resection can be followed by an adjuvant therapy which consists of radiation, radiochemotherapy or chemotherapy depending on the tumor stage and location.

Radiotherapy (RaT) should be applied, in case resection is impossible. If needed, it can be combined with adjuvant chemotherapy (ChT). The Manual by the Tumorzentrum Munich also recommends the application if the immune checkpoint inhibitor durvalumab after confirmed tissue expression of PD-L1 in stage IIIA patients.

Patients in stage IIIB and IV suffer from advanced stage lung cancer. They have already progressed in the disease to an extent that resection is, at least initially, impossible. Patients in stage IIIB should be treated with radiochemotherapy. If tissue PD-L1 expression is detectable, a treatment with durvalumab should follow. Patients diagnosed in stage IV should undergo molecular analysis searching for the known genetic alterations as well as PD-L1 expression investigation. Therapy decision depends on the outcome of the analysis and usually combines targeted with other approaches like ICIs and chemotherapy. Chemotherapeutic regimens are usually based on a platinum-drug which is combined with one or two other agents. The selection of the therapeutics is based on various prerequisites including general healthy status, tumor stage, contraindications and comorbidities (Tumorzentrum München, 2020). In December 2019, the National Comprehensive Cancer Network (NCCN) published an update on their NSCLC treatment guideline focusing on the reevaluated role of immunotherapy. Herein, the first line monotherapy with pembrolizumab is recommended in advanced stage NSCLC showing PD-L1 tissue expression rates ≥50%. If platinum-based chemotherapy is not tolerated, patients showing expression levels between one and 49% can also be treated likewise. For patients suffering from non-squamous NSCLC, a combinatory first line treatment of pembrolizumab and chemotherapy is recommended even independent from the PD-L1 expression status (Ettinger et al., 2019).

A standard chemotherapy regimen in advanced stage NSCLC is the combination of paclitaxel with a platinum-based drug.

Paclitaxel belongs to the family of taxanes and is a native biological substance found in the pacific yew tree. The cellular target of taxanes is the β- subunit of the microtubules. Target binding stabilizes the polymerized form of the microtubules. Due to a lack of free microtubules the mitotic spindle can no longer be built and the cell cycle is not able to proceed to the M-phase. Consequently the cell cycle is constantly arrested in the G2-phase. This process leads to cell death in the end.

The general digestibility of paclitaxel is very well, main adverse events are a short-term suppression of the bone marrow and peripheral neuropathy. Resistance to therapy is hypothesized to happen due to increased production of efflux transporters or mutation of the paclitaxel binding site on the β-subunit of the microtubule in course of therapy (Mutschler et al., 2013, p.895).

Platinum-based drugs belong to the class of alkylating agents. This class of anticancer drugs consists of reactive substances whose main mechanism of action is the alkylation of nucleic acids. The consequences are multiple DNA-alterations including cross-links which harm DNA-replication. Though the platinum-based drugs do not alkylate nucleic acids, they share the mechanism of cross-linking with the other substances of this group.

The three platinum-based drugs cisplatin, carboplatin and oxaliplatin are plane cis-diamine complexes with a platinum cation in the center. The drugs differ in their accompanying anion, which results in a higher stability of the latter. Platinum-based drugs activate by losing of the accompanying anions due to shift in intracellular chlorine concentration. This results in the building of an electrophile aquatic complex. The reactive complex forms cross-links, especially in single stranded DNA. Cross-linked strands cannot be replicated and lead to induction of apoptosis in the corresponding cell. All three substances have a high emetogenic potential which can be mitigated by the application of 5-HT_3 receptor antagonists (setrons) or dexamethasone. Additionally each substance has its special side effect that has to be considered while choosing between the three drugs. Cisplatin is highly nephron- and ototoxic. The toxic potential can be reduced by the application of a saline-glucose infusion. The application of carboplatin is limited by its bone marrow suppression whereas oxaliplatin shows a dose limiting neurotoxicity. Resistance against platinum-based drugs is also knows. Mechanisms are hypothesized to base on a reduced transport into the cell, an increased intracellular enzymatic clearance, increased expression on DNA-repair enzyme or an enlarged tolerance for DNA-damages meanwhile replication (Mutschler et al., 2013, p. 889; Steinhilber et al., 2010, pp. 474-476).

Currently, targeted therapies are only applied in advanced stage NSCLC (Deutsche Krebsgesellschaft et al., 2018; Griesinger et al., 2018). Targeted treatment bears the hope for a specific and effective therapy meanwhile reducing adverse effects. Three starting points for targeted therapies are postulated. The first idea is to identify and treat driver mutations (e.g. BRAF-mutation, MET-amplification). The second idea is to identify and block cell proliferation or survival molecules (e.g. Tyrosin kinase inhibitors).

The third aspect is to enhance the immune system (e.g. immune checkpoint inhibitors) (Griesinger et al., 2018; Hirsch et al., 2016). In the future these targeted approaches will gain more influence in therapy regimen as the accompanying diagnostics will be more accessible.

Table 2: Staging and TNM classification of lung cancers (NSCLC and SCLC)

Stage	**TNM-classification**
0	Tis
IA	T1N0M0
IB	T2aN0M0
IIA	T2bN0M0
IIB	T1N1M0; T2N1M0; T3N0M0
IIIA	T1N2M0; T2N2M0; T3N1M0; T4N0M0; T4N1M0
IIIB	T1N3M0; T2N3M0; T3N2M0; T4N2M0
IIIC	T3N3M0; T4N3M0
IVA	T1-4 N1-3 M1a,b
IVB	T1-4 N1-3 M1c

T: Tumor, N:Node, M: Metastatis, Tis: Carcinoma in situ, a: metastasis lung tissue, b: one extrathoraic metastasis, c: one or more extrathoraic metastasis

After the International Association for the Study of Lung Cancer (IASLC) and the Union for International Cancer Control (UICC), (Goldstraw et al., 2016; Union for International Cancer Control (UICC), 2020).

2.2 Immune checkpoint inhibitors

Immunotherapy conveys a relatively young field in cancer therapy resulting in amazing responses for previously hard-to-treat tumors and tumor stages. The approach uncovers an innovative way to eliminate cancer cells. Not the tumor cell itself is addressed by the medication but the immune system is enabled to identify and eradicate cancer cells more effectively.

Tumor cells, the same as normal cells, present specific antigens on their surface. Some of those antigens identify the cell as tumorous (tumor-specific antigens) and thus result in elimination by immune cells. Certain tumor cells developed the ability to downregulate the immune system as a survival mechanism. This process leads to a preselection of immunocompetent cells in cancer progression. The concept is referred to as immunoediting (Dunn et al., 2005; Escors et al., 2018; Smyth, 2005). Nevertheless immune cells are still able to identify and destroy cancer cells if being reactivated. Following this approach, the immune checkpoint inhibitors were developed.

2.2.1 Physiological background

The first explored immune checkpoint pathways were the cytotoxic T-lymphocyte-associated protein 4 (CTLA-4) and the programmed cell death protein (PD-1-PD-L1) pathway. Currently, several other proteins are investigated in the context of immune checkpoint inhibition (Schildberg et al., 2016).

The programmed-cell death protein pathway is targeted by the majority of ICIs because the PD-1-PD-L pathway represents an important mechanism to maintain peripheral immune tolerance (Patsoukis et al., 2012).

PD-1 (CD279) is a transmembrane receptor which is expressed on the surface of activated T-cells, B-cells, myeloid cells and macrophages (Blank et al., 2005; Freeman et al., 2000; Ishida et al., 1992; Schildberg et al., 2016). The amino acid structure of PD-1 is encoded in the *Pdcd1* gene. It consists of five exons, which can roughly be dedicated to the three distinct protein regions. Exon one and two belong to the extracellular region, exon three represents transmembrane component and Exon four and five belong to the intercellular part. Four splice variants are known of which two are lacking exon three and thus the transmembrane region. These can possibly represent soluble forms of the receptor (Keir et al., 2008; Wan et al., 2006). PD-1s extracellular region is a single Ig-like variable (IgV) domain, which is followed by a hydrophobic transmembrane motif. The intercellular region comprises of two motifes, an immunoreceptor tyrosine-based inhibitory motif (ITIM) and an immunoreceptor tyrosine-based switch motif (ITSM) (Freeman et al., 2000; Vivier & Daëron, 1997). Mutations in the ITSM region cause a loss of functionality, which indicates its importance in downstream signaling. PD-1 appearance on the cell surface is monomeric (Zhang et al., 2004).

Two ligands of PD-1 are described in literature, PD-L1 (CD274) and PD-L2 (CD273) (Freeman et al., 2000). As the PD-1 receptor shares main structure elements with CTLA-4, Freeman et al. hypothesized that the to-be-discovered ligand will have similarities with B7-1 (CD80) and B7-2 (CD86), the corresponding ligands of CTLA-4.

In order to test their hypothesis the group used the Basic Local Assignment Search Tool (BLAST). Finding a matching structure and confirmation cell culture experiments it was named it PD-L1. They also corroborated that the ligand PD-L1 was the same structure Dong and his group had identified already in 1999 as a so far receptorless ligand B7-H1 (Dong et al., 1999; Freeman et al., 2000; Vivier & Daëron, 1997). PD-L1 is expressed on the surface of a variety of hematopoetic and non-hematopoetic cells, for example antigen-presenting cells (APC) and epithelial cells. Its expression is balanced according to different factors including the location of the corresponding cell (Marzec et al., 2008). High levels of PD-L1 mRNA are found in several tissues, for examples those of lung and heart. PD-L1 consists of an extracellular structure including an IgV and an IgC domain, followed by a transmembrane element. The intracellular region only encompasses a few amino acids and its function is still unclear (Freeman et al., 2000).

In 2007 Butte et al. identified B7-1 (CD80) as a second binding partner for PD-L1, but not PD-L2. Receptor binding results in downregulation of T-cell proliferation as well as cytokine production (Butte et al., 2007). As both receptors are found on the surface of the same cell-type, their interaction causes bidirectional inhibitory signaling. Hence its effects basically resemble the ones by PD-1-PD-L1 interaction. The two signal pathways are likely to explain the greater efficacy of anti-PD-L1 drugs in vivo (Keir et al., 2008).

In 2001, PD-L2 was discovered as the second known ligand of PD-1. Its structure and functions are hypothesized to equal the ones of PD-L1, though its affinity to PD-1 is higher (Latchman et al., 2001; Tseng et al., 2001; Youngnak et al., 2003). Alike PD-L1, PD-L2 is expressed on the surface of hematopoietic and non-hematopoietic cells, for example B lymphocytes and dendritic cells (Francisco et al., 2010). Only recently a second binding partner for PD-L2 was identified. The interaction with repulsive guidance molecule b (RGMb) results in respiratory tolerance. This finding might contribute to an explanation for the observed side effect of (severe) pneumonitis during anti-PD-1 treatment (Xiao et al., 2014). The role of PD-L2 in cancer development has not intensively been investigated so far. Since the last few years more is understood about the function of immune checkpoint pathways in general. This also resulted in extended research on PD-L2, which will hopefully reveal more insights on its special functions in the near future (Solinas et al., 2020).

The interaction of the PD-1 receptor with its ligands PD-L1 or PD- (Figure 2) leads to phosphorylation of the aforementioned intracellular motifs ITIM and ITSM. Those recruit Src homology region 2 domain-containing phosphatases (SHP) which henceforth dephosphorylate signaling intermediates (Chemnitz et. al., 2004; Okazaki et al., 2001; Sheppard et al., 2004).

Consequently the signaling of PI3K-Akt and Ras-MEK-ERK pathways is inhibited (Patsoukis et al., 2012). Direct effects are decreases in the cytokine production of IFN-γ, TNF-α and IL-2 (Keir et al., 2008; Schildberg et al., 2016). Other than implied by the name, the interaction leads to cell cycle arrest rather than cell death (Brown et al., 2003).

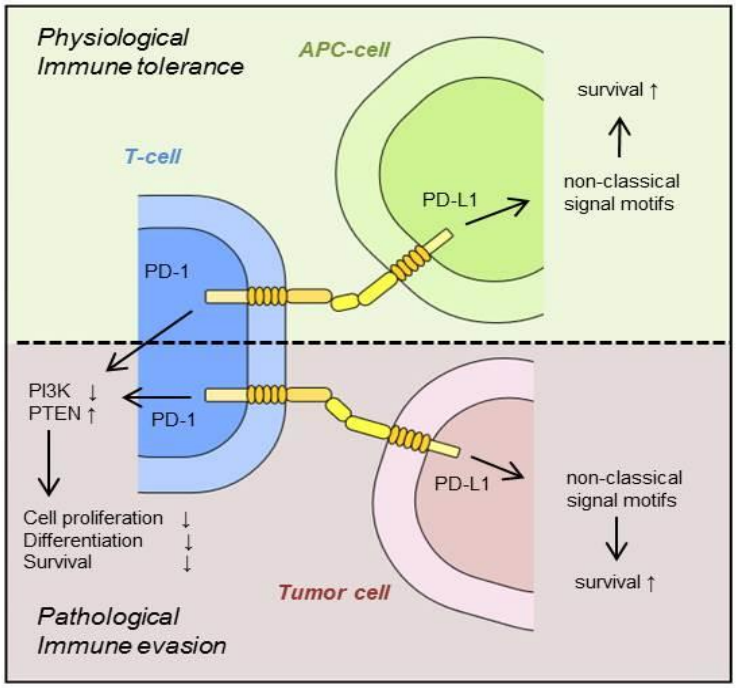

Figure 2: Signaling pathways of the programmed-cell death markers

The upper part of the figure (green) illustrates the physiological whereas the lower (red) part refers to the pathological PD-1-PD-L1 interaction and downstream signaling pathways.

Ligand expression can be upregulated by different inflammation stimulating mediators (Rozali et al., 2012; Topalian et al., 2015). PD-L1 expression, for example is induced by various inflammatory stimuli, like INF-γ. Parsa et al. detected an increased expression of PD-L1 due to loss of PTEN function and PI3K activation in cell culture of glioma cells (Parsa et al., 2007).

Upregulation of PD proteins expression was demonstrated in a variety of tumor types by different research groups. Dong et al. detected PD-L1 expression on different cancer cell culture by fluorescence-activated cell sorting (FACS) and used immunohistochemical staining to confirm the results on cancer biopsies (Brown et al., 2003; Dong et al., 2002). In the continuation, the tumor microenvironment (TME) evolved as the focus point for PD-1, PD-L1 and PD-L2 research (Keir et al., 2008). Cancer cells use immune checkpoint pathways to induce resistance against the immune system in two ways. These, innate and adaptive, mechanisms occur separately or in combination.

The consequence is always a high expression of PD-ligands on the cell surface. Genetic modifications form the basis of the innate pathway. These are amplifications of the PD-L genes or mutations in oncogenic signaling pathways. The adaptive pathway needs an environmental stimulus to induce the expression. This stimulus comes mainly from cytokines secreted by T cells aiming to eradicate tumor cells (Marzec et al., 2008; Pardoll, 2012; Parsa et al., 2007; Spranger et al., 2013; Taube et al., 2012; Topalian et al., 2015). It was shown that the infiltration with tumor infiltrating lymphocytes (TILs) results in IFN-γ secretion, which consequently fosters PD-L1 expression. This physiologically negative feedback loop therefore causes adaptive immune resistance in tumor cells (Spranger et al., 2013; Taube et al., 2012).

Just recently, the genetic element PD-L1L2-SE was identified. It is encoded between the PD-L1 and PD-L2 gene and represents an important enhancer sequence needed for the expression of PD-L1 and PD-L2 mRNA. Further research revealed it not to be depending on the presence of IFN-γ (Xu et al., 2019). The finding underlined the complexity of the regulation of signaling and expression of the PD-1-PD-L1 pathway.

Since the programmed cell death markers are shown to play a pivotal role in the regulation of the immune response they represent interesting biomarkers the context of cancer. A strong effect is expected to be found in ICI-treated patients due to the direct association with the corresponding target. An important prerequisite for the development of blood based biomarker analysis is the existence of soluble forms of the corresponding biomarkers. In 2005 Nielsen et al. were able to detect five splice variants of the PD-1 protein in cell culture of peripheral blood mononuclear cells. Special interest was payed to PD-1Δex3 which lacks the transmembrane domain (TMD) and is hence expected to represent a soluble splice variant. The group was able to stimulate the its expression though they, probably due to insensitive antibodies, were not able to confirm the secretion in cell culture supernatant (Nielsen et al., 2005). The existence of a soluble form of PD-L1 was shown by Frigola et al. in 2011. They were able to detect PD-L1 in the cell culture of tumor cells and blood samples of renal cell carcinoma patients. Since PD-L1 could not be found intracellularly, they follow the hypothesis of cleavage from the cell surface by metaloproteinases (Frigola et al., 2011). A TMD-lacking splice variant was also shown for PD-L2. The function of this variant is still unclear (Schildberg et al., 2016). The existence of soluble forms of PD-1, PD-L1 and PD-L2 was at least theoretically confirmed by literature research.

2.2.2 Application as biomarkers

This approach follows the idea of the immune checkpoint molecules PD-1, PD-L1 and PD-L2 representing interesting targets to evolve as biomarkers. Due to their central position in modulating immune response, they are hypothesized to play a pivotal role in all kinds of inflammatory diseases. Since cancer and cancer treatment results in immune activation it is proposed to find an effect by monitoring the biomarker concentrations.

Since tissue based analytic is expensive, only rarely accessible and cannot cover tumor heterogeneity, serum and plasma were chosen as analytes. Background research revealed it is likely that soluble forms of PD-1, PD-L1 and PD-L2 exist. A blood based screening method combined the advantages of a low cost and easily performable and objectively analyzable method.

The biomarkers can be of use in prediction, prognosis and monitoring of cancer patients treated with checkpoint inhibitors and other chemotherapeutic agents.

A further approach will be to evaluate the markers in differential diagnostic purposes on ICI-treated patients. Response rates of tumor patients to immunotherapy currently range in the low double-digit percent range. Hence, it is of great interest to establish a predictor to evaluate therapy success before application. In 2010 Brahmer et al. detected a correlation between tissue expression of PD-L1 and outcome in 39 patients treated with an anti-PD-1 study drug. The cohort suffered from a variety of solid tumors including metastatic melanoma, colorectal cancer, castrate-resistant prostate cancer, non-small-cell lung cancer and renal cell carcinoma (Brahmer et al., 2010). In the continuation other groups investigated the postulated correlation in larger cohorts and on different cancer types with varying outcomes.

2.2.3 Drugs

A variety of immune checkpoint inhibitors opens up a broad field of potentially later investigations on the new biomarker assays. Since the first approved drugs showed encouraging results in clinical practice, the research on new drugs was intensified. Especially melanoma patient data convinced with longterm survival observed former untreatable advanced stages. Some already received market approval for the treatment of a variety of cancer types. Table 3 lists all EMA-approved drugs with their corresponding indications. Currently two drugs targeting PD-1, pembrolizumab and cemiplimab, and four drugs targeting PD-L1, nivolumab, atezolizumab, durvalumab and avelumab, are available treatment options. Targeting PD-L1 combines two advantages. On the one hand this approach does not prevent PD-L2 from binding to the PD-1 receptor. This is assumed to reduce the rate and intensity of adverse events seen by anti-PD-1 blockade. On the other hand PD-L1 also induces downstream signaling by the B7-1 (CD80) receptor. The interaction with this second pathway is believed to enhance the immune stimulating effect. The general side effect profile of the drugs is similar as these are all explainable by the mechanism of action. The main difference between the drugs is based on the different approved indications. The picture will change in the future due to still ongoing studies.

Table 3: EMA-approved PD-1 and PD-L1 immune checkpoint inhibitors

Drug	**Target**	**Indication**	**Source**
Pembrolizumab	PD-1	Advanced melanoma	(MSD SHARP & DOHME GMBH, 2019)
		NSCLC	(MSD SHARP & DOHME GMBH, 2019)
		Recurrent cHL	(MSD SHARP & DOHME GMBH, 2019)
		Locally advanced urothelial carcinoma	(MSD SHARP & DOHME GMBH, 2019)
		Locally advanced SCCHN	(MSD SHARP & DOHME GMBH, 2019)
		RCC	(MSD SHARP & DOHME GMBH, 2019)

Drug	Target	Indication	Source
Cemiplimab	PD-1	Locally advanced CSCC	(Sanofi-Aventis Deutschland GmbH, 2019)
Nivolumab	PD-L1	Melanoma (adjuvant)	(Bristol-Myers Squibb GmbH & Co. KGaA, 2020)
		NSCLC	(Bristol-Myers Squibb GmbH & Co. KGaA, 2020)
		Advanced RCC	(Bristol-Myers Squibb GmbH & Co. KGaA, 2020)
		Recurrent cHL	(Bristol-Myers Squibb GmbH & Co. KGaA, 2020)
		Recurrent SCCHN	(Bristol-Myers Squibb GmbH & Co. KGaA, 2020)
		Locally advanced urothelial carcinoma	(Bristol-Myers Squibb GmbH & Co. KGaA, 2020)
Atezolizumab	PD-L1	Locally advanced urothelial carcinoma	(Roche Pharma AG, 2019b, 2019a)
		Advanced NSCLC	(Roche Pharma AG, 2019b, 2019a)
		Locally advanced triple-negative breast cancer	(Roche Pharma AG, 2019b)
		ES-SCLC	(Roche Pharma AG, 2019a)
Durvalumab	PD-L1	Advanced NSCLC	(AstraZeneca GmbH, 2018)
Avelumab	PD-L1	Metastatic MCC	(Merck Europe B.V., 2019a)
		Advanced RCC	(Merck Europe B.V., 2019a)

NSCLC: Non-small cell lung cancer, cHL: Classic Hodgkin-lymphoma, SCCHN: Squamous cell carcinoma of the head and neck, RCC: Renal cell carcinoma, CSCC: Cutaneous squamous cell carcinoma, ES-SCLC: Extensive Stage Small Cell Lung Cancer, MCC: Merkel cell carcinoma

2.2.3 Side effects

Due to immune system down-regulation, infectious diseases as pneumonitis, hepatitis, colitis, nephritis, endocrinopathies (including thyroid disorders, diabetes mellitus) and other immune-mediated side effects (including Guillain-Barré-Syndrom, myositis, meningitis, and more) occur in all drugs with market approval (AstraZeneca GmbH, 2018; Bristol-Myers Squibb GmbH & Co. KGaA, 2020; Merck Europe B.V., 2019a; MSD SHARP & DOHME GMBH, 2019; Roche Pharma AG, 2019a; Sanofi-Aventis Deutschland GmbH, 2019). Other adverse events are only reported in some of the medications, such as myocarditis (AstraZeneca GmbH, 2018; Bristol-Myers Squibb GmbH & Co. KGaA, 2020; Merck Europe B.V., 2019a; Roche Pharma AG, 2019a), reactions to infusion (AstraZeneca GmbH, 2018; Merck Europe B.V., 2019a; MSD SHARP & DOHME GMBH, 2019; Roche Pharma AG, 2019a) and skin reactions, especially rash (AstraZeneca GmbH, 2018; Bristol-Myers Squibb GmbH & Co. KGaA, 2020; MSD SHARP & DOHME GMBH, 2019; Roche Pharma AG, 2019a; Sanofi-Aventis Deutschland GmbH, 2019). All of the abovementioned reactions are severe diseases, which most need intensive treatment on their own. Consequently, it is very important to stratify patients before treatment application in order to protect those who will not benefit from therapy from severe side effects.

2.2.4 Developments in the field of immune checkpoint inhibitors

The therapeutic success of the first immune checkpoint inhibitors lead to intensified research on further pharmaceutical agents and targets. SHR-1210 (Ocrelizumab, anti-PD1, NCT03871855) and MK-1308 (anti-CTLA4) represent two drugs in the pipeline that are developed on already known targets (National Cancer Institute, 2020a; U.S. National Library of Medicine, U.S. National Institutes of Health, & U.S. Department of Health and Human Services, 2020b). The field of immune checkpoint inhibitors in broad though and offers a variety of new targets. MK-4280, for example, is developed to bind lymphocyte-activation gene 3 (LAG-3) (National Cancer Institute, 2020b). The majority of projects focus on the development of bifunctional molecules, for example bispecific antibodies. Some focus on the combination of already known targets. These include a for example the targets PD-1 with CTLA-4 (NCT03179436) or PD-1 with a tyrosine kinase inhibitor (NCT04203485), which are both part of clinical trials (Astra Zeneca, 2020; U.S. National Library of Medicine et al., 2020b). Another approach, M7824 (NCT03631706), combines PD-L1 with the cytokine TGF-β (Merck Europe B.V., 2019b). The combination with new checkpoint inhibitors is investigated in RGs 6160 and 7769 (Roche Pharma AG, 2020). The named substances only represent examples to illustrate the current pipeline due to many other companies and projects in the research field.

2.3 Biomarkers

2.3.1 Definition

The term biomarker is defined by the European Medicines Agency and the U.S. Food and Drug Administration.

The European Medicines Agency (EMA) defines the term as follows:

“A biological molecule found in blood, other body fluids, or tissues that can be used to follow body processes and diseases in humans and animals.”

(European Medicines Agency, 2019)

Whereas the U.S. Food and Drug Administration (FDA) states the following:

“A defined characteristic that is measured as an indicator of normal biological processes, pathogenic processes, or biological responses to an exposure or intervention, including therapeutic interventions. Molecular, histologic, radiographic, or physiologic characteristics are types of biomarkers. A biomarker is not an assessment of how an individual feels, functions, or survives. Categories of biomarkers include:

- susceptibility/risk biomarker
- diagnostic biomarker
- monitoring biomarker
- prognostic biomarker
- predictive biomarker
- pharmacodynamic/response biomarker
- safety biomarker” (Food and Drug Administration, 2019)

While the EMA definition is short but comprehensive, the one by the FDA encompasses more details by the introduction of subcategories. These can turn out to be useful in categorizing the markers, though it will not be possible to easily place all of them. Nevertheless, both understandings fit the latter presented biomarkers.

This work focuses on soluble biomarkers that can be detected in the blood stream. The advantages of such markers are easily accessible and comparably cheap sample drawing procedures. Thus, longitudinal monitoring is applicable and more information available. Samples are more stable and easier to store and transport. A limitation of the approach represents the impossibility to locate the origin of the biomarker. On the other hand, tumor heterogeneity and even metastases can be covered.

2.3.2 Tissue biomarkers in lung cancer

2.3.2.1 Staining

The Guideline established by the Association of the Scientific Medical Societies (Arbeitsgemeinschaft der Wissenschaftlichen Medizinischen Fachgesellschaften e.V., AWMF) from 2018 in Germany, announces the consent-based recommendation to assess the tissue PD-L1 expression status in untreated stage IV patients diagnosed with NSCLC. Different antibodies to perform immunohistochemical staining are available. According to the guideline, results are reported using a tumor proportion score (TPS) (Deutsche Krebsgesellschaft et al., 2018). Following Hutarew, “Tumor proportion scores (TPS) were defined as the percentage of tumour cells with complete or partial membranous staining at any intensity.” (Hutarew, 2016).

However, tissue staining with anti-PD-L1 antibodies faces various challenges. Results vary among different PD-L1 antibody clones, staining platforms, specimen type and observers. Consequently, different scoring systems and cut off values are used to interpret obtained results (Hutarew, 2016; Kerr et al., 2015).

Although hazard ratios for overall survival (OS) and progression free survival (PFS) rose for positive cohorts in many studies, other investigations also showed considerable response rates in negative tested patients (Hutarew, 2016). Limitation to the surveyed tissue biopsy and uncovered tumor heterogeneity and metastasis serve as an explanation for the finding. Moreover, it is not yet clear what effect prior chemotherapy or targeted therapy has on the tumorous PD-L1 expression status. This serves as a potential explanation for different results in the various studies as their prerequisite conditions might have been different (Kerr et al., 2015).The group of Herbst et al. showed than expression profiles on tumor infiltrating lymphocytes (TILs) correlated with therapy response, at least in an atezolizumab-treated cohort (Herbst et al., 2016). Nevertheless, PD-L1 expression patterns on immune cells cannot be reproducibly detected so far, though better training and guidelines are likely to improve the diagnostic value (Scheel et al., 2016).

2.3.2.2 Molecular markers

Especially the development of targeted therapies proved the necessity to introduce biomarkers to identify the target in advance to therapy application. Popular targets are genetic alterations including mutations, translocations and amplifications, for example BRAF, MET.

These are currently investigated in tumor biopsies using next generation sequencing (NGS) approaches. Different groups work on detecting the mutations on circulating tumor DNA (ctDNA) in blood samples. There have been already some impressive results, though the methods are not ready to enter broad clinical diagnostic setting yet (Tumorzentrum München, 2020).

2.3.3 Blood biomarkers in lung cancer

Tumor markers represent an important and easy to apply diagnostic tool. Although they cannot be relied on as single markers for diagnostic purposes they have found their role in supporting differential diagnosis, monitoring therapy and in early detection of recurrence in lung cancer. CYFRA 21-1, CEA, SCCA; NSE and ProGRP are known biomarkers in lung cancer (Table 4), whereas CA15-3, CA125 and HE4 are not.

Soluble cytokeratin 19 fragment (**CYFRA 21-1)** represents a promising tumor marker in lung cancer diagnostics. Cytokeratins are intermediate-sized filaments in epithelial cells. These filaments maintain an important functions in the structure of cell cytoplasm (Hatzfeld & Franke, 1985). So far, around 20 keratins are known which split into two subgroups (type I: 9-20; type II: 1-8). To form its final structure, the acidic (type I) and the basic (type II) combine to heteropolymers (Bodenmüller, 1995). Broers et al. investigated the presence of different cytokines in lung cancer tissues and detected cytokeratine 19 in a variety of them (Broers et al., 1988). Stieber et al. showed that CYFRA 21-1 allows for better distinguishing between malign and benign lung diseases than so far used carcinoembryonic antigen (CEA) and squamous cell carcinoma antigen (SCCA). Utility varied among the investigated lung cancer subtype (Stieber et al., 1993). Nowadays it is recommended to measure CYFRA-21 in monitoring and aftercare of NSCLC patients (Roche Diagnostics GmbH, 2012). It proved to be an independent prognostic factor in multivariate survival analysis. Additionally the efficacy of chemotherapy in advanced stage NSCLC can be monitored. Increasing concentrations after resection will indicate recurrence earlier than imaging. In summary, CYFRA 21-1 is currently the most important biomarker in NSCLC (Tumorzentrum München, 2020).

Carcinoembryonic antigen (**CEA**) was first described by the group of Gold et al. in 1964 (Gold & Freedman, 1964). Although the name indicates differently, CEA expression is not limited to fetal cells. It is detected in various healthy tissues, especially in the colon. Structurally, CEA belongs to the immunoglobulin superfamily. It is a highly glycosylated molecule, that is normally membrane-bound but can also be cleaved. Biologically it is important to enable cell-adhesion. Thus its utility as a biomarker candidate to diagnose and monitor cancer disease was hypothesized (Hammarström, 1999).

Nowadays, rising values indicate post-surgical cancer recurrence in colorectal cancer (CRC) (Herold, 2018, p. 493). Jong et al. strongly recommend to measure CEA values in order to monitor NSCLC (de Jong et al., 2020). Showing no organ specificity is one of the limitations faced by CEA. Nevertheless its pre-therapeutic concentrations are predictive for survival in the subgroup of adenocarcinomas. Additionally, its combination with other biomarkers improves overall specificity (Tumorzentrum München, 2020).

Squamous cell carcinoma antigen (**SCCA** or **SCC**) is a glycoprotein that is expressed in epithelial tissues. Biologically, it serves an enzyme inhibitor for serine and cysteine proteinases (Roche Diagnostics GmbH, 2020c; Schick et al., 1998). The tumor marker can be used to follow the status of cancers of squamous origin, for example located in the head and neck, oral cavity, esophagus and lung region. In lung cancer it is investigated in differential diagnosis, though its meaningfulness as a single marker is limited by its elevation in various benign diseases (Kagohashi et al., 2008; Tumorzentrum München, 2020).

Neuron-specific enolase (**NSE**) is an enzyme that catalyzes an important step in glucose metabolism. The corresponding enzyme family consists of three isoenzymes. NSE or enolase γ is characteristically expressed in neuronal tissue (Mu et al., 2020). Erythrocytes also contain NSE, in consequence blood samples that show signs of hemolysis cannot be analyzed (Scatena, 2015, p.137). Due to its specificity, NSE evolves as a promising biomarker for neuroendocrine type tumors. This characterization includes the histology of SCLC, which has been investigated in several studies. Marker concentrations have been found to correlate with the clinical stage as well as an increase in former stable concentrations is an early recurrence indicator. Pre-therapeutic NSE concentrations showed prognostic potential in lung cancer patients, SCLC and NSCLC (Muley et al., 2003; Tumorzentrum München, 2020).

ProGRP is a preliminary form of the gastrin-releasing protein (GRP). It is hypothesized to act as a neurotransmitter in the nervous system. Its release is highly specific to small cell lung cancers. Currently ProGRP is measured in differential diagnosis and to monitor therapy efficacy in SCLC patients. Due to its high specificity, it qualifies for a screening marker which has not been investigated yet. The combinatory analysis with the tumor marker NSE leads to a further increase in the diagnostic potential of ProGRP (Holdenrieder & von Pawel, 2013; Polak et al., 1988; Tumorzentrum München, 2020).

Table 4: Recommended tumor markers to assist in lung cancer diagnosis and monitoring

Histology	**Pre therapy**	**Monitoring**
Unknown	CYFRA 21-1, NSE, ProGRP, CEA, SCCA	Depending on histology
Adenocarcinoma	CYFRA 21-1 and CEA	CYFRA 21-1 and/or CEA
Squamous cell carcinoma	CYFRA 21-1 and SCCA	CYFRA 21-1 and/or SCCA
Large cell carcinoma	CYFRA 21-1 and CEA	CYFRA 21-1 and/or CEA
Small cell carcinoma	NSE and ProGRP	NSE and/or ProGRP

Obtained from the Tumorzentrum Munich (Tumorzentrum München, 2020)

Not being known as biomarkers in the field so far are the tumor markers CA 15-3, CA 125 and HE4. Due to their biology and locations, they might also represent interesting targets to evaluate. Hence these were included in the study investigations.

Cancer antigen 15-3 (**CA 15-3**, PEM (polymorphic epithelial mucin), MUC1 (mucin-1)) is a mucin protein, that belongs to the subfamily of membrane-associated mucins. It is a transmembrane protein although the majority of the protein is located extracellular. Repeated sequences of amino acids with alcoholic side chains explain the high abundance of O-glycosylation (Gendler et al., 1990; Hilkens et al., 1995). It is typically expressed in glandular and luminal epithelial tissue and participates in forming the glycocalyx. Its function is to protect the cells from various environmental influences. When cells experience stress conditions they lose their polarity and reposition mucins. These shifts result in different downstream signaling pathways including the MAPK-, PI3K/Akt- and Wnt-pathway. CA15-3 is also suggested to play a role in regulation of inflammation (Kufe, 2009). It is hypothesized to induce a downregulation in infections whereas activation was observed in tumor malignancies. Tumor associated CA 15-3 can be differentiated from physiological mucin-1 by its different glycosylation pattern. This resulting from the different expression of glycosylation enzymes compared to non-malignant cells. The hypoglycosylation is believed to result in extended extracellular shedding and intracellular uptake and therefore increased downstream signaling. Currently CA 15-3 is measured in order to stage and monitor relapse in cancers with glandular origin like breast or pancreatic cancer (Nath & Mukherjee, 2014). Since its omnipresent appearance on the cell surface it is also hypothesized to display an informative biomarker in other epithelial cancers like lung cancer.

Cancer or carbohydrate antigen 125 (**CA 125**), also known as MUC16, is a large glycoprotein. It represents a member of the membrane-bound mucin protein family, though it can also be secreted either by the Golgi apparatus or by enzymatic cleavage(Kaneko et al., 2009; O'Brien et al., 2002; Rump et al., 2004). The antigen is highly glycosylated with oligosaccharides bound to the protein by N- and O-linkage (O'Brien et al., 2002). The protein is known to be expressed by a variety of tissues including fallopian tubes, endometrium, endocervix, pleura, peritoneum, and pericardium (Miralles et al., 2003). It has several proposed functions including anti-adhesion, immune suppression and the observation that it ties various sugar-binding molecules. Rump et al demonstrated that CA125 binds to membrane-bound mesothelin in ovarian cancer. As the interaction mediates cell-adhesion, they hypothesize it promotes metastasis in ovarian cancer (Rump et al., 2004). CA125 has had a long history as a tumor marker in diagnosis and follow-up of ovarian cancer. Since it is expressed in many tissues and rises in a variety of benign diseases as well, combining the biomarker with other markers improves its clinical utility (Escudero et al., 2011). In this approach it could also allow further insights included in a multi-marker investigation in NSCLC.

Human epididymis protein 4 (**HE4**) is a secreted N-glycosylated protein. First found in epididymal tissue, it is also expressed in other tissues like the respiratory epithelium, especially the trachea (Drapkin et al., 2005). Its biological function is not exactly known yet. Structure homologies suggest it to be an extracellular proteinase inhibitor. It is assumed to be a decapacitation factor which are part of the seminal plasma and modulate the fertilizing ability of spermatozoa (Kirchhoff, 1998). At the moment it is used to detect ovarian and endometrial cancer, also in combination with CA125 which turns out to improve specificity (Escudero et al., 2011; Roche Diagnostics GmbH, 2011). HE4 investigations in lung cancer indicate that it can be predictive for tumor recurrence in the adenocarcinoma subtype (Tumorzentrum München, 2020). Choi et al. found that the pre-therapeutic concentrations of HE4 were able to assist diagnostic procedures. Marker concentrations were able to differentiate healthy controls from benign from tumor disease. The differentiation to healthy patients did not depend on a certain carcinoma subtype. Additionally a correlation between marker concentrations and stage was seen. The diagnostic value of HE4 was again shown in by a review in 2019 (Choi et al., 2017; He et al., 2019).

All of the abovementioned tumor markers present with their specific cut-off concentrations to differentiate between healthy or benign and malign disease. These are listed in Table 5.

Table 5: Tumor markers and their corresponding cut-off values

Biomarker	Cohort	Cut-off	Additional information	Source
CYFRA 21-1	Healthy vs. benign lung diseases Healthy vs. malignant lung diseases	3.3 ng/ml (specificity: 95%) 1.8 ng/ml (specificity: 95%)	Elevated levels possible in: acute pneumonia, tuberculosis, interstitial lung diseases, liver cirrhosis, renal insufficiency	(Roche Diagnostics GmbH, 2020a; Tumorzentrum München, 2020)
CEA	Healthy 20-69 years 40-69 years	 4.7 ng/ml 5.2 ng/ml (95% percentile)	Elevated levels in smokers	(Roche Diagnostics GmbH, 2018a)
SCCA	Healthy Lung cancer vs. benign lung diseases	2.3 ng/ml (95% percentile) 2.6 ng/ml (sensitivity: 39.1%)		(Roche Diagnostics GmbH, 2020c)
NSE	Healthy	16.3 ng/ml (95% percentile)		(Roche Diagnostics GmbH, 2017)

Biomarker	Cohort	Cut-off	Additional information	Source
ProGRP	Healthy	68.4 pg/ml (95% percentile)	Elevated in patients with renal failure	(Roche Diagnostics GmbH, 2020b)
	SCLC vs. NSCLC	80.1 pg/ml (sensitivity: 78.2%)		
	SCLC vs. benign Lung disease	80.8 pg/ml (sensitivity: 78.2%)		
	SCLC vs. other malignancies	191 pg/ml (sensitivity: 66%)		
CA 15-3	Healthy	26.4 U/ml (95% percentile)		(Roche Diagnostics GmbH, 2013)
CA 125	Healthy	35 U/ml (95% percentile)		(Roche Diagnostics GmbH, 2019)
HE4	Healthy			(Roche Diagnostics GmbH, 2018b)
	<40 years	60.5 pmol/l		
	41-59 years	~75 pmol/l		
	60-69 years	82.9 pmol/l		
	≥70 years	104 pmol/l (95% percentile)		

3 Aim

Therapy individualization is the basis for the desired goal of personalized cancer treatment. The approach needs to combine the employment of targeted therapies with comprehensive biomarker surveillance. A major challenge is still the introduction of informative biomarkers. Those offer great potential to initiate adjustments in therapy regimen and applied diagnostic methods. A biomarker-indicated early differentiation between responders and non-responders to therapy for example proves beneficial in two ways. On the one hand can non-responders be switched to a different therapy regimen which increases the individual probability of therapy response and also reduces the risk to experience side effects. On the other hand, it might be possible to enlarge the distances between follow-up investigations in good responders. This can, for example, contribute to a reduction radiation diagnostics in the patients.

There is still an unmet need for informative biomarkers to allow patients' response prediction, prognosis of outcome and therapy monitoring in all kinds of cancer therapy. On this behalf it is necessary to investigate already established but also introduce new biomarkers. The tumor markers CYFRA 21-1, CEA, SCCA, NSE, ProGRP, CA15-3, CA125 and HE4 and the new biomarkers PD-1, PD-L1 and PD-L2 were investigated in an NSCLC cohort. Analysis was performed with the focus on predictive value for therapy response and prognostic value for progression free and overall survival to address the following objectives.

- Pre-therapeutic concentrations predictive for poor and good response to chemotherapy objected by CT
- Concentration changes between C1 and C3 predictive for poor and good response to chemotherapy objected by CT
- Pre-therapeutic concentrations prognostic for PFS/OS
- C3 concentrations prognostic for PFS/OS
- Programmed cell death markers predictive for poor and good response to chemotherapy objected by CT

4 Patients, methods and materials

4.1 Patients

4.1.1 CESAR Biomarker Substudy

The Central European Society of Anticancer Research (CESAR) initiated a multicentric interventional study in cooperation with Saladax Biomedical Inc., the CESAR Study of Paclitaxel Therapeutic Drug Monitoring: CEPAC-TDM. The study protocol included blood collections for biomarker measurements, the CESAR Biomarker. The main study investigated whether pharmacokinetically-guided paclitaxel dosing could reduce neutropenia compared to conventional dosing. The findings of the study were already published (Joerger et al., 2016).

The blood collection for the CESAR Biomarker Substudy took place in a subset of the patients following the main study and focused on the first three treatment cycles. The blood-drawing scheme is visualized in Figure 3. The time points are indexed with a number consisting of two parts. The front part names the treatment cycle. The back part identifies the day in the treatment cycle, where one stands for before treatment application and two for the day after treatment application. Only patients where a blood sample before start of the study (1_1 or 1_0) was available were included in the measurements. The blood sample of the day after treatment (x_2) was included just, if a sample before treatment was available. Time point 3_2 was left out because of the low number of applicable samples. In case of cancer progression or study drop-outs, the last collected blood sample is automatically named end of treatment (EOT.)

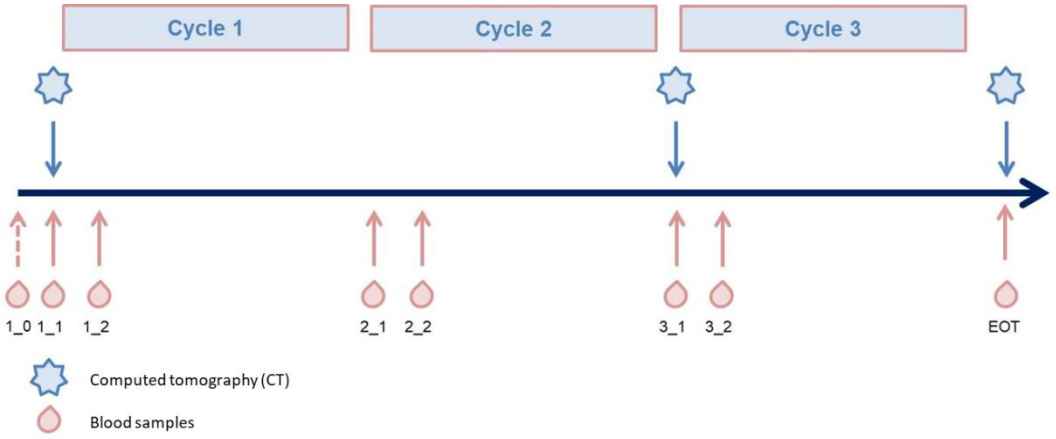

Figure 3: Blood collection scheme of the biomarker substudy

The dark blue arrow marks the time line. Blood collections are depicted as red arrows, whereas blue arrows stand for radiation investigations. The blue boxes at the top indicate the treatment cycles.

Table 6: Patient characteristics in the CESAR Biomarker Substudy

Characteristic	Amount	Characteristic	Amount
N	261	**Histology**	
Age/gender		Adenocarcinoma (%)	201 (77)
Mean age (range)	63 (40-77)	Squamous carcinoma (%)	60 (23)
Median age	63	**Staging**	
Female (%)	92 (35)	Stage IIIB (%)	40 (15)
Male (%)	169 (65)	Stage IV (%)	221 (85)
Smoking habits		**ECOG baseline**	
Current smoker (%)	97 (37)	0 (%)	135 (52)
Former smoker (%)	136 (52)	1 (%)	94 (36)
Never smoker (%)	28 (11)	2 (%)	10 (4)
Study arm		NA (%)	22 (8)
Arm A (BSA)	130 (50)	**Response**	
Arm B (PK)	131 (50)	Partial remission (%)	99 (38)
Study drug		Stable disease (%)	88 (34)
Carboplatin (%)	217 (83)	Progressive disease (%)	58 (22)
Cisplatin (%)	44 (17)	NA (%)	16 (6)

BSA: Body surface area guided dosing, PK: Pharmacokinetic guided dosing

Response was evaluated after the termination of the second treatment cycle by CT evaluation (Holdenrieder et al., 2020)

In preparation to the biomarker measurements, the whole sample set was properly organized and sorted. The shipped serum sample volume of 0.5 to 5 ml was divided in aliquots containing 500 µl each. Re-identification of the samples was carefully performed according to the reported clinical data. Whenever the sample identity remained unclear or no data was recorded, the corresponding sample was excluded from the biomarker study analyses.

All in all the background data of 243 patients was analyzable. 1/3 of the study population was female and 2/3 was male. 77% suffer from Non-Squamous adenocarcinoma and 85% reached stage IV of the disease. The characteristics of the patients were summarized in Table 6.

Patients were divided among their response to therapy assessed by computed tomography (CT) into responders and non-responders. Since 40% of the patients presented with stable disease, two approaches were differentiated. First, stable disease as well as partial remission was classified as response and progressive disease as non-response. The second approach investigated good response and as such only classified partial remission as response and summarized stable disease along with progressive disease as non-responsive.

Prediction of therapy response was investigated on the pre-therapy biomarker concentrations and on change in marker concentrations. The change period observed was start of therapy (1_1) until the end of treatment cycle two (3_1). Wherever data on 3_1 was not available, other time points were used when fulfilling the criteria. If only data on the end of treatment (EOT) was available, this data was used on the condition that the total amount of treatment cycles was less than three. If only data on the beginning of the second cycle (2_1) was available, this was used instead. In the case where data on both, 2_1 and EOT, was measured EOT data was preferred if the total amount of treatment cycles has been less than three, otherwise 2_1 data was used.

4.1.2 Healthy cohort

The set of healthy controls contained 136 heparin plasma samples. All study participants were males with a median age of 54 years (32-71). 96 participants showed cardiac abnormalities during the medical examination whereas the remaining 40 participants were categorized as healthy. All samples were analyzed with the newly developed PD-1, PD-L1 and PD-L2 ELISA assays.

4.1.3 Ethics

The CEPAC-TDM study protocol was written based on international standards of good clinical practice. It was accepted by local institutional review boards and also national authorities. Every participant agreed to study conditions by signing an informed consent (Joerger et al., 2016). The study is listed in the U.S. Library of Medicine (Clinical trials.gov) under the identifier: NCT01326767 (U.S. National Library of Medicine, U.S. National Institutes of Health, & U.S. Department of Health and Human Services, 2020a).

Informed consent was given by all patients included in the healthy cohort.

4.2 Tumor markers ECLIA

4.2.1 ECLIA method

The electrochemiluminescence immune assay (ECLIA) is an ELISA technology developed by Roche. The assays are based on two antibodies of which one is coupled with biotin and the other with a ruthenium complex. The sample is incubated with both antibodies in the first step. Next, streptavidin-covered beads are added which bind the biotinylated antibodies. The application of electricity activates the ruthenium complex to emit light which is then allows the sensitive quantification of the antigen. It takes 18 minutes to complete one sample analysis. All assays were fully validated by Roche Diagnostics GmbH. Measurements were performed on a Cobas Elecsys® e411 (Roche Diagnostics GmbH, 2012).

4.2.2 ECLIA quality control

Quality control was performed by a daily calibration and the measurement of supplied assay kit controls. Accepted calibration and controls were the prerequisite for sample measurements.

4.2.3 ECLIA materials

The analysis of the tumor markers based on assay kits purchased from Roche Diagnostics GmbH. The following tables list the reagents, additional reagents and consumables used to perform the analyses (Table 7, Table 8, Table 9).

Table 7: Tumor marker reagents

Reagent	Calibrator	Control
Elecsys® CYFRA 21-1	Elecsys® CYFRA 21-1 CalSet	PreciControl LC/ PreciControl Tumor Marker
Elecsys® CEA	Elecsys® CEA CalSet	PreciControl Tumor Marker
Elecsys® SCC	Elecsys® SCC CalSet	PreciControl LC
Elecsys® NSE	Elecsys® NSE CalSet	PreciControl LC/ PreciControl Tumor Marker
Elecsys® ProGRP	Elecsys® ProGRP CalSet	PreciControl LC/ PreciControl ProGRP
Elecsys® CA 15-3 II	Elecsys® CA 15-3 II CalSet	PreciControl Tumor Marker
Elecsys® CA 125 II	Elecsys® CA 125 II CalSet	PreciControl Tumor Marker
Elecsys® HE4	Elecsys® HE4 CalSet	PreciControl HE4

All manufactured by Roche Diagnostics GmbH (Roche Diagnostics GmbH, 2013, 2017, 2018a, 2018b, 2019, 2020a, 2020c, 2020b)

Table 8: Tumor marker additional reagents

Reagent	Purpose
Universal Diluent	Sample dilution (optional)
Diluent NSE	Sample dilution NSE (optional)
Diluent MultiAssay	Sample dilution (optional)
ProCell	Cleaning
CleanCell	Cleaning
CleanSys	Cleaning

All manufactured by: Roche Diagnostics GmbH

Table 9: Tumor markers consumables

Consumables	Purpose
AssayCups	Reagent tubes
AssayTips	Pipetting
Hitachi-Standard-Cup	Manual sample dilution

All manufactured by: Roche Diagnostics GmbH

4.3 PD-markers ELISA

4.3.1 ELISA method

The applied method is the sandwich-ELISA technology. In this method, two specific antibodies against different human epitopes are used to identify the antigen. Available information about the origin and antibody type is listed in Table 10.The assay procedure described applies to all three assays. It is also visualized Figure 4.

Table 10: Specification of PD-1, PD-L1 and PD-L2 antibodies

Name	Origin/ production cell line
Capture antibody PD-1	Goat
Detection antibody PD-1	Goat
Standard PD-1	Recombinant human protein
Capture antibody PD-L1	Mouse
Detection antibody PD-L1	Goat
Standard PD-L1	Recombinant human protein
Capture antibody PD-1	Mouse
Detection antibody PD-1	Mouse
Standard PD-1	Recombinant human protein

DuoSet manuals for PD-1, PD-L1 and PD-L2 (R&D Systems, 2018; R&D Systems Inc., 2016a, 2016b)

The assays are performed on bare (=uncoated) plates with a carbon surface. The carbon surface fulfills two purposes as it on the one hand binds biological material with high affinity and on the other hand serves as the electrode during the detection process. In the first step all wells are mixed with phosphate buffered saline (PBS) for 5 minutes at 700 rpm. This step is included to moisten the dry well bottom. It will allow for the capture antibody dilution to spread alongside the whole well bottom. After discarding the PBS 25 µl of the capture antibody dilution is added to each well. Following five minutes of shaking at 700 rpm the plate is placed in the fridge (2-8 °C) for an overnight incubation. After this step the plate is washed. This is done three times with a volume of 200 µl of wash buffer per well. Next, 150 µl of blocking reagent is added to satiate the unbound capacity of the carbon surface. This step is important to avoid sample components to bind to the plate and thereby probably cause disturbing detections signals. After one hour incubation step at 500 rpm the washing step is repeated. Subsequently, 25 µl of standards, controls and samples are added to the plate and incubated for two hours at 500 rpm. After another washing step, 25 µl of detection antibody solution is applied and again incubated for two hours at 500 rpm. Followed by another washing step, 25 µl of SULFO-TAG streptavidin dilution is pipetted to each well. This introduced one part of the needed detection reagents, which is bound to the biotin-coupled detection antibody via its streptavidin component. The assay procedure is concluded by another washing step and the introduction of 150 µl MSD GOLD Read Buffer per well. Within the next 15 minutes the plate is measured on the MESO QuickPlex SQ 120 reader. The instrument applies voltage to the plate to start the light emission, which is captured by a high sensitive camera. As the electricity destroys the plate bottom, every plate can be only detected once. The described process is visualized in Figure 6. All assays were performed according to a self-developed assay protocol (Figure 5).

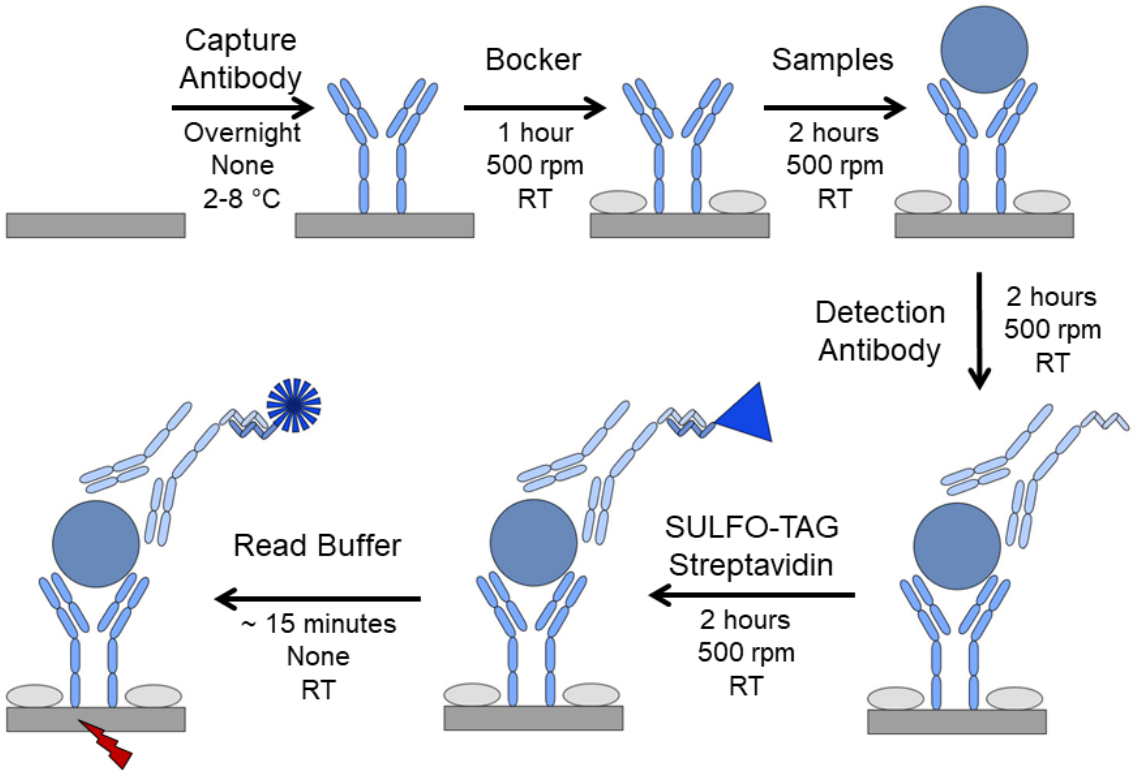

Figure 4: ELISA processing scheme

Starting with an overnight incubation with the capture antibody which is followed by a blocking step, the sample incubation step, the detection antibody the assay procedure terminates introducing the detection agent (SULFO-TAG). Finally the read buffer is added, voltage is applied to the plate by the MESO QuickPlex SQ120 and emitted light is detected.

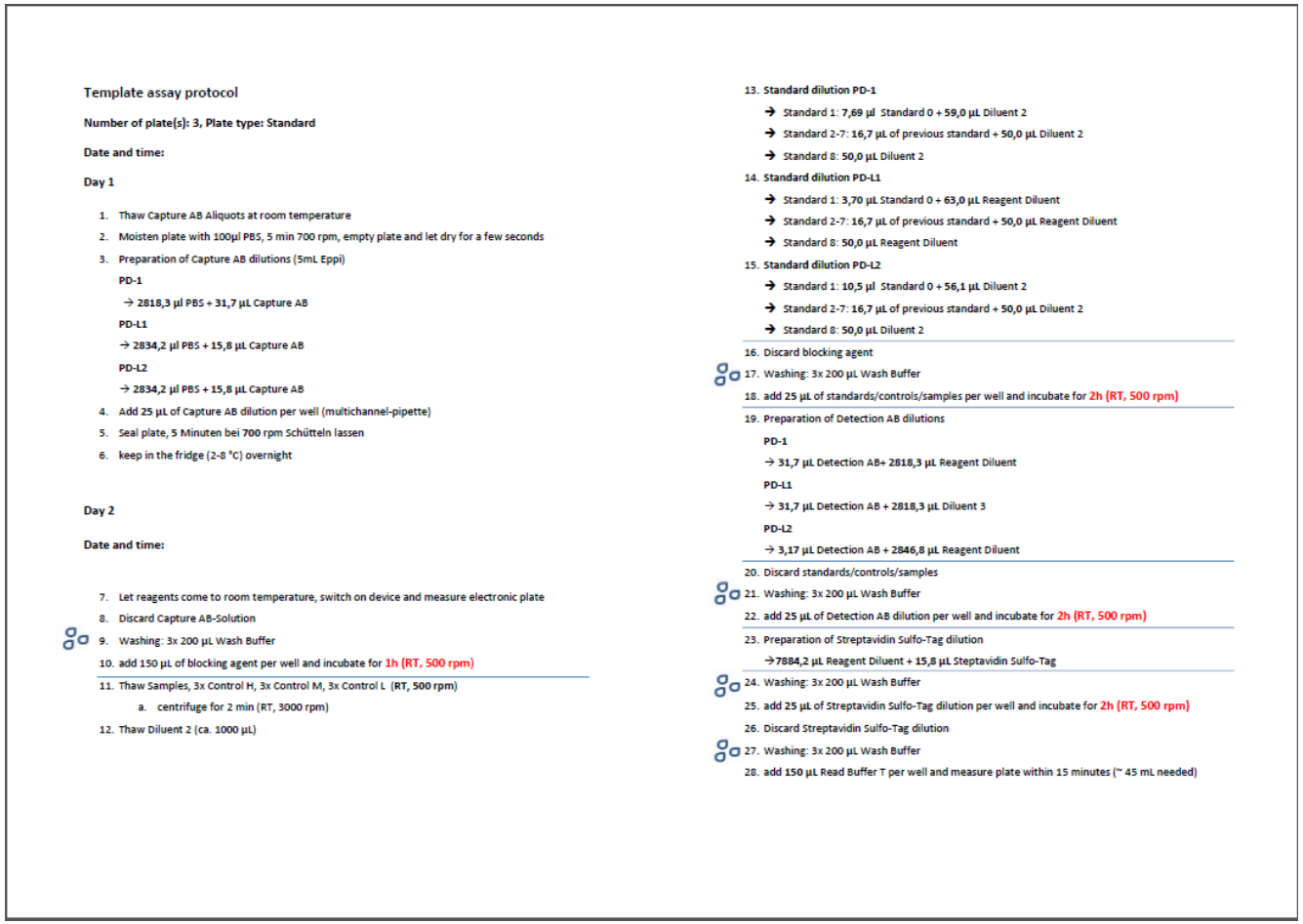

Template assay protocol

Number of plate(s): 3, Plate type: Standard

Date and time:

Day 1

1. Thaw Capture AB Aliquots at room temperature
2. Moisten plate with 100µl PBS, 5 min 700 rpm, empty plate and let dry for a few seconds
3. Preparation of Capture AB dilutions (5mL Eppi)
   PD-1
   → **2818,3 µl PBS + 31,7 µL Capture AB**
   PD-L1
   → **2834,2 µl PBS + 15,8 µL Capture AB**
   PD-L2
   → **2834,2 µl PBS + 15,8 µL Capture AB**
4. Add **25 µL** of Capture AB dilution per well (multichannel-pipette)
5. Seal plate, **5** Minuten bei **700** rpm Schütteln lassen
6. keep in the fridge (2-8 °C) overnight

Day 2

Date and time:

7. Let reagents come to room temperature, switch on device and measure electronic plate
8. Discard Capture AB-Solution
9. Washing: 3x 200 µL Wash Buffer
10. add 150 µL of blocking agent per well and incubate for 1h (RT, 500 rpm)
11. Thaw Samples, 3x Control H, 3x Control M, 3x Control L **(RT, 500 rpm)**
    a. centrifuge for 2 min (RT, 3000 rpm)
12. Thaw Diluent 2 (ca. 1000 µL)
13. **Standard dilution PD-1**
    → Standard 1: **7,69 µl** Standard 0 + **59,0 µL** Diluent 2
    → Standard 2-7: **16,7 µL** of previous standard + **50,0 µL** Diluent 2
    → Standard 8: **50,0 µL** Diluent 2
14. **Standard dilution PD-L1**
    → Standard 1: **3,70 µL** Standard 0 + **63,0 µL** Reagent Diluent
    → Standard 2-7: **16,7 µL** of previous standard + **50,0 µL** Reagent Diluent
    → Standard 8: **50,0 µL** Reagent Diluent
15. **Standard dilution PD-L2**
    → Standard 1: **10,5 µl** Standard 0 + **56,1 µL** Diluent 2
    → Standard 2-7: **16,7 µL** of previous standard + **50,0 µL** Diluent 2
    → Standard 8: **50,0 µL** Diluent 2
16. Discard blocking agent
17. Washing: 3x 200 µL Wash Buffer
18. add **25 µL** of standards/controls/samples per well and incubate for 2h (RT, 500 rpm)
19. Preparation of Detection AB dilutions
    PD-1
    → **31,7 µL** Detection AB+ **2818,3 µL** Reagent Diluent
    PD-L1
    → **31,7 µL** Detection AB + **2818,3 µL** Diluent 3
    PD-L2
    → **3,17 µL** Detection AB + **2846,8 µL** Reagent Diluent
20. Discard standards/controls/samples
21. Washing: 3x 200 µL Wash Buffer
22. add **25 µL** of Detection AB dilution per well and incubate for 2h (RT, 500 rpm)
23. Preparation of Streptavidin Sulfo-Tag dilution
    →**7884,2 µL** Reagent Diluent + **15,8 µL** Steptavidin Sulfo-Tag
24. Washing: 3x 200 µL Wash Buffer
25. add **25 µL** of Streptavidin Sulfo-Tag dilution per well and incubate for 2h (RT, 500 rpm)
26. Discard Streptavidin Sulfo-Tag dilution
27. Washing: 3x 200 µL Wash Buffer
28. add **150 µL** Read Buffer T per well and measure plate within 15 minutes (~ 45 mL needed)

Figure 5: Template assay protocol PD-1, PD-L1 and PD-L2 DHM assays

The developed assays use electrochemilumincescence (ECL) as the detection method. In this technology, voltage is used to create highly reactive substances whose interaction then emits light. This emission is detected by a highly sensitive camera. The principle of ECL is depicted in Figure 6.

The bottom of each ELISA-plate consists of carbon which serves as an electrode in the detection process. In the instrument voltage is applied to the plate. This leads to the development of two reactive substances. One is a ruthenium-complex as part of the SULFO-TAG, bound to the detection antibody via biotin-streptavidin-coupling. The second, tripropylamine (TPA), is part of the MSD GOLD Read Buffer. The interplay of the ruthenium-complex and the TPA emits light that is detected by a camera in the instrument. The amount of light emitted correlates with the amount of the ruthenium-complex, and in consequence with the concentration of the antigen.

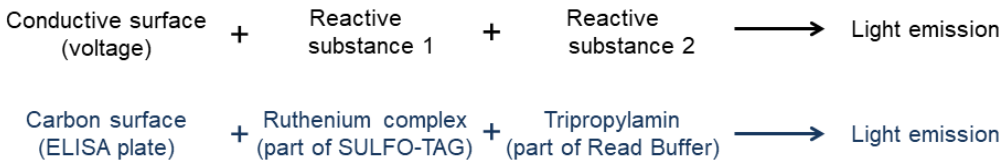

Figure 6: Detection based on electrochemiluminescence

The upper part of the figure describes the necessary compounds for an electrochemiluminescence detection system. The lower part describes which components fulfill the corresponding part in the system supplied by MSD.

ELC convinces with several advantages over conventional ELISA-detection technology. It provides a highly sensitive detection method due to signal amplification. Nevertheless the background signals are very low. The detection technology is compatible with a variety of sample matrices, namely serum, plasma and cell culture supernatant. Its broad dynamic range over several magnitudes enables the measurement of differently concentrated samples without pre-dilution on one plate (Meso Scale Discovery, 2020).

Data procession and analysis was performed with the supplied DISCOVERY WORKBENCH 4.0.12 (LSR_4_0_12) (Meso Scale Discovery, LLC., Rockville, USA). Analyses are performed using Microsoft Office Home and Student 2010, Microsoft excel version 14.0.7249.5000 (Microsoft Corporation, Redmond, USA).

4.3.2 ELISA validation

The three ELISAs to quantify soluble PD-1, PD-L1 and PD-L2 were based on antibody pairs and recombinant protein standards. Chessboard titrations experiments were performed to identify capture and detection antibody concentrations exhibiting the highest signals. Additionally, different diluents were explored to optimize assay performance. Following methodical validation comprised imprecision, limit of quantification, dilution linearity and selectivity testing. A standard curve was prepared as a serial dilution of the corresponding recombinant protein. This calibration was used for quantification purposes (Krueger et al., 2020).

Knowledge about preanalytcial influence factors on sample quality is a key factor to receive high quality data in the end. Centrifugation speed, duration before sample processing and storage temperature were varied. Investigations included time intervals and storage temperatures before blood centrifugation (3h/ 6h/ 24h/ 48h/ 168h at 4°C/ 25°C/ 37°C) and after blood centrifugation (3h/ 6h /24h at 4°C/ 25°C). Additionally, the effect of the freezing process and repeated freeze- thaw cycles were investigated (Krueger et al., 2020).

4.3.3 ELISA quality control

Quality control represents an important aspect to verify and monitor assay quality. Therefore serum control pools were produced for each assay. A number of samples were measured and split into a high, a medium and a low group according to obtained concentrations. The samples from each group were pooled, mixed thoroughly and aliquoted. In this way three controls were created for each assay separately. The control aliquots are measured in duplicate on each performed plate. Thereby the plate performance of several plates can be compared directly and if necessary adjusted or decided to be re-measured.

4.3.4 ELISA materials

Different materials, supplies instruments were needed to perform all experiments. These were structured into tables which separate the topics chemicals (Table 11), solutions (Table 12), consumables (Table 13), instruments (Table 14), and centrifugation programs (Table 15).

Table 11: Applied chemicals and their corresponding suppliers

Chemical agent	**Supplier**
Albumine Fraktion V	Carl Roth GmbH+Co.KG, Karlsruhe, Germany
ROTI®-CELL 10x PBS	Carl Roth GmbH+Co.KG, Karlsruhe, Germany
TWEEN®20	Merck KGaA, Darmstadt, Germany
Diluent 2/ 3	Meso Scale Discovery, LLC., Rockville, USA
SULFO-TAG Streptavidin	Meso Scale Discovery, LLC., Rockville, USA
MSD GOLD Read Buffer	Meso Scale Discovery, LLC., Rockville, USA
Human PD-1 DuoSet® ELISA	R&D Systems, Inc., Minneapolis, USA
Human PD-L1 DuoSet® ELISA	R&D Systems, Inc., Minneapolis, USA
Human PD-L2/B7-DC DuoSet® ELISA	R&D Systems, Inc., Minneapolis, USA

PBS: Phosphate buffered saline

Table 12: Solutions and their composition

Name	**Component**
Blocking reagent	PBS + 5% BSA
Reagent diluent	PBS + 1%BSA
Wash Buffer	PBS + 0,05% TWEEN®20

PBS: Phosphate buffered saline, BSA: Bovine serum albumin.

Table 13: Consumables and their corresponding suppliers

Consumables	Supplier
Sample tubes	
0.5/ 1.5/ 2.0 ml	BRAND GMBH+CO KG, Wertheim, Germany
5.0 ml	Carl Roth GmbH+Co.KG, Karlsruhe, Germany
Falcon™ tubes	
15/50 ml	Fisher Scientific GmbH, Schwerte, Germany
Cyro® tubes	
0.5/1.8 ml	Thermo Fisher Scientific Inc., Waltham, USA
Sample tips	
0.5-10 ml	BRAND GMBH+CO KG, Wertheim, Germany
100-1000/ 10-100 µl/ 0.5-10 µl	BRAND GMBH+CO KG, Wertheim, Germany
50-1250 µl	Eppendorf AG, Hamburg, Germany
Seal foils	Carl Roth GmbH+Co.KG, Karlsruhe, Germany
Plates	
QUICKPLEX®96-Well Standard	Meso Scale Discovery, LLC., Rockville, USA
QUICKPLEX®96-Well High Bind	Meso Scale Discovery, LLC., Rockville, USA
Blood sampling tubes	SARSTEDT AG&Co.KG, Nümbrecht, Germany
Serum: S-Monovette® 5.5ml Z	
Heparin: S-Monovette® 5.5ml LH	
EDTA: S-Monovette® 9ml K3E	
Citrate: S-Monovette® 5ml 9NC	

Table 14: Instruments and their corresponding suppliers

Instrument	Supplier
Stirring plate	Heidolph Instruments GmbH & CO. KG, Schwabach, Germany
Scales	Ohaus corporation, Parsippany, USA
Centrifuges	
Rotina 380	Andreas Hettich GmbH & CO.KG, Tuttlingen, Germany
5415D	Eppendorf AG, Hamburg, Germany
Shaker	
Unimax 1010	Heidolph Instruments GmbH & CO. KG, Schwabach, Germany
Bioshake IQ	Quantifoil Instruments GmbH, Jena, Germany
ThermoMixer C	Eppendorf AG, Hamburg, Germany
Tube shaker	IKA®-Werke GmbH & CO. KG, Staufen, Germany
Pipettes	
0.5-10ml	BRAND GMBH+CO KG, Wertheim, Germany
100-1000 /10-100/ 0.5-10 µl	BRAND GMBH+CO KG, Wertheim, Germany
Multichannel-pipettes	
5-100/ 50-1250 µl	Eppendorf AG, Hamburg, Germany

Continuation of Table 14

Instrument	Supplier
Timer	Bresser GmbH, Rhede, Germany
Incubator	
memmert Type U26	Memmert GmbH + Co.KG
Storage	
Refridgerator	Skyport GmbH, Amberg, Germany
Freezer (-20°C)	Liebherr-Hausgeräte GmbH, Ochsenhausen, Germany
Freezer (-80°C)	Thermo Fisher Scientific Inc., Waltham, USA
Analyzers	
MESO QuickPlex SQ120	Meso Scale Discovery, LLC., Rockville, USA

Table 15: Specification of centrifugation programs

Program	Specimen	Speed/ Time/ Temperature
Normal	Full blood	3000/ 10/ rt
½x velocity	Full blood	1500/ 10/ rt
2x velocity	Full blood	6000/ 10/ rt
Sample preparation (ELISA)	Serum, Heparin-/EDTA-/Citrate-plasma	3000/ 2/ rt

Speed in g (=rcf), time in min, temperature in °C; rt: room temperature.

4.4 Statistic tools clinical evaluation

Comprehensive data analysis was performed independently from sample collection and analysis with support by the QuoData Statistics GmbH. The results of the tumor marker evaluation are part of a publication that is currently prepared (Holdenrieder et al., 2020). Mean, median, standard deviation and coefficient of variation (CV) are basic statistic tools to analyze the data. Describing boxplots, also the fifth and the 95th quartile are listed. Line, dot, bar and pie charts were constructed with excel. Boxplots and scatter plots were drawn in R and RStudio version 3.4.0 (2017-04-21). The Wilcox- , Mann-Whitney-U-Test and Spearman correlations were also calculated in R.

Results were drawn as receiver operating characteristic (ROC) curves and analyzed on the corresponding area under the curve (AUC). The AUC was classified as not discriminating (<0.6), poor (0.6-0.7), acceptable (0.7-0.8), excellent (0.8-0.9) and outstanding (>0.9). Following single marker assessments covariates were added in order to try to improve prognosis and prediction. Last, multi-marker analysis was performed including all tumor marker data.

Kaplan-Meier curves were applied to visualize progression free survival (PFS) and overall survival (OS) in the whole NSCLC cohort. In order to investigate prognostic value of the pre-therapeutic tumor marker concentrations, they were split into four groups. The cohort was split into quartiles based on all measured single marker concentrations. Each patient was allocated to the corresponding group. Kaplan-Meier curves were drawn to compare the performance of the groups. Hazard ratios (HRs) were calculated to compare the lowest and the highest concentration group on the basis of a p-value of ≤0.05 and also providing a 95% confidence interval. HRs equaling 1 meant no discrimination between the two groups. HRs >1 represented an elevated risk for the investigated group to suffer from decreased median survival whereas HRs <1 conversely indicated a lower risk.

Cox proportional hazard regression analysis was performed to estimate the influence of covariates on progression free and overall survival. Accounted covariates included gender, stage, histology, study arm, study drug, ECOG-status at study entry and prior therapies. Results of analysis were reported again in form of hazard ratios.

Paired and unpaired t-Tests can be used to calculate whether means differ significantly. The applied significance level in this study is 95% (p=0.05). As prerequisites for the t-Test were not fulfilled, Mann-Whitney-U-Test and Wilcoxon test were used to compare the groups instead. In case the values come from different cohorts, the Mann-Whitney-U-Test was used. When two measurements in the same cohort were compared the Wilcox-Test was applied. Significant differences between the compared groups existed, where the calculated p-value was smaller than 0.05.

The Shapiro-Wilk test determines whether the investigated data is normally distributed. The decision is based on the applied significance level. In this approach, all data sets with p-value >0.05 were normally distributed.

To assess linear correlation between two variables, two tests Pearson or Spearman correlation are applicable. The Pearson correlation has the following prerequisites: metric scaling, no (extreme) outliers and bivariate normal distribution of the data. The obtained correlation coefficient r can range von -1 to 1. Its three possible interpretations are: r~0: no correlation, r<0: negative correlation and r>0: positive correlation. If at least one precondition is violated, the Spearman correlation can be used instead. The calculation reports two numbers, the p-value of the correlation and the correlation coefficient (rho). P-values >0.05 indicate a significant correlation. The Rho value, also effect size, is interpreted according to a classification published by Cohen in 1992. Effect size is weak between 0.10 and 0.29, medium between 0.30 and 0.49 and strong ≥0.50 (Cohen, 1992). The coefficient of determination represents the amount of variances in two variables determined by the same source. It is calculated from the squared rho and listed in [%].

5 Results

The measurement data of the tumor markers and the newly developed assays quantifying soluble PD-1, PD-L1 and PD-L2 in the NSCLC cohort were reported. Analyses were performed to assess predictive value regarding response to therapy as well as prognostic value in regard to progression free survival and overall survival. The newly developed markers PD-1, PD-L1 and PD-L2 were additionally measured in a cohort of healthy males and compared with the concentrations obtained in NSCLC patients.

5.1 Tumor markers CESAR Biomarker Substudy

The tumor markers CYFRA 21-1, CEA, SCCA, NSE, ProGRP, CA 15_3, CA 125 and HE4 and the PD-markers PD-1, PD-L1 and PD-L2 were analyzed in the NSCLC cohort.

The results of the tumor marker evaluation are part of a publication that is currently prepared (Holdenrieder et al., 2020).

Time-point 1_1, 2_1 and 3_1 were blood samples collected before the start of the respective treatment cycles' medication application. The last sample taken before study termination was related to as end of treatment (EOT). Those samples allowed a monitoring of the biology of cancer development under treatment. Two additional samples at day two after treatment application were collected in the first and the second cycle of treatment, referred to as 1_2 and 2_2. These specifically visualize the direct effect of treatment on the biomarker concentrations.

The time points 1_1 and 3_1, as well as the relative change in biomarker concentrations between both time points were chosen for intensive analysis. 1_1 represented pre-therapeutic concentrations. The largest potential for predictive and prognostic biomarkers is associated with this time point because it offers answers on cancer development and choice of therapy even before start of application. Since the meaningfulness of biomarkers is expected in course of therapy due to separation of responders and non-responders a second time point within the therapy was analyzed. In this approach the data for before the application of the third treatment cycle was chosen. CT was performed at that time point which allowed for a very precise evaluation of therapy response.

Tumor markers associated with lung cancer CYFRA 21-1, CEA, SCCA NSE and ProGRP were measured. Additionally, CA 15-3, CA 125 were investigated. Boxplots visualized the tumor marker concentration distributions on the six blood sample time points without differentiating according to the response (Figure 7).

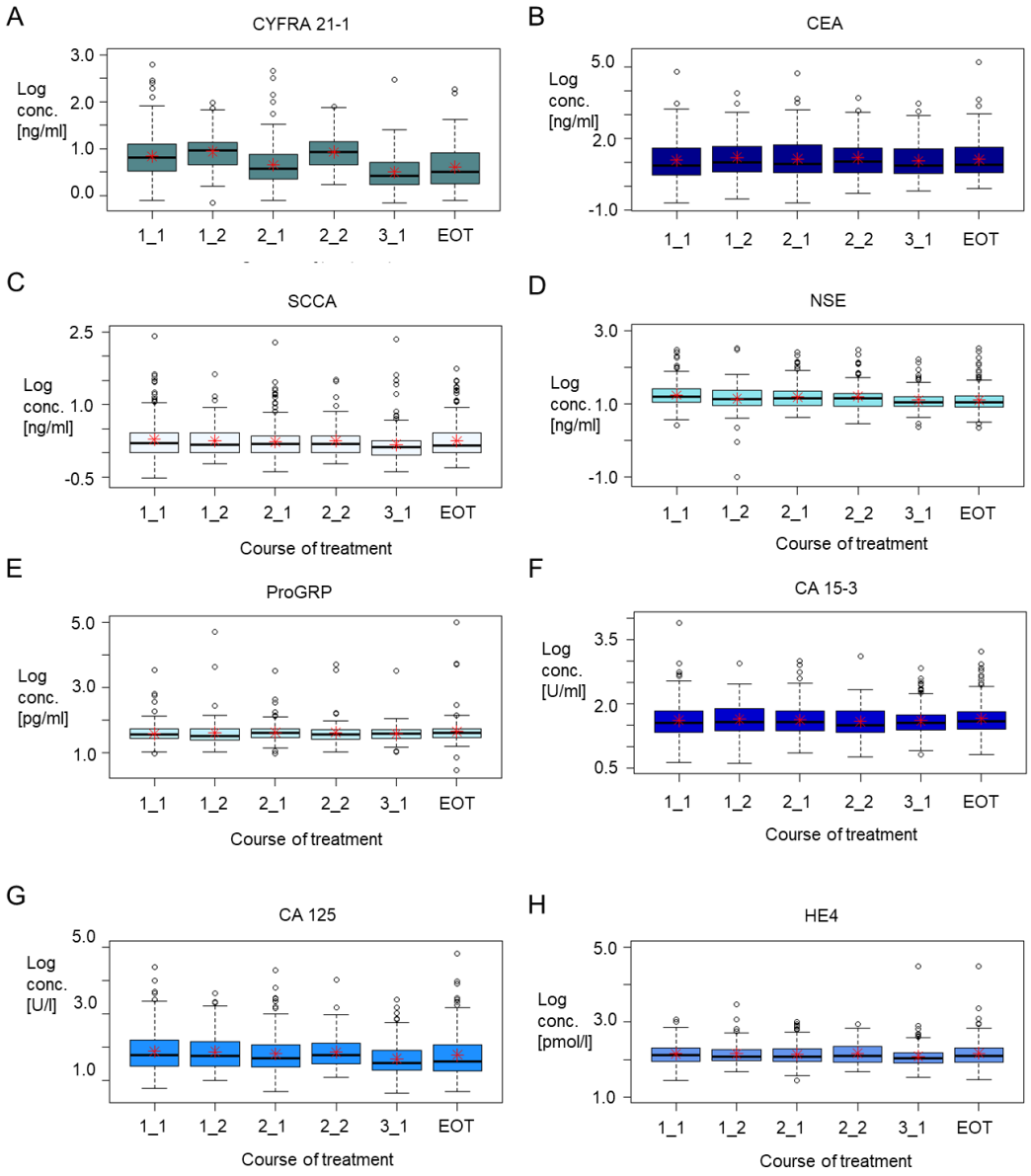

Figure 7: Tumor marker concentrations development during cancer therapy

Boxplots visualize the distribution of the concentration of the different tumor markers CYFRA 21-1 (A), CEA (B), SCCA (C), NSE (D), ProGRP (E), CA 15-3 (F), CA 125 (G) and HE4 (H) in course of therapy. Red starts indicate the calculated mean concentration.

The development of the tumor marker concentrations was evaluated with a focus on the general marker development in course of therapy. Additionally the direct effect of chemotherapy application of the markers was investigated. In this approach the time point X_1 was compared with the time point X_2.

CYFRA 21-1 concentrations varied among the whole investigation period. A slight decrease was seen during the end of treatment time point. Increasing CYFRA 21-1 concentrations were detected in response to therapy application in treatment cycle 1 and also cycle 2. Median CEA concentrations stayed stable across all six time points and no direct effect of treatment was seen. The measured SCCA concentrations resulted in narrow boxes. No variations in median concentrations were observed throughout the observation period and as reaction to therapy.

A non-significant shift towards lower median concentrations was observed in the NSE biomarker levels. No change in marker concentrations in response to therapy was reported. Stable median biomarker concentrations of ProGRP were measured throughout therapy, although strong outliers were detected at the time points 1_2, 2_2 and end of treatment. Again no concentration change in response to therapy was detected.

CA 15-3 and CA 125 also presented with stable marker levels. CA 125 concentrations were very high in a fraction of the patients and concentrations did not change in response to therapy application.. Median HE4 concentrations did not change during the treatment. HE4 concentrations stayed stable when chemotherapy was applied.

Downstream analysis was performed with regard to four questions. First the predictive value for progression of disease, categorizing stable disease and remission as responders and progressive disease as not responsive was investigated. The evaluation was based on the pre-treatment tumor marker concentrations and the relative change in concentrations from the beginning to the end of treatment cycle 2. Second, the same was approach was applied to assess good response regrouping the stable disease patients to the non-responders. The third and fourth question dealt with the idea of estimating the prognostic value for progression free survival (PFS) and overall survival (OS).

5.2 Prediction of therapy response

245 patients were eligible for the analysis of response to therapy in the pre-therapeutic concentrations. Due to missing data for a second time point, the number reduced to 230 patients for the analysis of the effect of concentration changes in course of therapy (Figure 8).

For predicting response to therapy, the patients were grouped into three parties among the observed tumor growth in imaging (CT). The differentiation was made between partial remission (PR; N=99), stable disease (SD; N=88) and progressive disease (PD; N=58). Patient numbers were a little lower in the assessment of relative changes due to a lack of a second data point in some patients. Since 34% of the patients experienced stable disease, two downstream evaluations were followed. For estimation of poor response to therapy, patients with progressive disease were classified as non-responders and SD together with PR as responders. When good response to therapy was investigated, only PR was classified as response and SD and PD were combined in the non-responder group.

The comparison of the response groups was performed in pre-therapeutic concentration first. In a second approach, the relative change in biomarker concentrations between the beginning of therapy and the end of treatment cycle 2 (3_1) was compared.

In the first approach the absolute concentrations in both groups were depicted as histograms. The peak as well as the overlapping area gave a first idea whether the marker concentration in the two response groups differ. For further assessment, receiver operating characteristic (ROC) curves were drawn. The respective area under the curve (AUC) calculated the predictive potential of the corresponding biomarker.

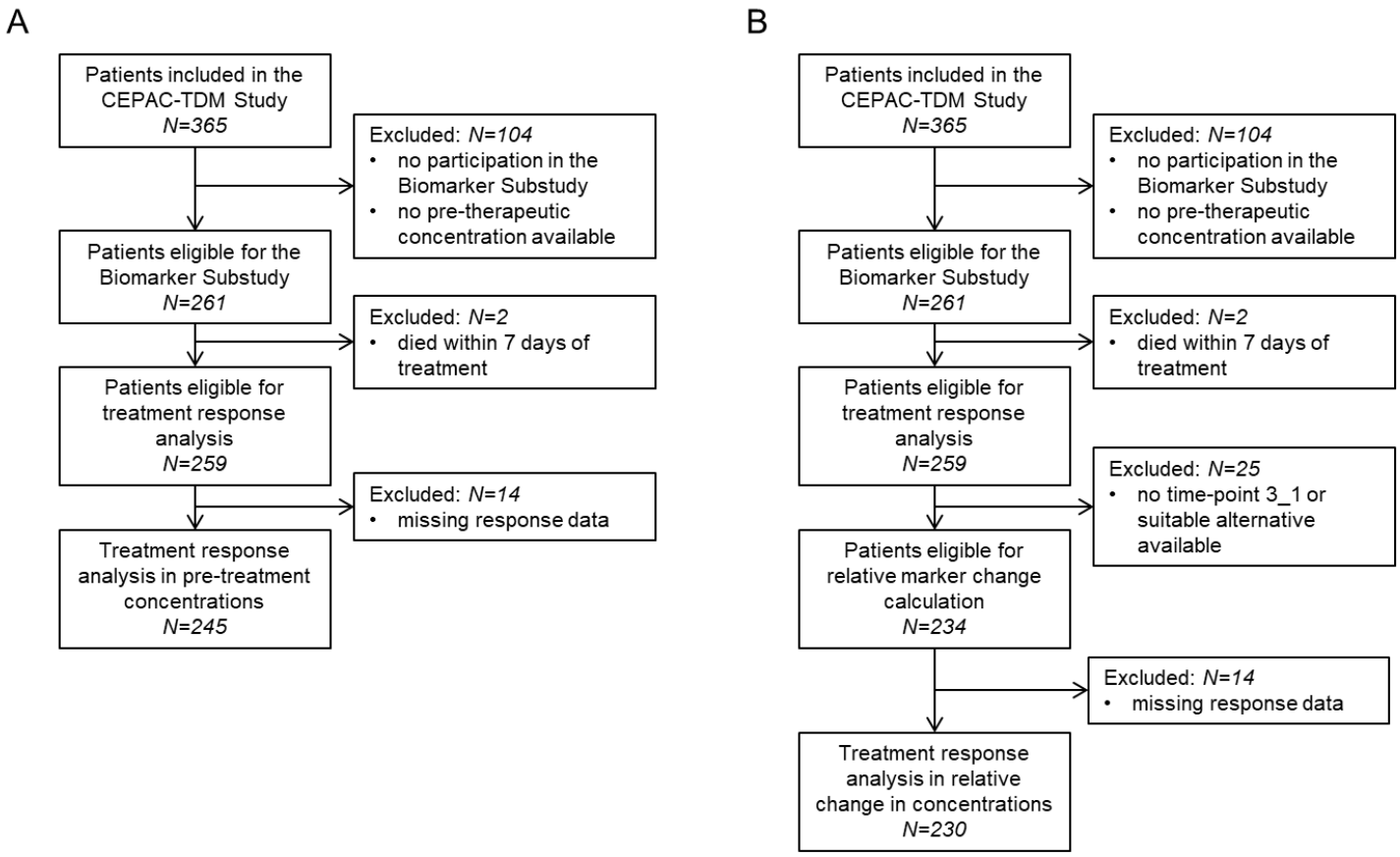

Figure 8: Decision tree outlining included samples in the analysis for prediction of response

The depicted decision trees illustrate the sample inclusion process for the analysis of the prediction potential of poor and good response to therapy. The decision tree for pre-therapeutic study samples was shown on the left (A) and the one for the relative concentration change between C1 and C3 on the right (B).

5.2.1 Prediction of poor response to therapy

Patients were grouped according to CT results into responders (SD/PR; N=187) and non-responders (PD; N=58). The concentrations were depicted in a histogram to compare the distribution in both response groups.

Pre-therapeutic concentrations

Pre-therapeutic concentrations were depicted in histograms (Figure 9). The curves drawn for CYFRA 21-1 showed a considerable overlap. The non-responders curve showed a plateau, whereas the responders curve showed a clear peak. The density evaluation showed a maximum at higher concentrations for responders compared to non-responders. Both curves for CEA present with a large overlap covering the whole concentration range. The maximum density of concentrations is very slightly shifted to lower concentrations for responders. The responders' curve in the biomarker SCCA formed a considerable peak around a concentration of 1 ng/ml. The peak of the non-responder curve was detected at the same concentration. But the whole concentration range distribution was broader resulting in a notably lower density at 1 ng/ml for non-responders.

No differentiation between the two curves was possible when analyzing NSE concentration distribution and density. The results obtained in ProGRP almost resemble those of NSE. Contrary in this biomarker a slight shift of the maximum density of responders to higher concentrations was observed.

Concentrations obtained for CA 15-3 showed large overlapping fractions with a minimal shift of the maximum density in responders towards lower concentrations. The concentrations for responders form one defined peak for the tumor marker CA 125. The concentrations for non-responders instead spread widely across the concentration range, though the highest density of concentrations was comparable with the one in the responder group. The curves constructed for responders and non-responders for HE4 formed normal peaks. A minimal shift of the peak for responders towards lower concentrations was visible.

Receiver operating characteristic (ROC) curves were drawn to further analyze predictive value of pre-therapeutic concentrations on poor response to therapy. Calculated AUCs were 0.573 (CYFRA 21-1), 0.517 (CEA), 0.536 (SCCA), 0.521 (NSE), 0.563 (ProGRP), 0.570 (CA 15-3), 0.587 (CA 125) and 0.563 (HE4). The AUCs were smaller than 0.6 for all eight investigated markers. Pre-therapeutic single marker concentrations were not predictive for poor therapy response. The combination of pre-therapeutic concentration of different tumor markers was not able to improve overall predictive value (Figure 10).

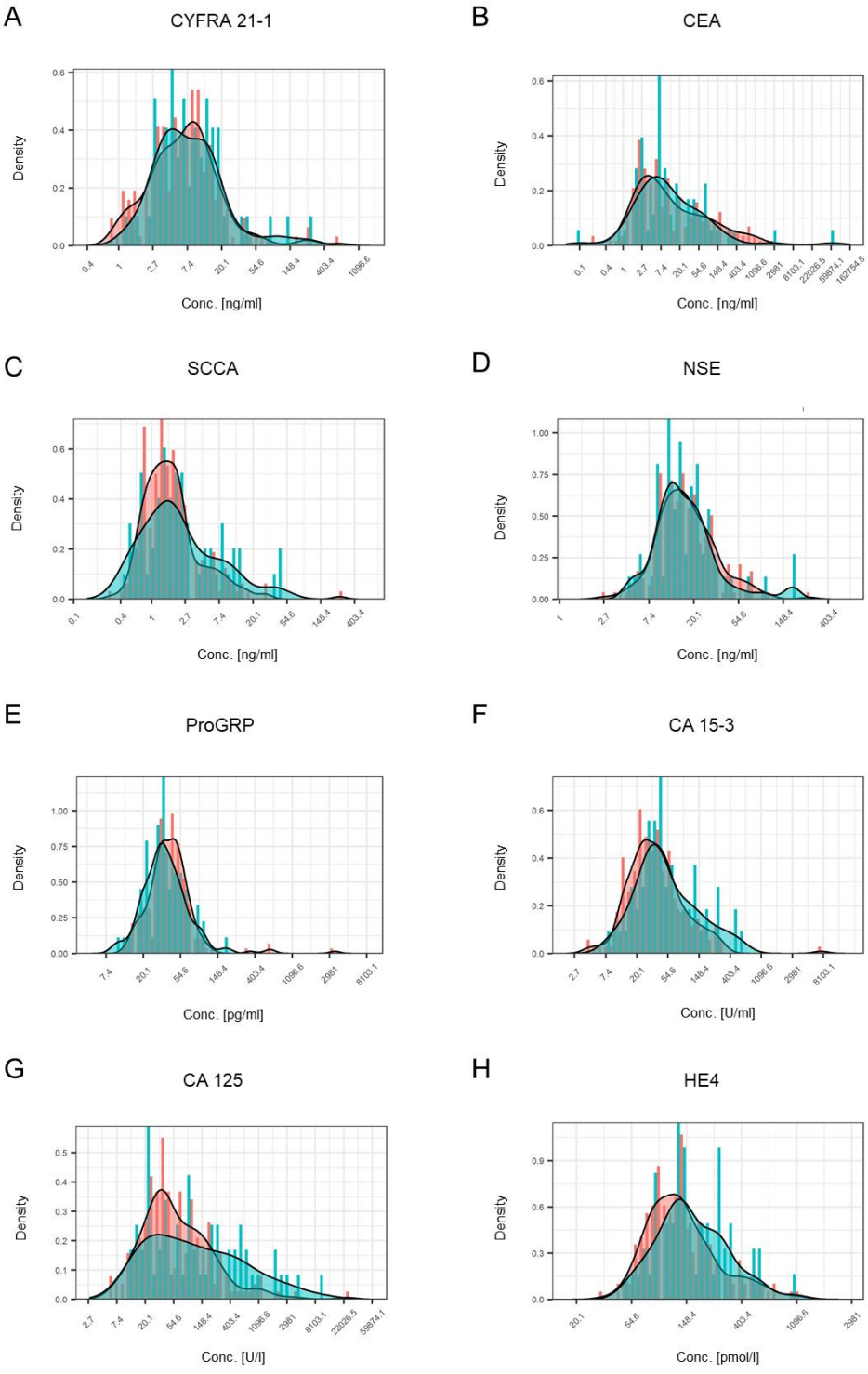

Figure 9: Comparison of the pre-therapeutic concentrations in the response groups based on poor response to therapy

Histograms illustrate the distribution of the single tumor markers based on the measured pre-therapeutic concentrations for CYFRA 21-1 (A), CEA (B), SCCA (C), NSE (D), ProGRP (E), CA 15-3 (F), CA 125 (G) and HE4 (H) separated into response groups. Non-responders (PD) are shown in turquoise and responders (SD/PR) in orange.

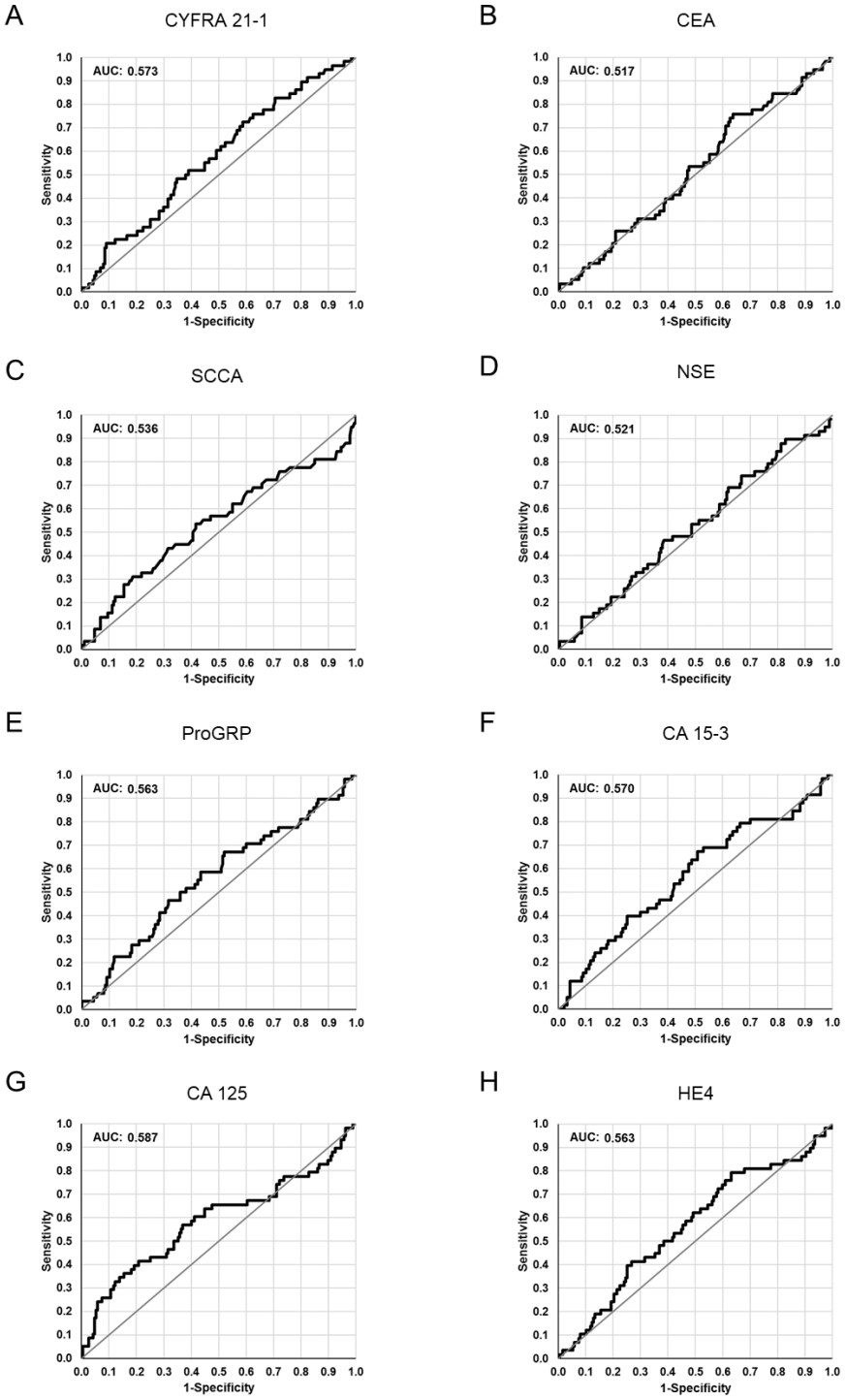

Figure 10: Predictive value of pre-therapeutic marker levels on therapy response

ROC curves illustrate the predictive value of the single tumor markers based on the measured pre-therapeutic concentrations for CYFRA 21-1 (A), CEA (B), SCCA (C), NSE (D), ProGRP (E), CA 15-3 (F), CA 125 (G) and HE4 (H). Corresponding AUCs were calculated and displayed on the upper right of the graph for each marker. AUCs lower than 0.6 represent poor prognostic performance regarding prediction of response to therapy.

Relative concentration changes between Cycle 1 and Cycle 3

In the next step the predictive value of relative concentrations between the beginning of therapy and the end of treatment cycle 2 were investigated. The end of treatment cycle 2 equaled the beginning of treatment cycle 3 before application of therapy which was represented by the blood sample 3_1 (Figure 11).

The curve for responders in CYFRA 21-1 showed a peak in the negative range of the scale. This translated into a decrease in concentrations for the majority of responders. The peak for the non-responder distribution curve was located around zero and presented a shoulder towards increases relative changes. Non-responders consequently tend to experience stable or even increasing CYFRA 21-1 concentrations. CEA concentrations for both response groups peaked at zero equaling no change in biomarker concentrations. Regardless the density for responders was considerably higher since the non-responder curve additionally showed a tiny plateau in the positive scale ranges. Meaning some non-responders experienced an increase in CEA concentration. The peaks for SCCA showed an overlap at concentrations slightly below zero. Again, the density for responders was much higher since the non-responder peak formed a shoulder because some patients of the non-responder group exhibited increased concentrations during treatment.

Both curves for responders and non-responders formed defined peaks depicting the relative change in NSE concentrations. Whereas the peak for the non-responders was located at zero meaning no observed marker changes in response to treatment, the peak for responders was shifted towards decreasing biomarker concentrations. In ProGRP both response groups showed no change in biomarker concentration indicated by sharp overlapping peaks at the zero value. Interestingly the responder analysis exhibited an additional peak at a relative change of -1 with considerable density. A subgroup of the patients experienced a decrease in ProGRP concentrations in response to treatment. Separating the stable disease from the partial remission patients in later evaluation might lead to further insights.

CA 15-3 curves looked alike throughout the whole depicted course. A peak at zero meant no change in concentrations in the marker in the majority of patients. Both response groups showed an additional peak at decreasing concentrations. Due to the resemblance of both curves no differentiation potential was expected. The picture observed for CA 125 is different. The responders curve formed a sharp peak at zero with the majority of patients experiencing a decrease to stable marker concentrations in course of chemotherapy. The curve characterizing the non-responders was comparably flatter. Although the maximum density was also seen at zero, a considerable part of the patients experienced increasing marker concentrations. Responder and non-responder curve in HE4 showed a large overlap with a joined peak at a stable biomarker concentration during therapy course. A subgroup of the responders showed decreasing concentrations towards the end of treatment cycle 2. Alike ProGRP, further investigations on good response to therapy might offer explanations for the observed phenomenon.

ROC curves were also drawn to investigate predictive value of a relative change in tumor marker concentrations between beginning and end of treatment cycle 2 on response to therapy. Corresponding AUCs were 0.747 (CYFRA 21-1), 0.638 (CEA), 0.668 (SCCA), 0.691 (NSE), 0.518 (ProGRP), 0.583 (CA 15-3), 0.702 (CA 125) and 0.634 (HE4). The relative change measured in ProGRP concentrations was not discriminative between responders and non-responders. AUCs for CEA, SCCA, CA 15-3 and HE4 only show poor predictive value. Nevertheless the predictive value for CYFRA 21-1, NSE and CA125 proved to be acceptable. Multi-marker approaches could not increase the predictive value significantly (Figure 12).

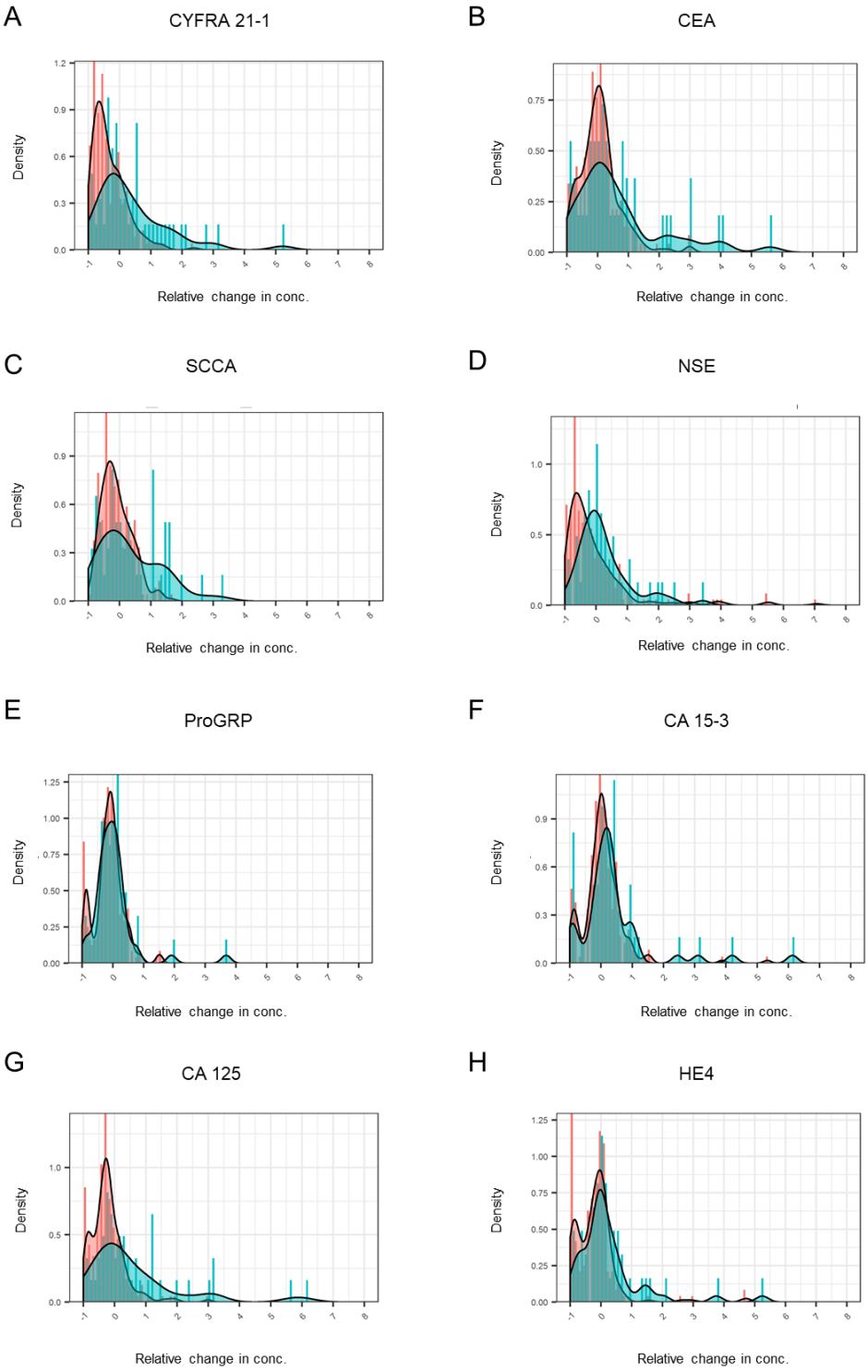

Figure 11: Comparison of the relative change in concentrations in the response groups based on poor response to therapy

Histograms illustrate the distribution of the single tumor markers based on the measured pre-therapeutic concentrations for CYFRA 21-1 (A), CEA (B), SCCA (C), NSE (D), ProGRP (E), CA 15-3 (F), CA 125 (G) and HE4 (H) separated into response groups. Non-responders (PD) are shown in turquoise and responders (SD/PR) in orange.

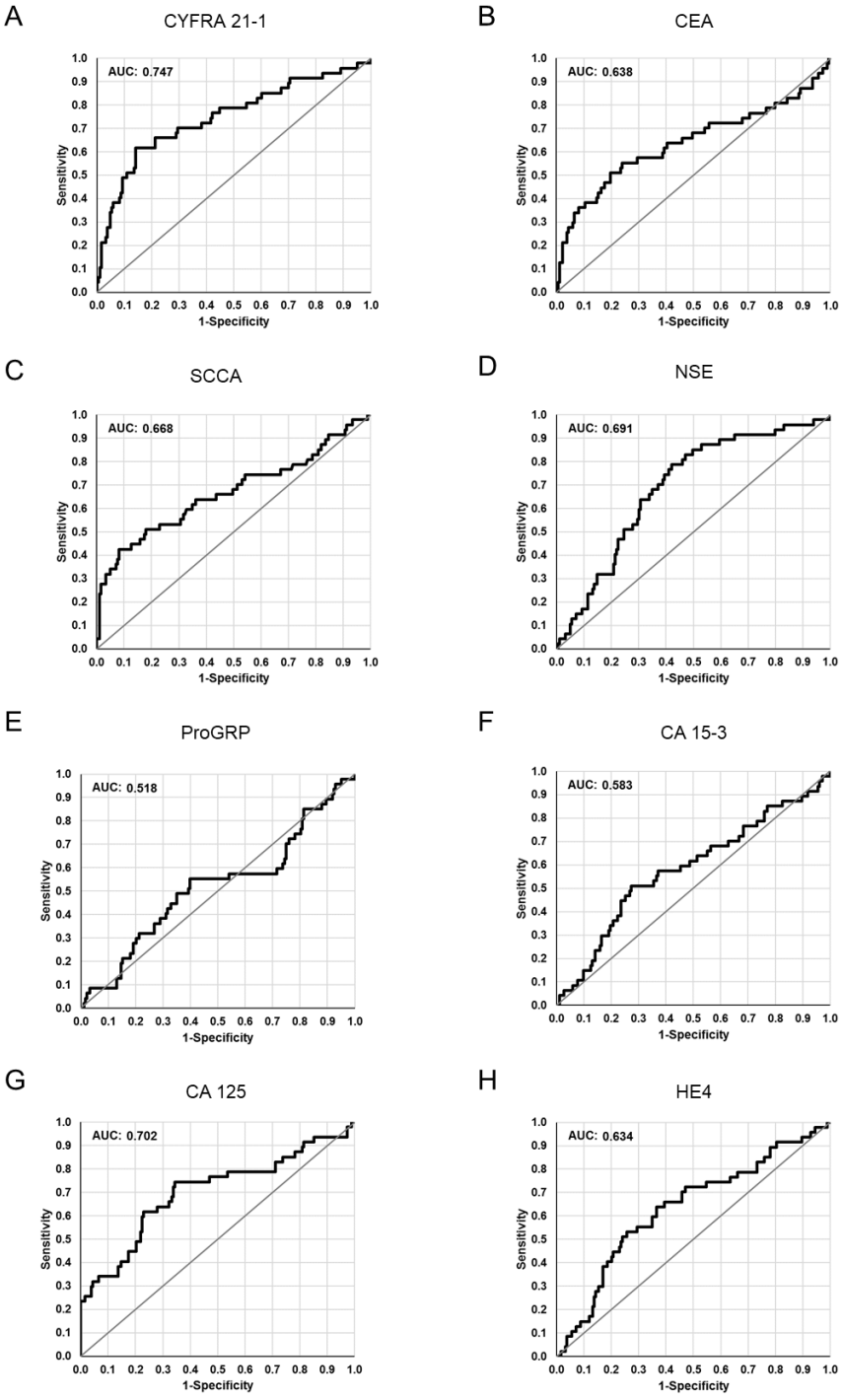

Figure 12: Predictive value of relative change in marker levels between cycle 1 and end of cycle 2 on therapy response

ROC curves illustrate the predictive value of the single tumor markers based on the measured relative change in concentration from beginning of therapy until the end of treatment cycle 2 for CYFRA 21-1 (A), CEA (B), SCCA (C), NSE (D), ProGRP (E), CA 15-3 (F), CA 125 (G) and HE4 (H). Corresponding AUCs were calculated and displayed on the upper right of the graph for each marker. AUCs lower than 0.6 represent poor prognostic performance regarding prediction of response to therapy.

5.2.2 Prediction of good response to therapy

Patients were grouped according to CT results into responders (PR; N=99) and non-responders (SD/PD; N=146). The concentrations were depicted in a histogram to compare the distribution in both response groups (Figure 13).

Pre-therapeutic concentrations

The curves of the responders and non-responders showed a large overlap in the tumor marker CYFRA 21-1. The peak of the non-responder group was slightly but clearly not significantly shifted towards lower pre-treatment concentrations. CEA curves covered each other very well which meant no difference between the two groups was shown. The same observation was made for SCCA concentrations.

Alike the other markers no differentiation between responders and non-responders was seen in absolute pre-therapeutic concentrations for the biomarkers NSE and ProGRP.

Histograms depicting the concentrations of CA 15-3 showed no differentiation between the two response groups. Both curves for CA 125 peaked at a concentration around 30 ng/ml. The density for the responder curve was considerably higher as the non-responder curve exhibited a generally flatter course. The higher concentrations were more likely to belong to a patient in the non-responder group. HE4 investigations revealed peaks that showed a comparable shape. The responder peak was slightly shifted towards lower pre-therapeutic concentrations.

The good response to therapy was investigated using ROC curves. Assessing pre-therapy tumor marker concentrations the following AUCs were reported for the single marker analyses: 0.558 (CYFRA 21-1), 0.569 (CEA), 0.552 (SCCA), 0.511 (NSE), 0.558 (ProGRP), 0.581 (CA 15-3), 0.588 (CA 125) and 0.612 (HE4). The prognostic value of all single markers ranges between from not discriminative to poor. The combination of different markers did not elevate the AUCs and thus not the predictive value of pre-therapeutic concentrations (Figure 14).

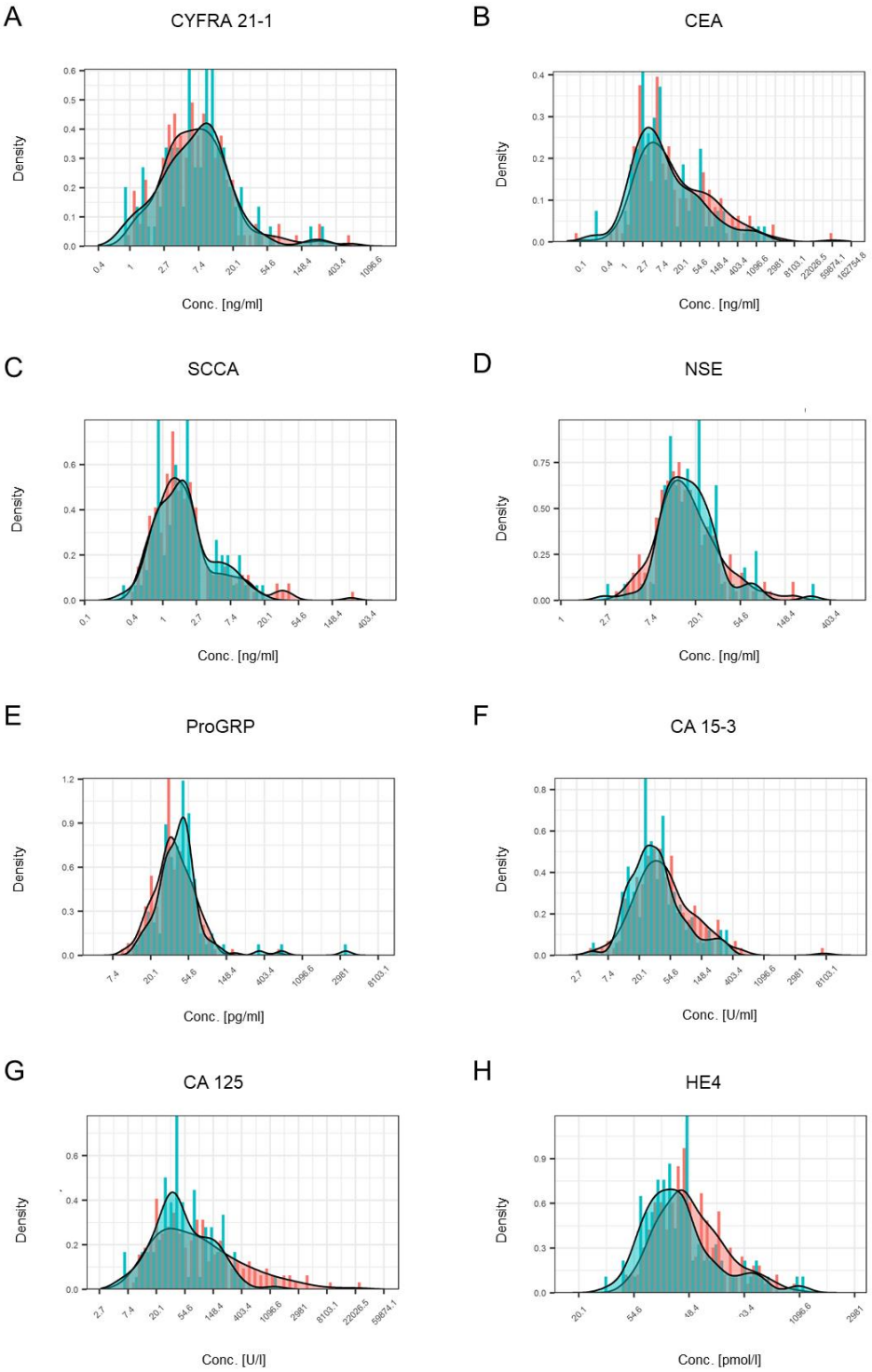

Figure 13: Comparison of the pre-therapeutic concentrations in the response groups based on good response to therapy

Histograms illustrate the distribution of the single tumor markers based on the measured pre-therapeutic concentrations for CYFRA 21-1 (A), CEA (B), SCCA (C), NSE (D), ProGRP (E), CA 15-3 (F), CA 125 (G) and HE4 (H) separated into response groups. Non-responders (PD/SD) are shown in turquoise and responders (PR) in orange.

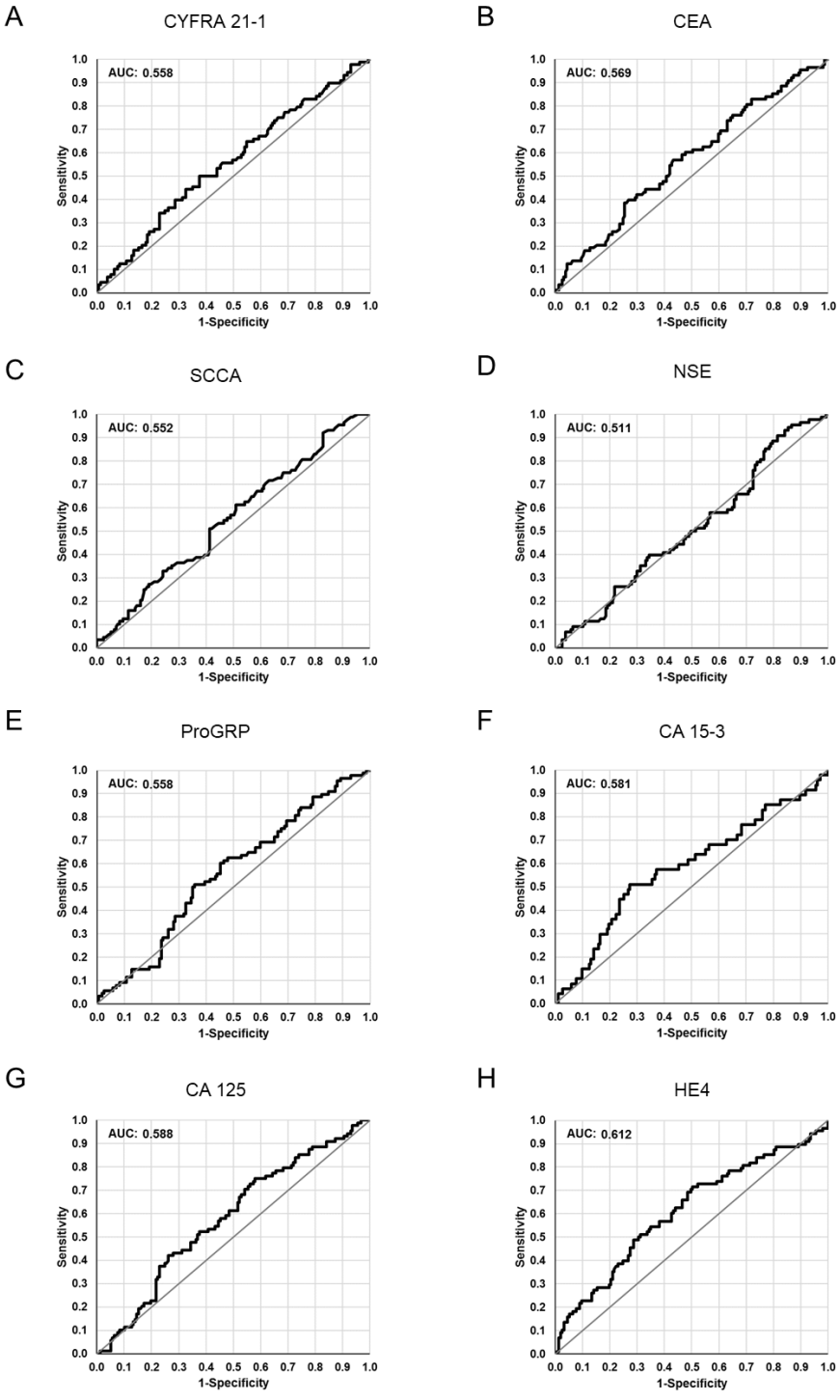

Figure 14: Predictive value of pre-therapeutic marker levels on well response to therapy

ROC curves illustrate the predictive value of the single tumor markers based on the measured pre-therapeutic concentrations for CYFRA 21-1 (A), CEA (B), SCCA (C), NSE (D), ProGRP (E), CA 15-3 (F), CA 125 (G) and HE4 (H). Corresponding AUCs were calculated and displayed on the upper right of the graph for each marker. AUCs lower than 0.6 represent poor prognostic performance regarding prediction of well response to therapy.

Relative concentration changes between Cycle 1 and Cycle 3

In a second approach the relative change in biomarker concentration was compared between beginning of therapy and the end of treatment cycle 2 (Figure 15).

The highest density for CYFRA 21-1 was observed in the negative scale of the graph which equaled a decrease in biomarker concentrations in both response groups. Whereas patients that respond well to therapy almost never experienced an increase in biomarker concentration during therapy, a considerable part of the non-responders did. Stable concentrations were seen in CEA biomarker concentrations for both response groups. The same picture was observed when analyzing the SCCA concentrations.

The majority of responders to therapy experienced a decrease in NSE concentrations during the first two therapy cycles. The concentrations in the non-responders varied from decrease to increase but the peak was located in decreasing concentrations. Further calculations will reveal whether the differences are significant. Both curves for ProGRP showed almost complete overlap. The majority of patients in either response group showed stable concentrations of the biomarker. A small group of patients in responders and non-responders experienced a decrease in concentrations. Since a similar observation was made when analyzing poor response to therapy. Thus the response to therapy cannot be the explanation for this separates peaks.

The observations made when analyzing the curves for CA 15-3 mirrored the results obtained when analyzing the ProGRP graph, CA 125 curves showed a large overlap for both response groups. Both peak concentrations ranged around the zero concentration which meant stable biomarker concentrations during treatment. No differentiation between the curves drawn for HE4 was feasible. The majority of patients in both groups experienced stable values. A subpopulation in both groups had a decrease on HE4 concentration.

Again also the relative change in tumor marker concentrations between beginning of therapy and end of treatment cycle 2 was assessed on the predictive value for a good response to therapy. Calculated AUCs were 0.718 (CYFRA 21-1), 0.600 (CEA), 0.585 (SCCA), 0.630 (NSE), 0.542 (ProGRP), 0.590 (CA 15-3), 0.670 (CA 125) and 0.622 (HE4). ProGRP data again showed no discriminative value whereas poor predictive value was calculated for CEA, SCCA, NSE, CA15-3 and HE4. CYFRA 21-1 and CA 125 showed acceptable results regarding prediction of therapy response. Predictive value was not increased by a multi marker approach (Figure 16).

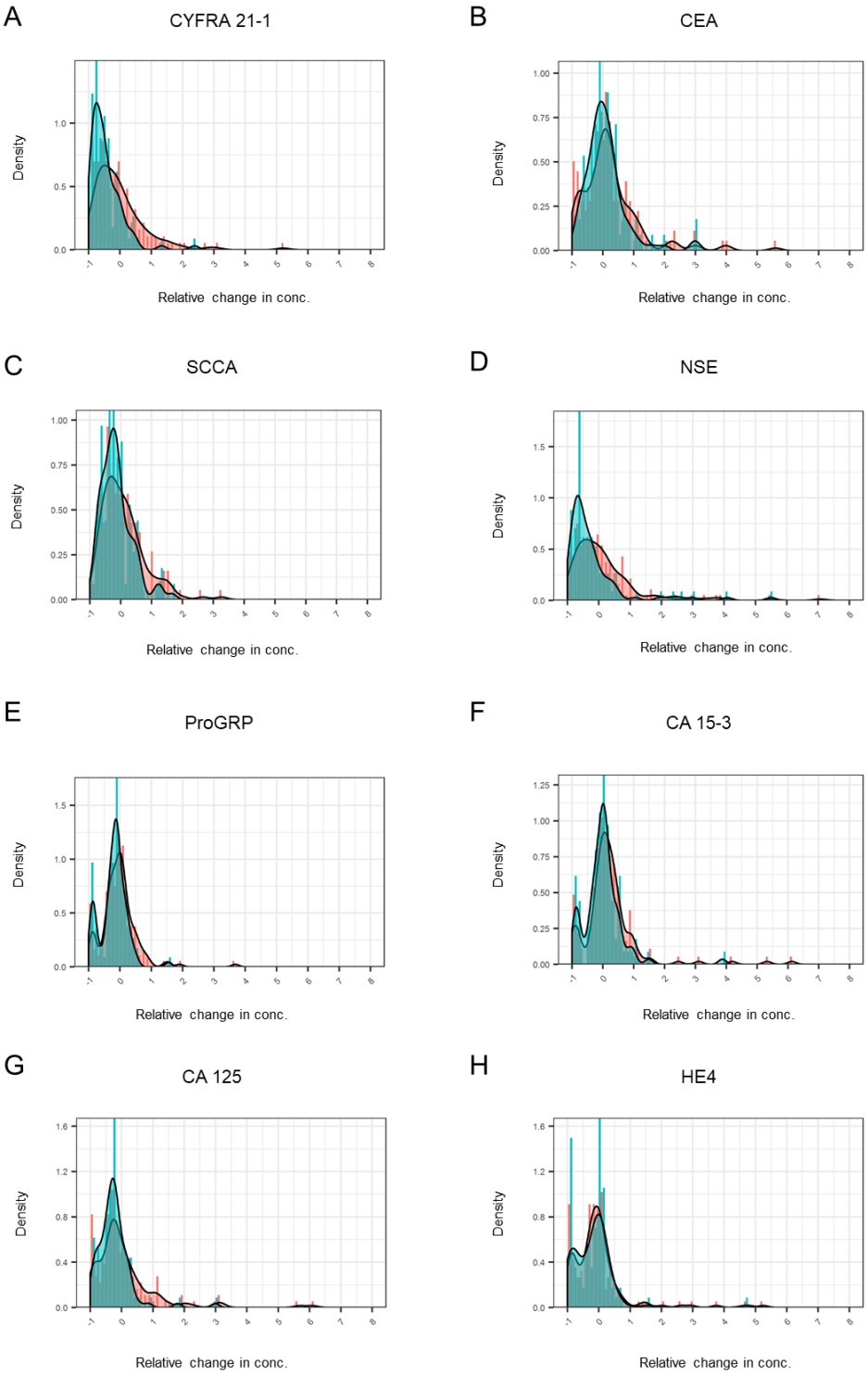

Figure 15: Comparison of the relative change in concentrations in the response groups based on good response to therapy

Histograms illustrate the distribution of the single tumor markers based on the measured pre-therapeutic concentrations for CYFRA 21-1 (A), CEA (B), SCCA (C), NSE (D), ProGRP (E), CA 15-3 (F), CA 125 (G) and HE4 (H) separated into response groups. Non-responders (PD/SD) are shown in turquoise and responders (PR) in orange.

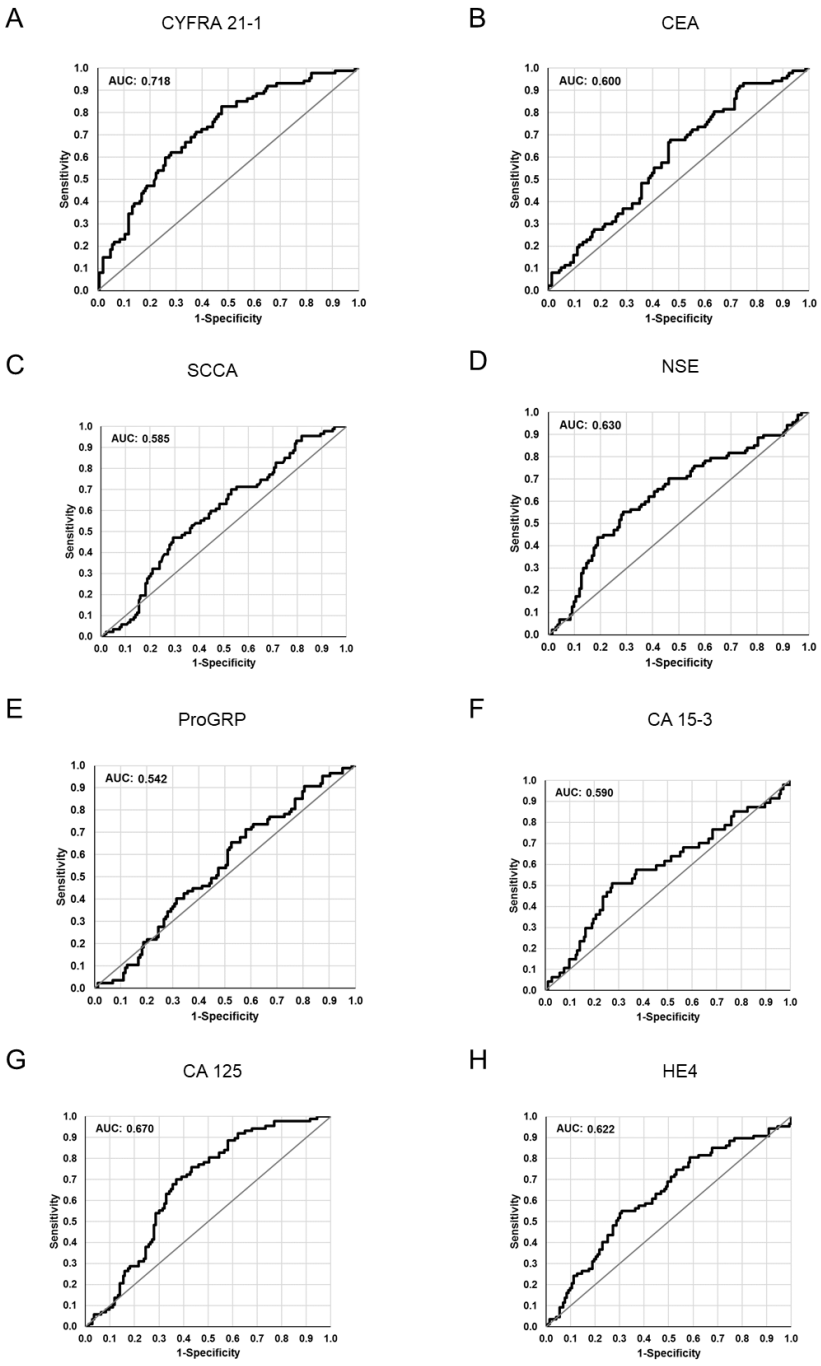

Figure 16: Predictive value of relative change in marker levels between cycle 1 and end of cycle 2 on well response to therapy

ROC curves illustrate the predictive value of the single tumor markers based on the measured relative change in concentration from beginning of therapy until the end of treatment cycle 2 for CYFRA 21-1 (A), CEA (B), SCCA (C), NSE (D), ProGRP (E), CA 15-3 (F), CA 125 (G) and HE4 (H). Corresponding AUCs were calculated and displayed on the upper right of the graph for each marker. AUCs lower than 0.6 represent poor prognostic performance regarding prediction of well response to therapy.

5.3 Prognosis of survival probability

193 patients were eligible for the analysis of probability of PFS in the pre-therapeutic concentrations. Due to missing data for a second time point, the number reduced to 175 patients for the corresponding analysis. Equally, 197 patients were eligible for the analysis of probability of PFS in the pre-therapeutic concentrations. Due to missing data for a second time point, the number reduced to 182 patients for the corresponding analysis (Figure 17).

Prognostic value of the tumor markers regarding progression free survival (PFS) and overall survival (OS) was investigated by Kaplan-Meier curves and further confirmed by hazard ratio (HR) and cox proportional hazard regression analysis.

Kaplan-Meier curves were dawn to visualize PFS and OS in the whole cohort. Later the patients were clustered depending on their smoking status into current smokers, former smokers and never smokers. The never smokers outperform former and current smoker in progression free and overall survival. The former smoker showed a very slightly beneficial course in progression free survival during the first six months compared to the current smokers. In the following months, both curves were comparable. There were only minor differences observed in the course of both overall survival curves which were consequently regarded as equal (Figure 18). Never-smokers were not included in the probability analysis for prognosis of PFS and OS since their PFS/OS performance was different from the remaining cohort. A single analysis of the never-smokers was not feasible due to the small amount of patients in this group. Two time points were investigated in this approach. First, the pre-therapeutic concentrations were analyzed. Second, the biomarker concentrations before the start of the third treatment cycle were taken into account.

For the analysis of the prognostic value of tumor marker concentrations, the patients were split into four groups. Quartiles were calculated from the whole cohort's concentrations and the patients were placed based on their corresponding tumor marker concentration. The data was depicted in Kaplan-Meier curves. Hazard ratios were calculated comparing a low and high quartile to objectively assess whether there is a difference in the median survival.

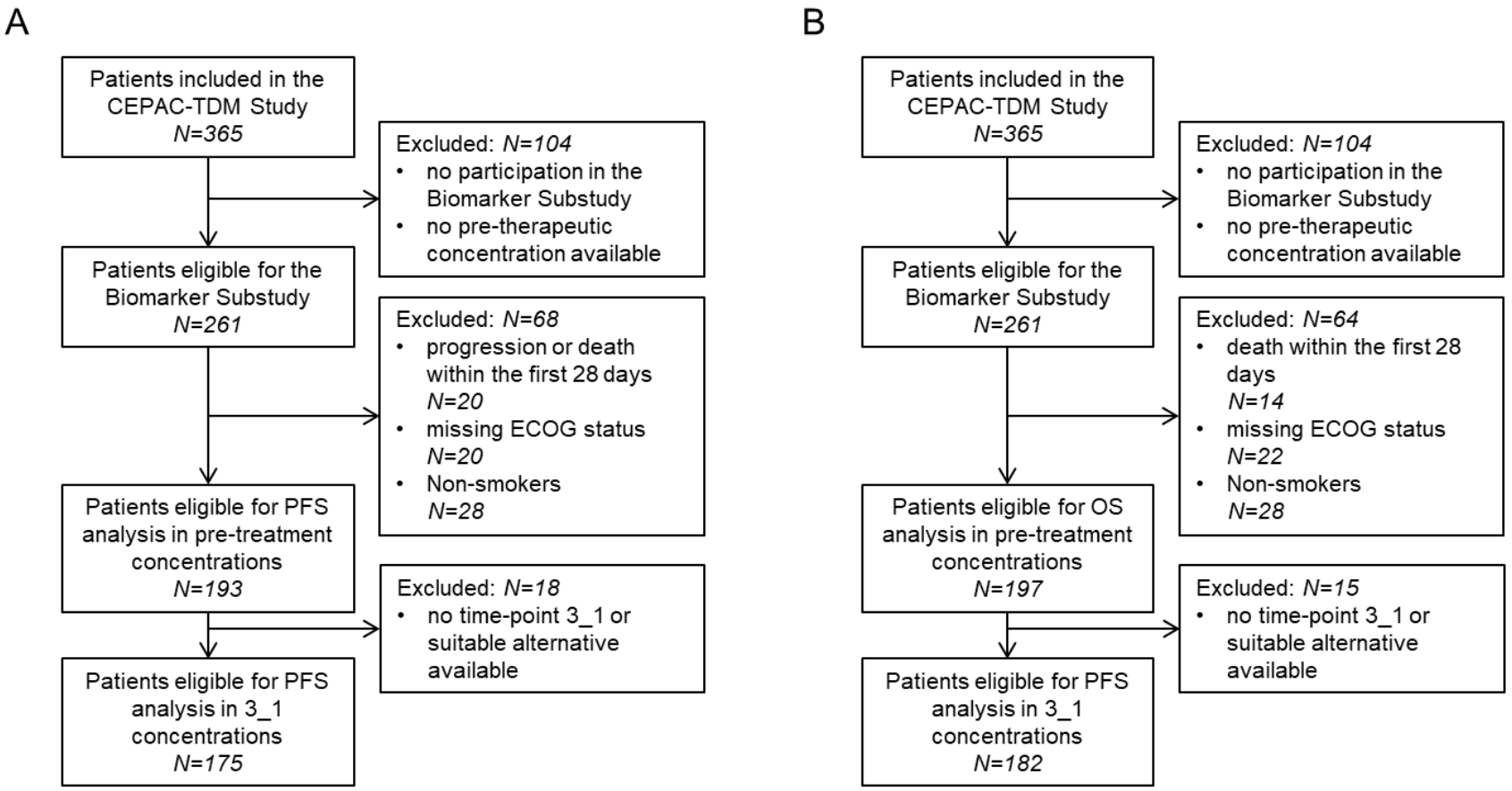

Figure 17: Decision tree outlining included samples in the analysis for prognosis of survival

The depicted decision trees illustrate the sample inclusion process for the analysis of the prognosis of progression free and overall survival. The decision tree for pre-therapeutic study samples was shown on the left (A) and the one for the C3 samples on the right (B).

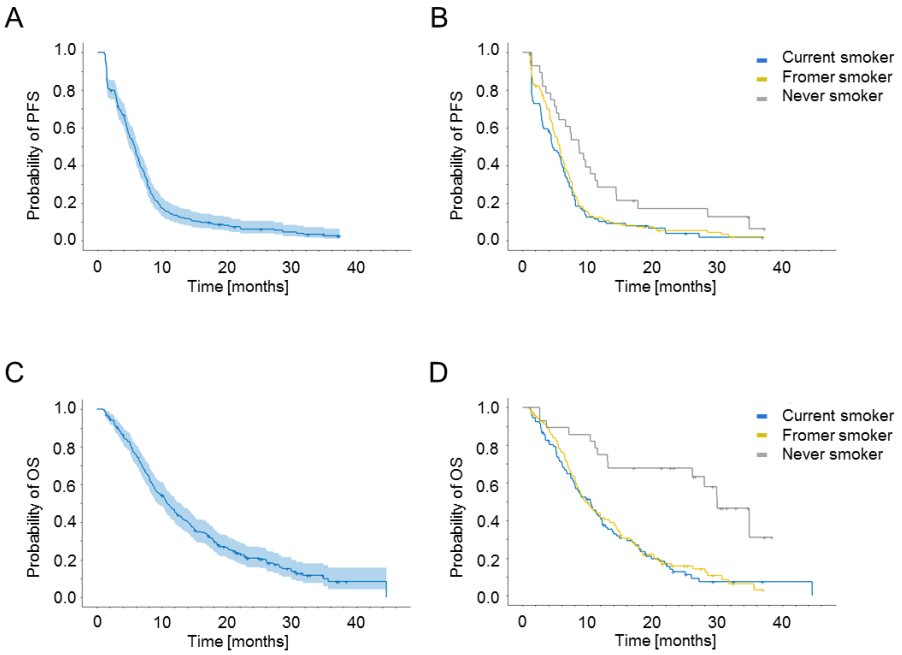

Figure 18: Kaplan-Meier curves on progression free survival and overall survival

Kaplan-Meier curves were drawn to illustrate the progression free and overall survival of the NSCLC study cohort. The dark blue line represented the mean progression free survival (A) or the mean overall survival (C) incorporating data of all patients. Light blue shades marked the confidence interval. The cohort was split by the reported smoking status into current smokers, former smokers and never smokers. Kaplan-Meier curves compared the performance of the three groups for progression free survival (B) and overall survival (D).

The influence of covariates was also illustrated by Kaplan-Meier curves comparing two conditions of the corresponding covariate with each other. Regarding the histology, a better performance of the squamous cell carcinoma patients was observed over the whole observation period. Only minor differences were observed for the different patient stages. The Kaplan-Meier curves investigating the influence of gender and study arm showed a large overlap of both curves. Whereas in exploring the study drug the cisplatin-treated group visibly outperformed the carboplatin group. The comparison of ECOG-status zero with the combined higher ECOG states one and two revealed no difference in the groups. Patients that did not underwent prior therapy, performed slightly better than those with adjuvant therapy. Still, the effect is rather weak and the patients with adjuvant therapies small (Figure 19).

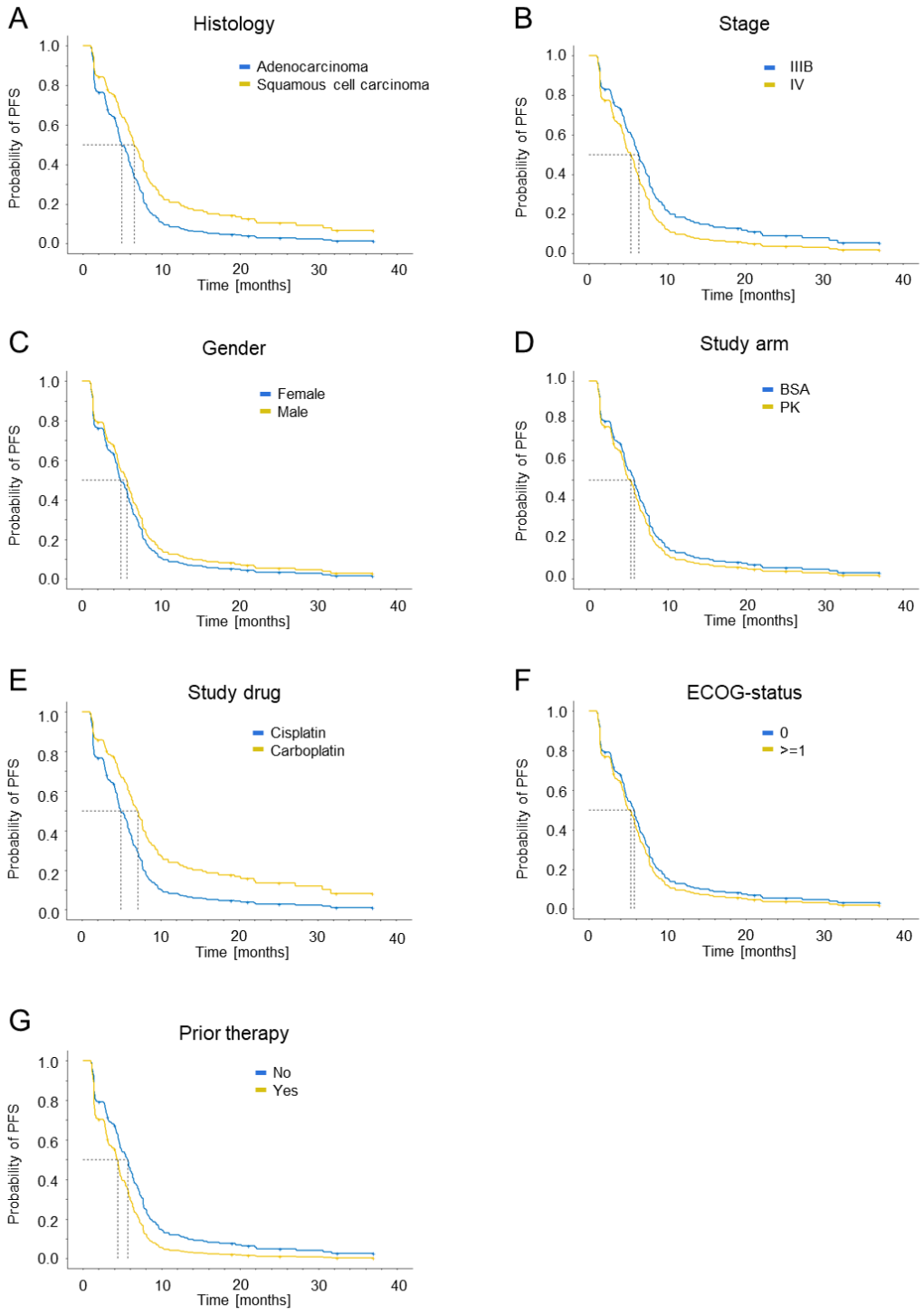

Figure 19: Kaplan-Meier curves analyzing the influence of different covariates on PFS

Kaplan-Meier curves were drawn to visually analyze the influence of the covariates histology (A), stage (B), gender (C), study arm (D), study drug (E), ECOG-status (F) and prior therapy (G) on the probability of progression free survival.

5.3.1 Progression free survival

The probability of progression free survival was investigated by Kaplan-Meier curves and the calculation of hazard ratios. Hazard ratios were accepted as significant when the calculated 95% confidence interval did not include one.

Pre-therapeutic concentrations

To assess the prognostic value of pre-therapeutic CYFRA 21-1 concentrations Kaplan-Meier curves were alike comparing all four groups. This was also seen in the corresponding hazard ratio (HR) which equals 1.07 (CI: 0.94-1.22) and proved no significant difference between the groups. The curves for CEA showed the same course for the first months. Later the patients showing the lowest pre-treatment concentrations presented with a more favorable outcome regarding PFS. Considering the median progression free survival there was no difference seen between the groups (HR: 1.07; CI: 0.99-1.16). The same applied to the tumor marker SCCA with a reported HR of 1.11 (CI: 0.93-1.31).

NSE and ProGRP curves were comparable among the four examined groups. Hazard ratios of 1.20 (CI: 0.96-1.50) for NSE and 0.84 (CI: 0.64-1.08) for ProGRP were calculated but the broad confidence interval negated prognostic value for both markers.

Regarding the Kaplan-Meier curves for CA 15-3 a separation between the four quartile concentration curves was detected. Q1 patients seemed to outperform the whole cohort regarding progression free survival after one year. The calculated median survival showed a benefit for the cohort displayed by a HR of 1.34 (CI: 1.17-1.54). A median progression free survival time of 6.4 months was shown in the cohort with a low concentration of CA 15-3, whereas a median progress was observed after 4.4 months in patients with high concentrations. Kaplan-Meier curves for CA 125 differed significantly for the four investigated groups. The observation was confirmed by a HR of 1.22 (CI: 1.09-1.36) indicating a median survival advantage for patients with low pre-treatment concentrations over the ones with a high concentration (6.3 versus 4.3 months). The four groups showed equal course examining HE4 tumor marker concentrations. Although the resulting HR was 1.20 (CI: 0.79-1.27) the broad confidence interval proved no discrimination between the quartiles (Table 16, Figure 20).

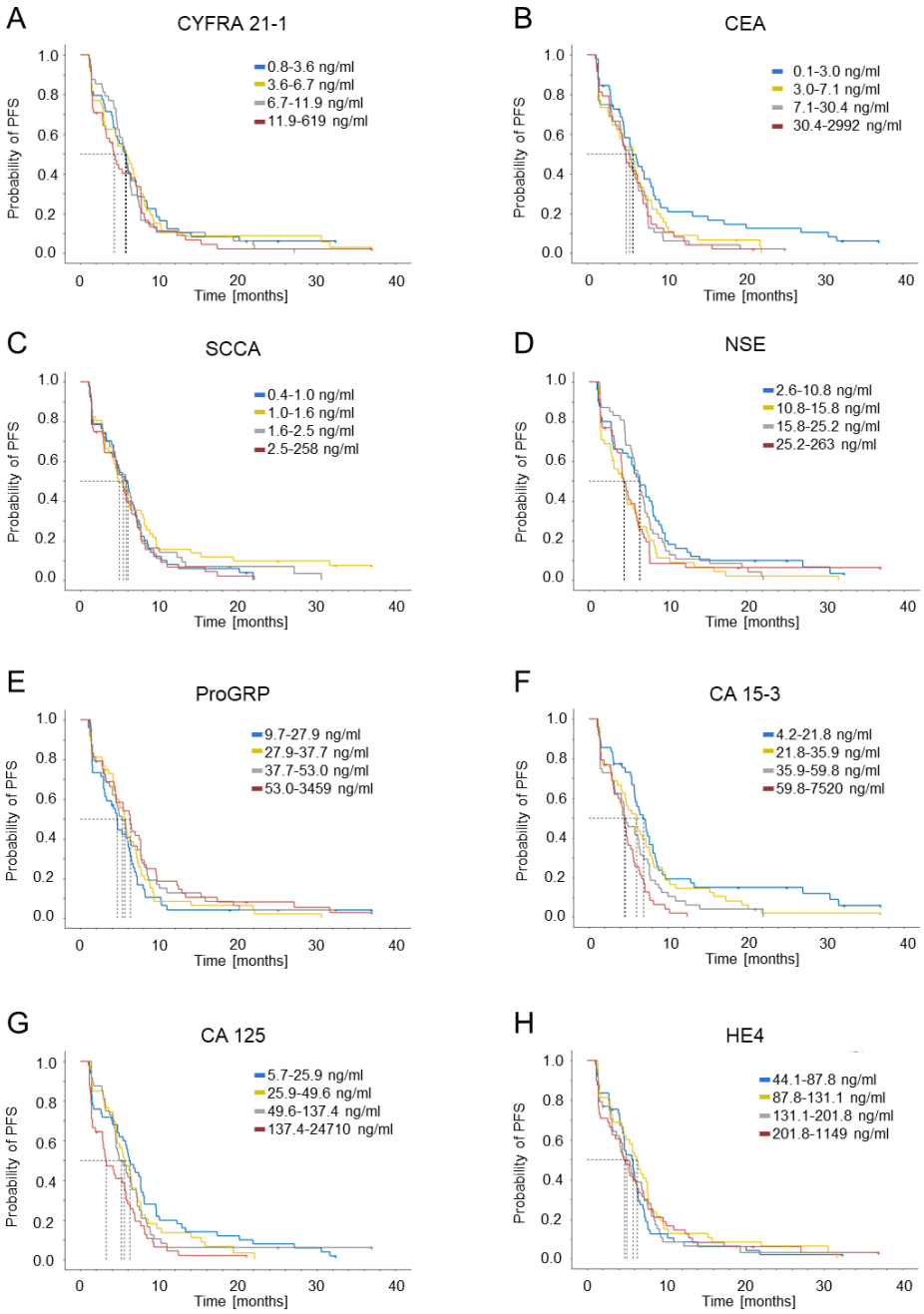

Figure 20: Kaplan-Meier curves showing progression free survival distributed among the quartiles of the measured pre-therapeutic concentration range

Patients were categorized into four groups according to their reported concentration among the quartiles calculated from the whole cohort. The four resulting Kaplan-Meier curves were compared for the markers CYFRA 21-1 (A), CEA (B), SCCA (C), NSE (D), ProGRP (E), CA 15-3 (F), CA 125 (G) and HE4 (H). The quartiles were differentiated by color starting with the lowest (Q1) in blue, followed by Q2 in yellow, Q3 in grey and the highest (Q4) in red. The results were compared by the median survival depicted by the dashed black line for the prognostic value of progression free survival (PFS).

Table 16: Hazard ratios for the single markers investigating progression free survival of pre-therapeutic concentrations

Marker	Hazard ratio (95% CI)	Median PFS low conc.	Median PFS high conc.
CYFRA 21-1	1.07 (0.94-1.22)	5.7 (4.7-6.5)	5.3 (4.5-6.1)
CEA	1.07 (0.99-1.16)	5.8 (4.9-6.9)	4.7 (4.2-5.8)
SCCA	1.11 (0.93-1.31)	5.8 (4.7-6.7)	4.9 (4.3-6.1)
NSE	1.20 (0.96-1.50)	5.8 (4.9-6.7)	4.7 (4.3-6.0)
ProGRP	0.84 (0.64-1.08)	4.9 (4.4-6.0)	5.8 (4.8-6.7)
CA 15-3	1.34 (1.17-1.54)	6.4 (5.8-7.5)	4.4 (3.6-5.3)
CA 125	1.22 (1.09-1.36)	6.3 (5.7-7.4)	4.3 (3.2-5.3)
HE4	1.20 (0.79-1.27)	5.5 (4.6-6.3)	5.4 (4.5-6.4)

Median PFS in months

Cox proportional hazard regression analysis was performed on the single biomarkers and also a variety of covariates including gender, stage, histology, study arm, study drug, ECOG at study entry and prior therapies. As single markers, the pre-therapeutic concentrations of SCCA (HR: 1.30), CA 15-3 (HR: 1.35) and CA 125 (HR: 1.23) evolved as prognostic for progression free survival. For all three markers the probability of PFS decreased with increasing pre-therapeutic marker levels. The covariates stage, gender, study arm, ECOG status and prior therapy had no influence on the PFS probability. The incorporation of histology revealed a longer PFS probability for squamous cell cancers for the markers CYFRA 21-1, CEA, SCCA, NSE, ProGRP and HE4 (HRs: 0.50-0.64). Additionally patients treated with cisplatin were more likely to experience longer PFS. This was shown by all six markers with calculated hazard ratios ranging from 0.56 to 0.60 (Table 17).

Table 17: Hazard ratios resulting from Cox regression analysis of covariates on progression free survival in pre-therapeutic concentrations

	CEA	CYFRA 21-1	NSE	ProGRP	SCCA	CA 15-3	CA 125	HE4
ln(Marker)	1.05	1.11	1.18	0.80	1.30	1.35	1.23	0.91
Histo (Squamous)	0.64	0.57	0.60	0.60	0.50	0.70	0.69	0.59
Stage (IV)	1.05	1.02	1.03	1.10	1.02	1.05	0.93	1.09
Gender (Male)	0.93	0.88	0.93	0.91	0.83	0.90	0.89	0.92
Arm (PK)	1.16	1.19	1.17	1.17	1.12	1.14	1.22	1.17
Drug (Cisplatin)	0.56	0.59	0.57	0.56	0.55	0.60	0.59	0.56
ECOG (≥1)	1.19	1.21	1.22	1.22	1.17	1.28	1.27	1.20
PriorTx (yes)	1.18	1.24	1.20	1.14	1.23	1.48	1.48	1.15

End of treatment cycle 2 concentrations

The same investigations were performed at the end of treatment cycle 2. It was expected to confirm or even increase the prognostic potential of the markers detected in pre-therapeutic concentrations. Kaplan-Meier curves were drawn to follow the survival in the grouped quartiles.

For CYFRA 21-1, the three curves for Q1-Q3 run in close proximity to each other whereas the curve for Q4 showed a good separation from the other three. The same observation was made for the tumor marker CEA although the separation between the curves was visibly smaller. Also marker SCCA showed similar curve slopes in the Kaplan-Meier analysis. The four Kaplan-Meier curves drawn for the quartiles of NSE concentrations showed some variations. Nevertheless no clear differentiation between the curves was possible. Also the curves for ProGRP presented with a large overlap for most of the observation period. For CA 15-3, the curves for Q1-Q3 showed a large overlap and differed from the course of the Q4 curve during the first moths of the observation period. Around the eight moth mark the probability for progression free survival changed in Q3 and looked more like the one observed for Q4. A separation of all four curves drawn for CA 125 was visible for the first few months. In the continuation Q1/Q2 and Q3/Q4 showed equal time courses. The curve for Q4 in HE4 showed a variation from the other three quartiles within the first four months. In the following time period, all four curves ran in close proximity to each other and no difference was visible. Calculation of hazard ratios confirmed the prognostic potential of five tumor markers in single marker investigations (Figure 21). The three biomarkers CYFRA 21-1 (HR: 1.66; CI: 1.39-1.99), CEA (HR: 1.14; CI: 1.04-1.25) and SCCA (HR: 1.34; CI: 1.06-1.66) showed significant HRs at the 95% confidence interval. The median progression free survival period increases for CYFRA 21-1 from 3.6 to 7.2, for CEA from 4.4 to 6.3 and for SCCA from 4.5 to 6.3 months. NSE and ProGRP did not reveal prognostic quality (HRs: 1.05; CI: 0.90-1.23 and 1.16; CI: 0.98-1.36). The mucins CA 15-3 and CA 125 already showed prognostic potential in the pre-therapeutic concentrations. The potential was also seen in the investigation at the end of treatment cycle 2 with corresponding HRs of 1.29 (CA 15-3; CI: 1.10-1.52) and 1.35 (CA 125; CI: 1.20-1.52). The median time until progression increased from 4.4 to 6.5 months in CA 15-3 and from 3.3 to 6.7 months in CA 125. HE4 concentrations did not allow discrimination between the responders and non-responders (HR: 1.06; CI: 0.92-1.21) (Table 18).

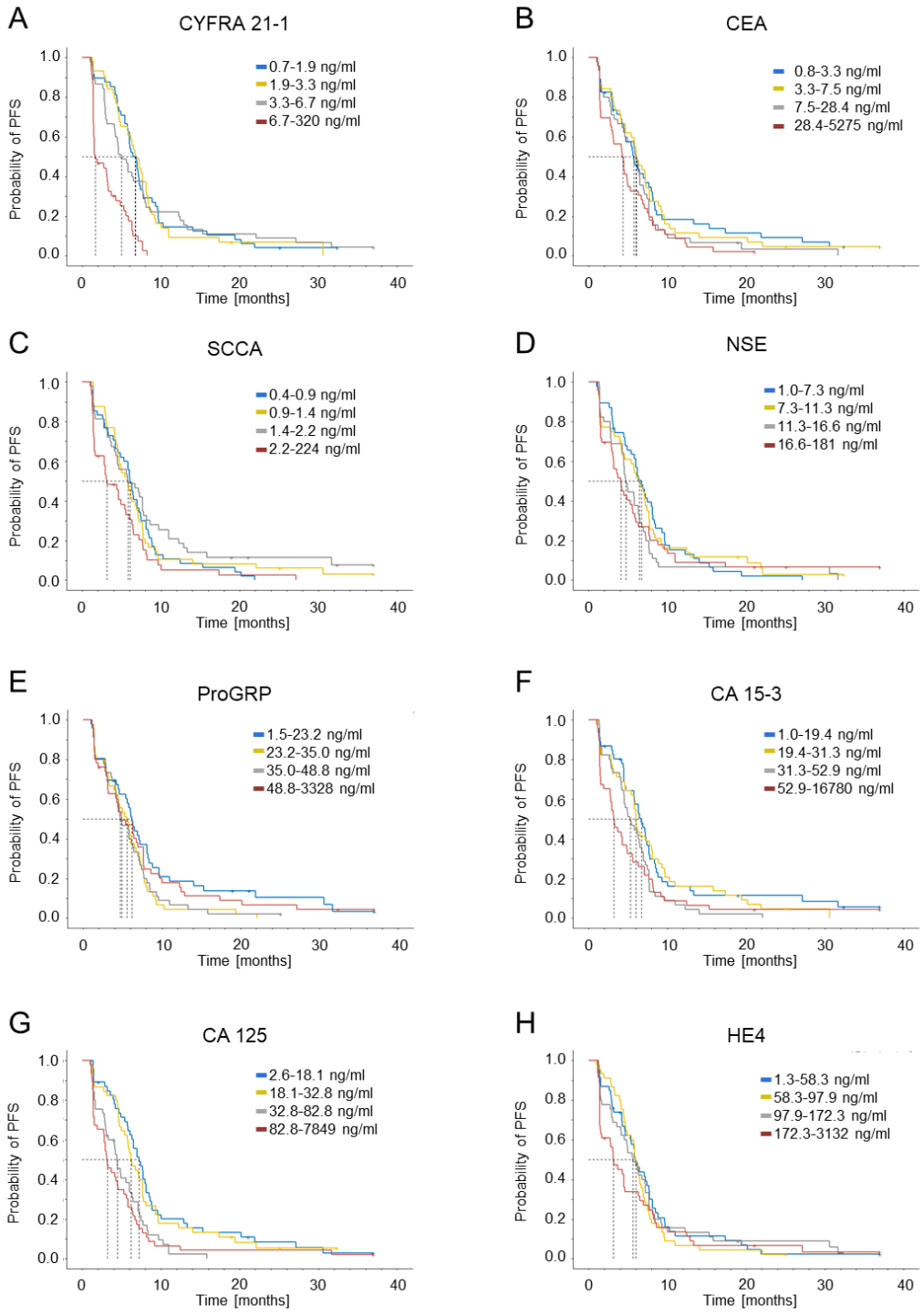

Figure 21: Kaplan-Meier curves showing progression free survival distributed among the quartiles of the measured concentration range at the end of treatment cycle 2

Patients were categorized into four groups according to their reported concentration among the quartiles calculated from the whole cohort. The four resulting Kaplan-Meier curves were compared for the markers CYFRA 21-1 (A), CEA (B), SCCA (C), NSE (D), ProGRP (E), CA 15-3 (F), CA 125 (G) and HE4 (H). The quartiles were differentiated by color starting with the lowest (Q1) in blue, followed by Q2 in yellow, Q3 in grey and the highest (Q4) in red. The results were compared by the median survival depicted by the dashed black line for the prognostic value of progression free survival (PFS).

Table 18: Hazard ratios for the single markers investigating progression free survival of end of treatment cycle 2 concentrations

Marker	Hazard ratio (95% CI)	Median PFS low conc.	Median PFS high conc.
CYFRA 21-1	1.66 (1.39-1.99)	7.2 (6.3-8.0)	3.6 (2.9-4.5)
CEA	1.14 (1.04-1.25)	6.3 (5.6-7.4)	4.4 (3.3-5.7)
SCCA	1.34 (1.09-1.66)	6.3 (5.6-7.4)	4.5 (4.1-5.8)
NSE	1.05 (0.90-1.23)	5.8 (4.6-6.9)	5.4 (4.4-6.3)
ProGRP	1.16 (0.98-1.36)	6.3 (5.3-7.7)	4.9 (4.4-6.1)
CA 15-3	1.29 (1.10-1.52)	6.5 (5.8-7.7)	4.4 (3.2-5.6)
CA 125	1.35 (1.20-1.52)	6.7 (6.0-7.7)	3.3 (2.9-4.6)
HE4	1.06 (0.92-1.21)	5.8 (4.7-7.1)	5.3 (4.4-6.3)

Cox proportional hazard regression analysis was performed to evaluate the effects of covariates on the predictive value. Single marker investigations confirmed the results obtained in the previous analysis step. Calculated HRs were 1.66 (CYFRA 21-1), 1.14 (CEA), 1.51 (SCCA), 1.28 (CA 15-3) and 1.39 (CA 125). The analysis of covariates showed the influence of the histology and the treatment drug. The probability for progression free survival was in favor of squamous histology in CYFRA 21-1, CEA, SCCA, NSE, ProGRP, CA 15-3 and HE4 with calculated hazard ratios between 0.49 and 0.65. All eight biomarkers showed a benefit of the treatment with cisplatin over carboplatin with hazard rations ranging from 0.56 to 0.59 (Table 19).

Table 19: Hazard ratios resulting from Cox regression analysis of covariates on progression free survival in end of treatment cycle 2 concentrations

	CEA	CYFRA 21-1	NSE	ProGRP	SCCA	CA 15-3	CA 125	HE4
ln(Marker)	1.14	1.66	1.07	1.12	1.51	1.28	1.39	1.05
Histo (Squamous)	0.65	0.63	0.57	0.57	0.49	0.57	0.69	0.56
Stage (IV)	1.06	1.07	1.06	1.06	0.98	0.98	1.01	1.07
Gender (Male)	0.91	0.86	0.86	0.89	0.79	0.89	0.80	0.88
Arm (PK)	1.31	1.24	1.30	1.28	1.25	1.24	1.35	1.28
Drug (Cisplatin)	0.56	0.56	0.59	0.59	0.58	0.59	0.59	0.59
ECOG (≥1)	1.08	1.01	1.16	1.13	1.03	1.24	1.20	1.14
PriorTx (yes)	1.16	1.20	1.14	1.12	1.17	1.24	1.42	1.10

5.3.2 Overall survival

Pre-therapeutic concentrations

Next, the prognostic value of pre-therapeutic tumor marker concentrations regarding overall survival was analyzed. Again the patients were split into four groups among the concentrations quartiles. The resulting data was graphically transferred into Kaplan-Meier curves (Figure 22). Hazard ratios were calculated comparing low and high concentrations of the biomarker to objectively assess whether there is a difference in the median survival (Table 20).

Kaplan-Meier curves depicting the four groups for CYFRA 21-1 ran close to each other. Consequently the hazard ratio of 1.09 (CI: 0.95-1.25) proved no difference between the lowest and highest quartile. The curves for CEA showed a reasonable overlap over the whole time period. The resulting HR was 1.07 (CI: 0.95-1.13) which meant no discrimination between the groups. The same applied to the curves of the tumor marker SCCA with a recorded HR of 1.04 (CI: 0.89-1.28).

The Kaplan-Meier curves for NSE ran in close proximity to each other. The observation was confirmed by a calculated HR of 0.99 (CI: 0.78-1.25). The graph displaying ProGRP results showed a considerable overlap of the curves in the first weeks and after more than fourteen months. In between, the four quartiles of patients appear to be separable from each other. Nevertheless hazard ratio assessment was not able to allow discrimination between highest and lowest quartile for median survival (HR: 0.94; CI: 0.73-1.21).

Regarding the Kaplan-Meier curves for CA 15-3 a separation of the curves for Q1, Q2/3 and Q4 was possible. The calculated median survival confirmed a benefit for the cohort displayed by a HR of 1.27 (CI: 1.11-1.44). The median overall survival duration increased from 8.2 to 12.2 months. Kaplan-Meier curves for CA 125 displayed only minor differences for the four investigated groups. The observation was confirmed by a HR of 1.10 (CI: 0.99-1.22) indicating no prognostic value for the median survival. The four groups showed equal course examining HE4 tumor marker concentrations. The reported HR was 1.00 (CI: 0.79-1.26) which proved no potential for median survival prognosis.

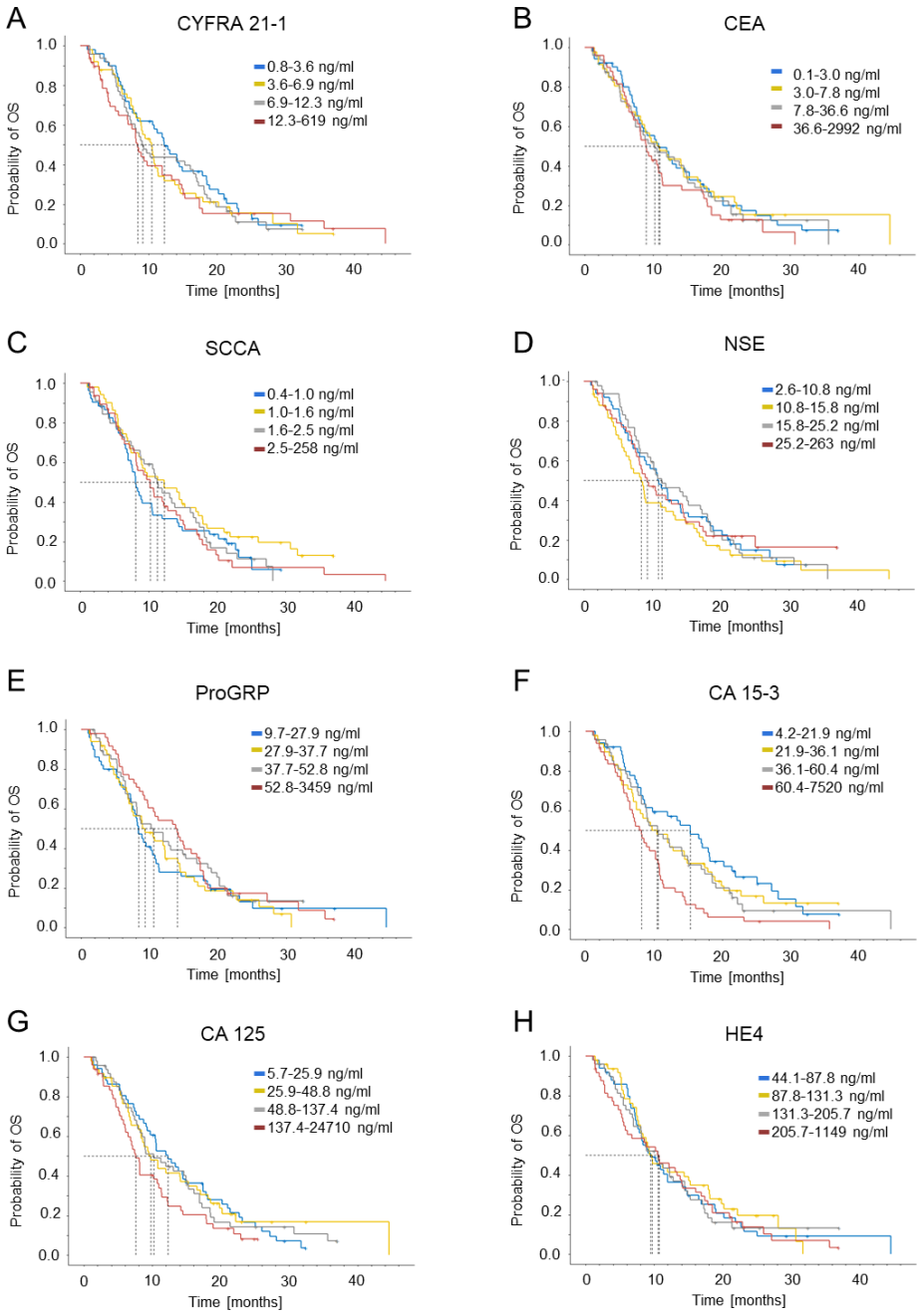

Figure 22: Kaplan-Meier curves showing overall survival distributed among the quartiles of the measured pre-therapeutic concentration range

Patients were categorized into four groups according to their reported concentration among the quartiles calculated from the whole cohort. The four resulting Kaplan-Meier curves were compared for the markers CYFRA 21-1 (A), CEA (B), SCCA (C), NSE (D), ProGRP (E), CA 15-3 (F), CA 125 (G) and HE4 (H). The quartiles were differentiated by color starting with the lowest (Q1) in blue, followed by Q2 in yellow, Q3 in grey and the highest (Q4) in red. The results were compared by the median survival depicted by the dashed black line for the prognostic value of overall survival (OS).

Table 20: Hazard ratios for the single markers investigating overall survival of pre-therapeutic concentrations

Marker	Hazard ratio (95% CI)	Median OS low conc.	Median OS high conc.
CYFRA 21-1	1.09 (0.95-1.25)	10.7 (8.9-14.2)	9.2 (8.1-12.0)
CEA	1.04 (0.95-1.13)	10.5 (8.8-14.1)	9.2 (8.1-12.2)
SCCA	1.07 (0.89-1.28)	10.5 (8.7-14.4)	9.2 (8.1-12.3)
NSE	0.99 (0.78-1.25)	10.2 (8.4-12.3)	10.2 (8.4-13.8)
ProGRP	0.94 (0.73-1.21)	9.7 (8.2-12.3)	10.5 (8.7-13.4)
CA 15-3	1.27 (1.11-1.44)	12.2 (10.4-16.1)	8.2 (7.3-10.2)
CA 125	1.10 (0.99-1.22)	11.2 (9.1-14.6)	8.7 (7.4-11.2)
HE4	1.00 (0.79-1.26)	10.2 (8.4-13.1)	10.2 (8.4-13.8)

Median OS in months

Cox proportional hazard regression analysis was performed on the single biomarkers and under consideration of covariates to assess the probability of overall survival. The incorporated covariates were gender, stage, histology, study arm, study drug, ECOG at study entry and prior therapies. Concerning single marker assessments, only CA 15-3 evolved as prognostic for overall survival (HR: 1.30). The probability of overall survival increases with decreasing pre-therapeutic CA 15-3 concentrations. The inclusion of the covariates, histology, stage, gender, study arm, study drug, ECOG status and prior therapy had no influence on the OS probability (Table 21).

Table 21: Hazard ratios resulting from Cox regression analysis of covariates on overall survival in pre-therapeutic concentrations

	CEA	CYFRA 21-1	NSE	ProGRP	SCCA	CA 15-3	CA 125	HE 4
ln(Marker)	1.03	1.08	0.95	0.92	1.11	1.30	1.11	0.98
Histo (Squamous)	0.97	0.91	0.93	0.93	0.88	1.09	1.01	0.92
Stage (IV)	1.08	1.07	1.11	1.11	1.12	1.03	1.03	1.10
Gender (Male)	0.90	0.90	0.89	0.89	0.88	0.90	0.90	0.90
Arm (PK)	1.13	1.12	1.12	1.13	1.11	1.14	1.16	1.12
Drug (Cisplatin)	0.81	0.82	0.80	0.81	0.79	0.86	0.82	0.81
ECOG (≥1)	1.11	1.10	1.11	1.11	1.09	1.19	1.13	1.11
PriorTx (yes)	0.98	1.02	0.93	0.93	0.94	1.12	1.04	0.93

End of treatment cycle 2 concentrations

CYFRA 21-1 showed prognostic potential in estimating overall survival with a clear separation of the Kaplan-Meier curves of Q1 and Q4. It was confirmed by a calculated hazard ratio of 1.27 (CI: 1.11-1.46). The median overall survival increase was 3.8 months from 8.4 to 12.2 months. The Kaplan-Meier curves for CEA showed close proximity of the curves for Q1, Q3 and Q4. The curve for Q2 ranged above the other three curves. As the hazard ratio was investigated between Q1 and Q4, CEA was not able to prove discrimination between the groups (HR: 1.06; CI: 0.96-1.17). The curves for SCCA did not differ much in their slope. But a small difference was observed at the median overall survival. Nevertheless the calculated HR of 1.15 (CI: 0.93-1.42) for SCCA was not discriminative due to its broad confidence interval.

The four curves for NSE showed good discrimination at the median overall survival probability. The curves for ProGRP ranged in close proximity to each other so no discriminative value was expected. The same held true for the squamous cell carcinoma markers NSE and ProGRP with HRs of 1.12 (CI: 0:94-1:32) and 1.15 (CI: 0.97-1.38), respectively.

Kaplan-Meier curves for CA 15-3 showed discrimination between the curve for Q1 and the three other curves. Hence the prognostic value that already revealed in the pre-therapeutic values showed again. A corresponding HR of 1.26 (CI: 1.07-1.48) was calculated for the time point end of cycle two. The median overall survival increased from 8.4 to 13.4 months. Additionally, CA 125 proved prognostic potential in this investigation (HR: 1.16; CI: 1.03-1.31). This resulted in a longer median overall survival of 3.5 months (8.5 versus 12.0). The Kaplan-Meier curves for Q3 and Q4 looked alike but were visibly different than those of Q2 and Q1. All four curves four HE4 ranged in close proximity to each other. In consequence HE4 was not able to discriminate between the groups with a calculated HR of 1.08 (CI: 0.94-1.25) (Figure 23, Table 22).

Cox proportional hazard regression analysis to assess the influence of covariates on the prognostic potential of the single tumor markers proved the previous findings. CYFRA 21-1 (HR: 1.27), CA 15-3 (HR: 1.27) and CA 125 (HR: 1.18) were confirmed as interesting markers. None of the other covariates, gender, stage, histology, study arm, study drug, ECOG at study entry and prior therapies, was able to further improve prognostic quality of the tumor markers (Table 23).

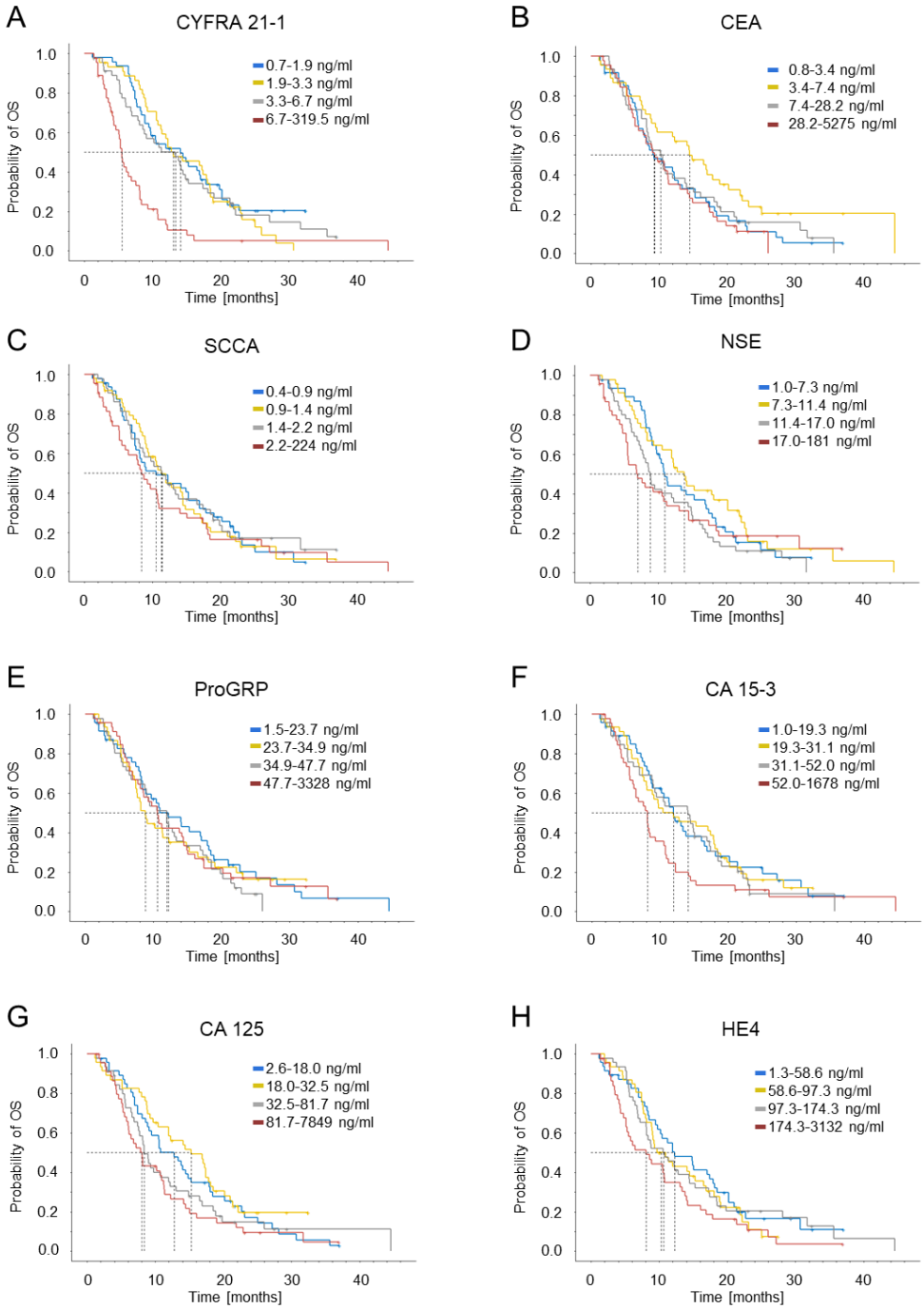

Figure 23: Kaplan-Meier curves showing overall survival distributed among the quartiles of the measured concentration range at the end of treatment cycle 2

Patients were categorized into four groups according to their reported concentration among the quartiles calculated from the whole cohort. The four resulting Kaplan-Meier curves were compared for the markers CYFRA 21-1 (A), CEA (B), SCCA (C), NSE (D), ProGRP (E), CA 15-3 (F), CA 125 (G) and HE4 (H). The quartiles were differentiated by color starting with the lowest (Q1) in blue, followed by Q2 in yellow, Q3 in grey and the highest (Q4) in red. The results were compared by the median survival depicted by the dashed black line for the prognostic value of overall survival (OS).

Table 22: Hazard ratios for the single markers investigating overall survival of end of treatment cycle 2 concentrations

Marker	Hazard ratio (95% CI)	Median OS low conc.	Median OS high conc.
CYFRA 21-1	1.27 (1.11-1.46)	12.2 (10.5-15.3)	8.4 (7.4-10.5)
CEA	1.06 (0.96-1.17)	11.2 (9.1-14.9)	9.2 (8.1-12.3)
SCCA	1.15 (0.93-1.42)	11.3 (9.2-14.9)	9.2 (8.1-12.2)
NSE	1.12 (0.94-1.32)	12.0 (9.2-16.1)	9.3 (8.2-12.2)
ProGRP	1.15 (0.97-1.38)	12.2 (9.7-17.3)	9.5 (8.4-12.0)
CA 15-3	1.26 (1.07-1.48)	13.4 (10.5-17.4)	8.4 (7.4-10.7)
CA 125	1.16 (1.03-1.31)	12.0 (10.2-15.3)	8.5 (7.4-10.8)
HE4	1.08 (0.94-1.25)	11.4 (9.1-16.5)	9.5 (8.2-12.2)

Median OS in months

The results of the tumor marker analysis can be summarized as follows:

No pre-therapeutic tumor marker concentration, single or combination, was predictive for poor response to therapy. When the changes in marker levels between start of therapy and cycle two were investigated CYFRA 21-1, CA 125 and NSE revealed predictive qualities as single markers.

The same as for good response to therapy, no pre-therapeutic tumor marker or tumor marker combination showed a predictive potential estimating good response to therapy. The change in the biomarkers CYFRA 21-1 and CA 125 predicted the response to therapy.

Pre-therapeutic levels CA 15-3 and CA 125 showed potential in the prognosis of progression free survival. Increasing levels of all three markers resulted in a decreasing probability for progression free survival. Investigations after treatment cycle two revealed a prognostic value for five markers. Increasing values of CYFRA 21-1, CEA, SCCA, CA 15-3 and CA 125 decreased the probability for progression free survival.

Prognostic value concerning overall survival (OS) was only seen in the pre-therapeutic levels of CA 15-3. Evaluating the concentrations at cycle two, increasing concentrations of CYFRA 21-1, CA 15-3 and CA 125 decreased median overall survival.

Table 23: Hazard ratios resulting from Cox regression analysis of covariates on overall survival in end of treatment cycle 2 concentrations

	CEA	CYFRA 21-1	NSE	ProGRP	SCCA	CA 15-3	CA 125	HE 4
ln(Marker)	1.07	1.27	1.14	1.14	1.17	1.27	1.18	1.07
Histo (Squamous)	1.01	1.04	0.95	0.93	0.91	0.95	1.05	0.93
Stage (IV)	1.08	1.10	1.08	1.05	1.10	1.01	1.08	1.10
Gender (Male)	0.88	0.95	0.85	0.90	0.86	0.88	0.85	0.87
Arm (PK)	1.27	1.14	1.25	1.23	1.21	1.23	1.30	1.21
Drug (Cisplatin)	0.84	0.82	0.83	0.83	0.80	0.83	0.87	0.84
ECOG (≥1)	1.03	0.93	1.05	1.04	0.99	1.14	1.05	1.04
PriorTx (yes)	1.00	1.04	0.98	0.91	0.92	1.01	1.04	0.94

5.4 Programmed cell death markers

Programmed cell death markers represent important proteins in the regulation of immune cell activity. PD-1, PD-L1 and PD-L2 were investigated as new biomarkers. Three ELISAs to reliably quantify soluble markers in blood were invented on the basis of purchased antibody DuoSets and electrochemiluminescence detection technology. During the establishment process the best assay performance conditions were identified. A comprehensive set of analytical and preanalytical experiments were executed to validate the assays. The data was submitted for publication.

5.4.1 Analytical validation

The analytical validation showed a broad quantification range starting at 30 ng/ml down to 0.0073 ng/ml for PD-1, PD-L1 and PD-L2. Intra-assay imprecision presented with coefficients of variations (CVs) under ten percent obtained in three patient pools of different concentrations for all three markers (PD-1: 6.4%, 6.5%, 7.8%, PD-L1: 7.1%, 4.2%, 6.8%; PD-L2: 4.5%, 10.0%, 9.9%). Dilution linearity experiments proved good linearity from a 1:4 dilution downwards. Selectivity was tested against the each two other biomarkers. No interference was shown for neither of the markers for concentrations of at least 15 ng/ml of the possible influencing marker (Krueger, Mayer, Gerckens, et al., 2020).

5.4.2 Preanalytical validation

PD-1 concentrations were stable for 24 hours before and after centrifugation either at room temperature or at 4°C. PD-L1 concentrations fluctuate with a variations coefficient of ± 40%, especially because of signals close to the lower limit of quantification. PD-L2 marker levels are stable in full blood for 24 hours at 4°C and for six hours at room temperature or even 37°C. Stability after centrifugation was for 24 hours either at room temperature or at 4°C. The freezing process did not change the concentrations for PD-1, PD-L1 or PD-L2. Reproducibility of results was proven for up to three freeze-thaw cycles with obtained variation coefficients of 9.1% for PD-1, 6.8% for PD-L1 and 4.8% for PD-L2 (Krueger, Mayer, Kottmaier, et al., 2020).

5.4.3 CESAR Biomarker substudy

The self-developed assays for soluble PD-1, PD-L1 and PD-L2 were used to quantify the programmed cell death markers in the NSCLC cohort. Samples from all six blood drawing time points were investigated. The number of measurements varied among the time points due to limited availability of patient samples. An overview of the measured data is given in Table 24.

The marker concentrations for PD-1, PD-L1 and PD-L2 in course of the intervention were visualized in boxplots (Figure 24). During all time points the majority of concentrations for PD-1 range between 0.01 and 0.02 ng/ml. at all observation time points, a few concentrations are very high. Most PD-L1 concentrations were below or at the quantification limit. Still located in the lower third of the standard curve, the highest measured concentration equaled 0.17 ng/ml. The majority of PD-L2 concentration ranged between 0.18 and 2.1 ng/ml. Neither of the markers showed a significant change in concentration in response to therapy application on the day after treatment (X_2).

For analysis of response to therapy the patients were categorized according to the response obtained in CT-staging after completion of treatment cycle 2. Response groups included 58 patients with progressive disease (PD), 99 patients with stable disease (SD) and 86 patients with partial remission (PR). Investigating poor response to therapy, PR and SD (N=185) were classified as response and PD (N=58) as non-response. When assessing good response to therapy, stable and progressive disease were classified as non-responders (N=157) and only partial remission (N=86) as responsive (Figure 25).

Pre-therapeutic programmed cell death marker concentrations were analyzed for their potential of predicting poor and good response to therapy. For all three biomarkers, no difference in mean concentration or in the distribution of concentrations was detected regarding pre-therapeutic marker concentrations. Neither PD-1, nor PD-L1 or PD-L2 concentrations before therapy start was predictive for poor or good therapy response (Figure 26).

The same analysis was performed with the concentrations obtained from time point 3_1. Where no data for this time point existed, the data from 2_1 was used instead. The same observations that were made in the pre-therapeutic data showed also in this examination. No difference between mean marker concentrations or marker distributions revealed by separating the two response groups. Just like pre-therapeutic concentrations, concentrations obtained during treatment were not predictive for poor or good response to therapy (Figure 27).

Table 24: Data summary of PD-1, PD-L1 and PD-L2 values for the cancer cohort

PD-1	**1_1**	**1_2**	**2_1**	**2_2**	**3_1**	**EOT**
N	264	95	218	73	164	174
Median	**0.12**	**0.11**	**0.11**	**0.10**	**0.12**	**0.13**
Mean	**0.45**	**0.21**	**0.32**	**0.60**	**0.27**	**0.63**
5th	0.048	0.047	0.049	0.049	0.04	0.045
95th	0.74	0.68	0.64	0.75	0.63	1.046
Minimum	0.023	0.038	0.020	0.045	0.012	0.022
Maximum	30.00	2.29	21.69	30.00	8.33	30.00
N >ULOQ	1	0	0	1	0	1
N <LLOQ	0	0	0	0	0	0
PD-L1	**1_1**	**1_2**	**2_1**	**2_2**	**3_1**	**EOT**
N	266	96	220	73	165	175
Median	**0.0073**	**0.0073**	**0.0073**	**0.0073**	**0.0073**	**0.0073**
Mean	**0.0093**	**0.0085**	**0.0096**	**0.0090**	**0.0099**	**0.0099**
5th	0.0073	0.0073	0.0073	0.0073	0.0073	0.0073
95th	0.020	0.014	0.017	0.013	0.019	0.025
Minimum	0.0073	0.0073	0.0073	0.0073	0.0073	0.0073
Maximum	0.12	0.042	0.11	0.083	0.17	0.085
N >ULOQ	0	0	0	0	0	0
N <LLOQ	222	87	179	64	135	143
PD-L2	**1_1**	**1_2**	**2_1**	**2_2**	**3_1**	**EOT**
N	266	96	220	73	165	175
Median	**0.61**	**0.57**	**0.62**	**0.52**	**0.64**	**0.70**
Mean	**0.92**	**0.87**	**1.00**	**1.021**	**1.15**	**0.84**
5th	0.22	0.25	0.21	0.18	0.25	0.21
95th	1.81	2.08	1.66	1.89	1.66	1.63
Minimum	0.029	0.029	0.032	0.12	0.071	0.018
Maximum	19.21	9.034	21.98	21.88	30.00	8.51
N >ULOQ	0	0	0	0	1	0
N <LLOQ	0	0	0	0	0	0

ULOQ: Upper limit of quantification, LLOQ: Lower limit of quantification

Units for all markers [ng/ml], except for N

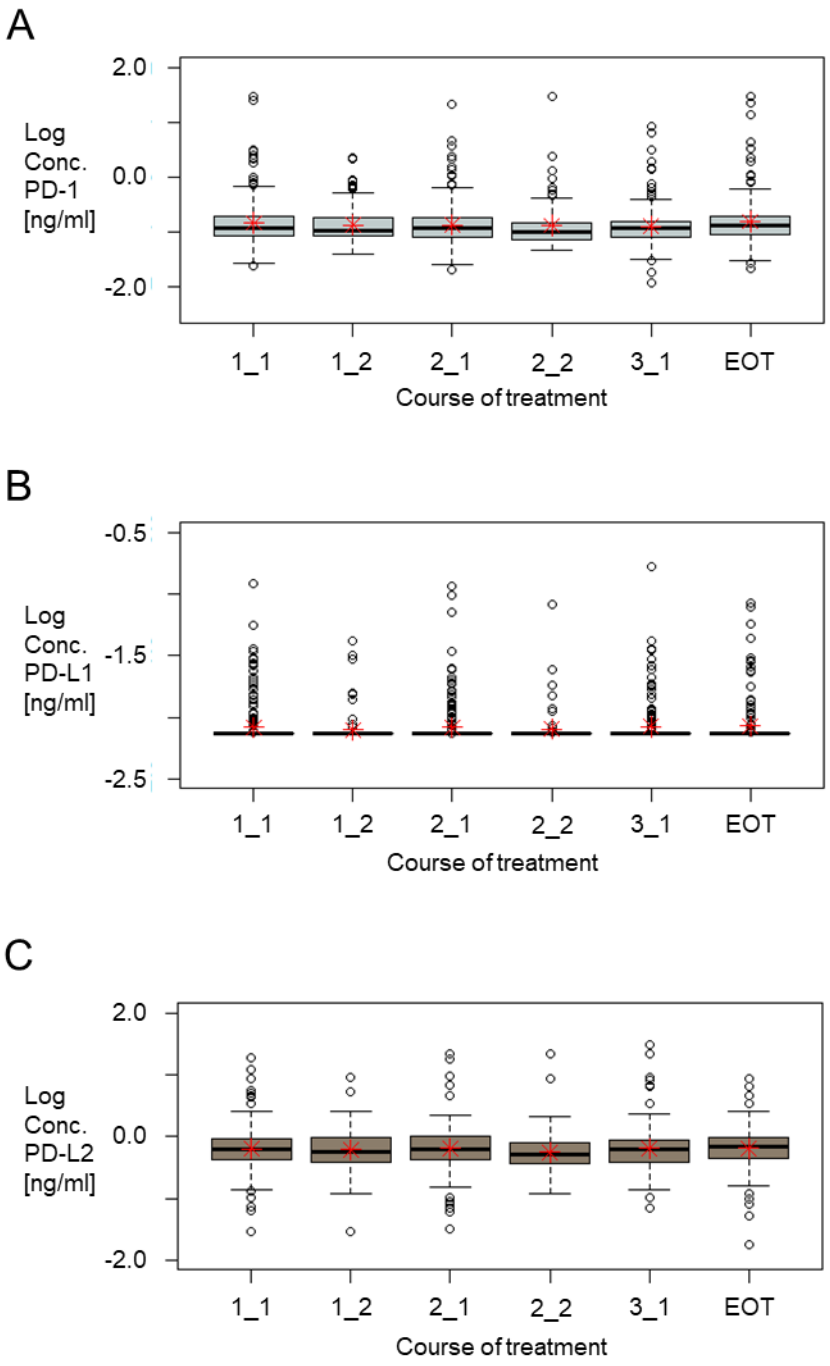

Figure 24: PD-1, PD-L1 and PD-L2 biomarker concentrations at the six different time points during treatment

The figure depicts the distribution of the biomarker concentrations at each of the blood collection time points in direct comparison for PD-1 (A), PD-L1 (B) and PD-L2 (C).Red stars in each box indicate the mean values.

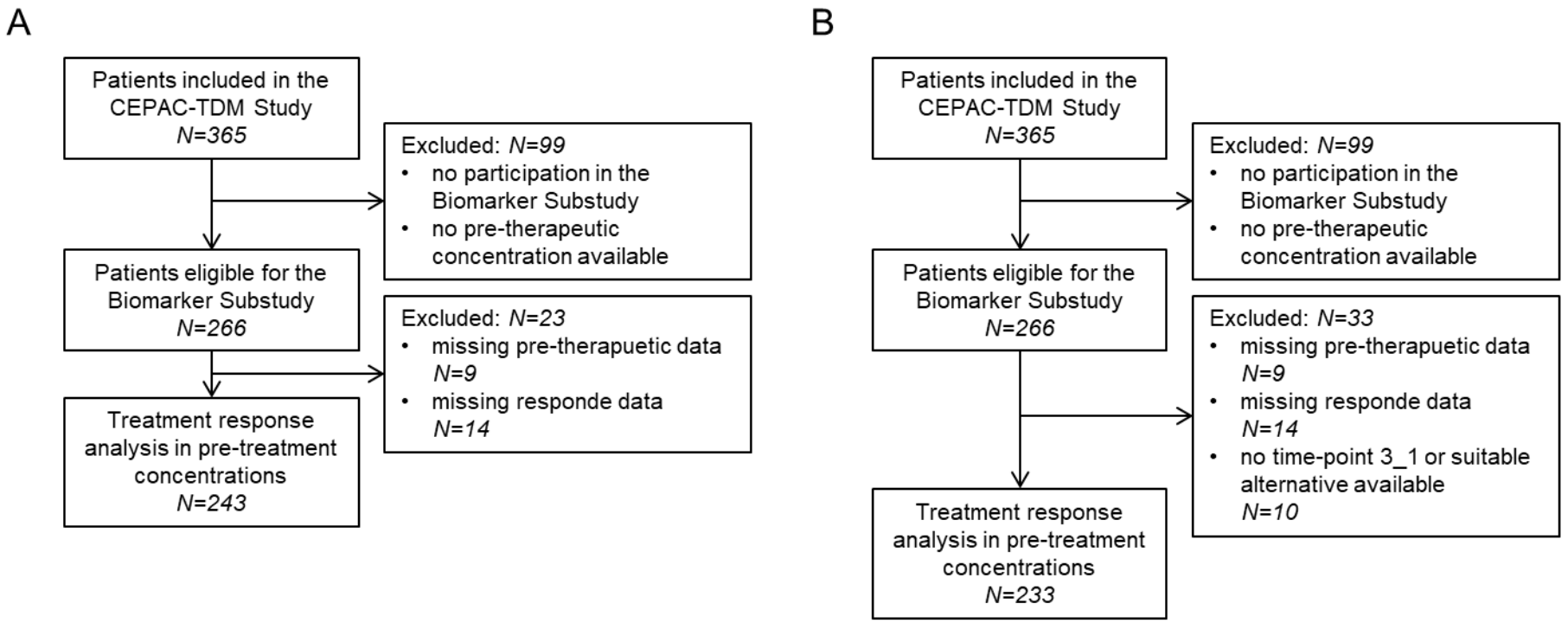

Figure 25: Decision tree outlining included samples in the analysis for prediction of response in the programmed cell death markers

The depicted decision trees illustrate the sample inclusion process for the analysis of the prediction potential of poor and good response to therapy. The decision tree for pre-therapeutic study samples was shown on the left (A) and the one for the relative concentration change between C1 and C3 on the right (B).

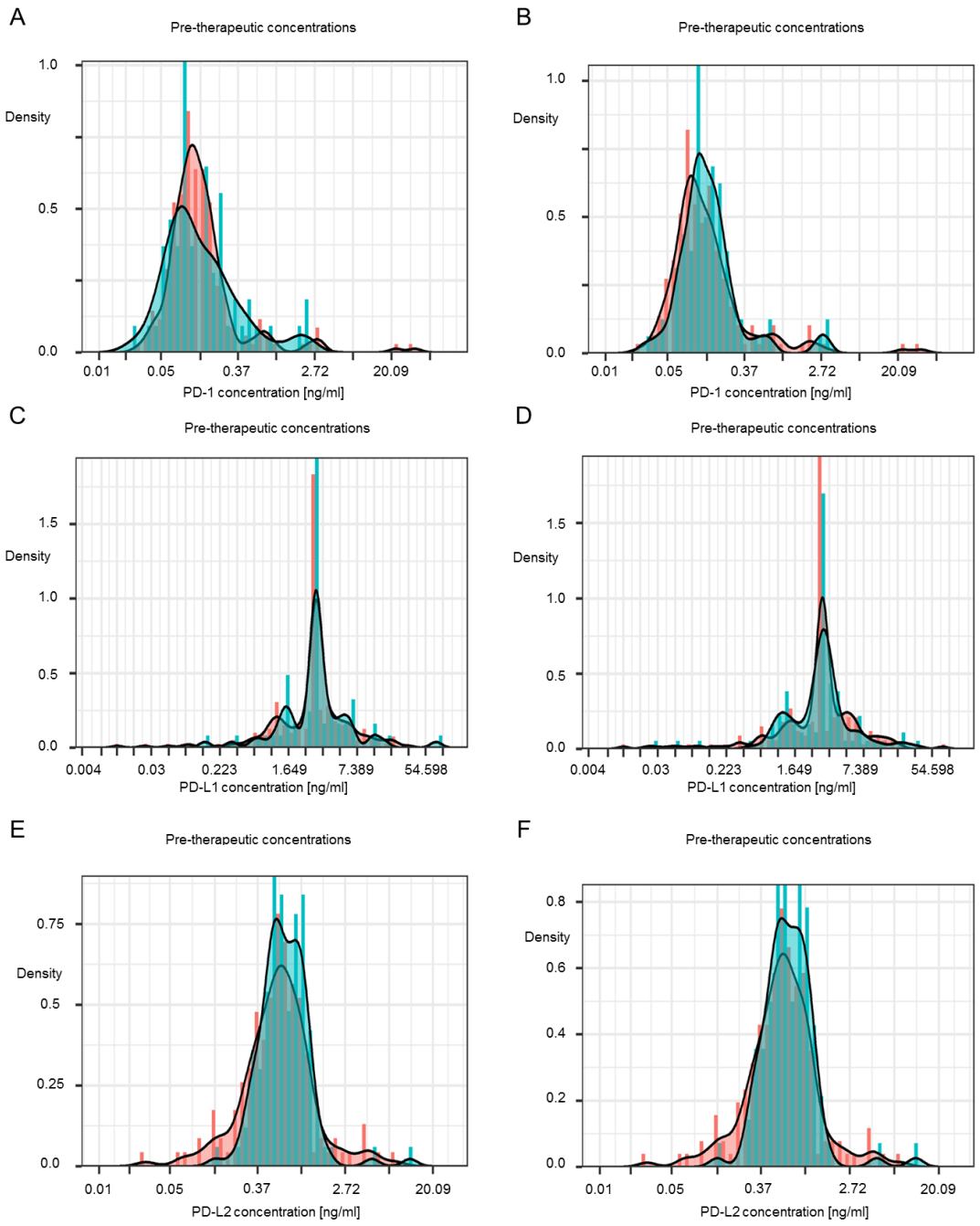

Figure 26: Pre-therapeutic concentrations of responders versus non-responders in PD-1, PD-L1 and PD-L2

Pre-therapeutic biomarker concentrations were plotted separated into responders and non-responders for PD-1 (A, B), PD-L1 (C, D) and PD-L2 (E, F). Stable disease was classified as response in the left column (poor response) and as non-response (good response) in the right column. Non-responders (PD) are shown in turquoise and responders (SD/PR) in orange for poor response to therapy (left). Responders (PR) are shown in turquoise and non-responders (SD/PD) in orange for good response to therapy (right).

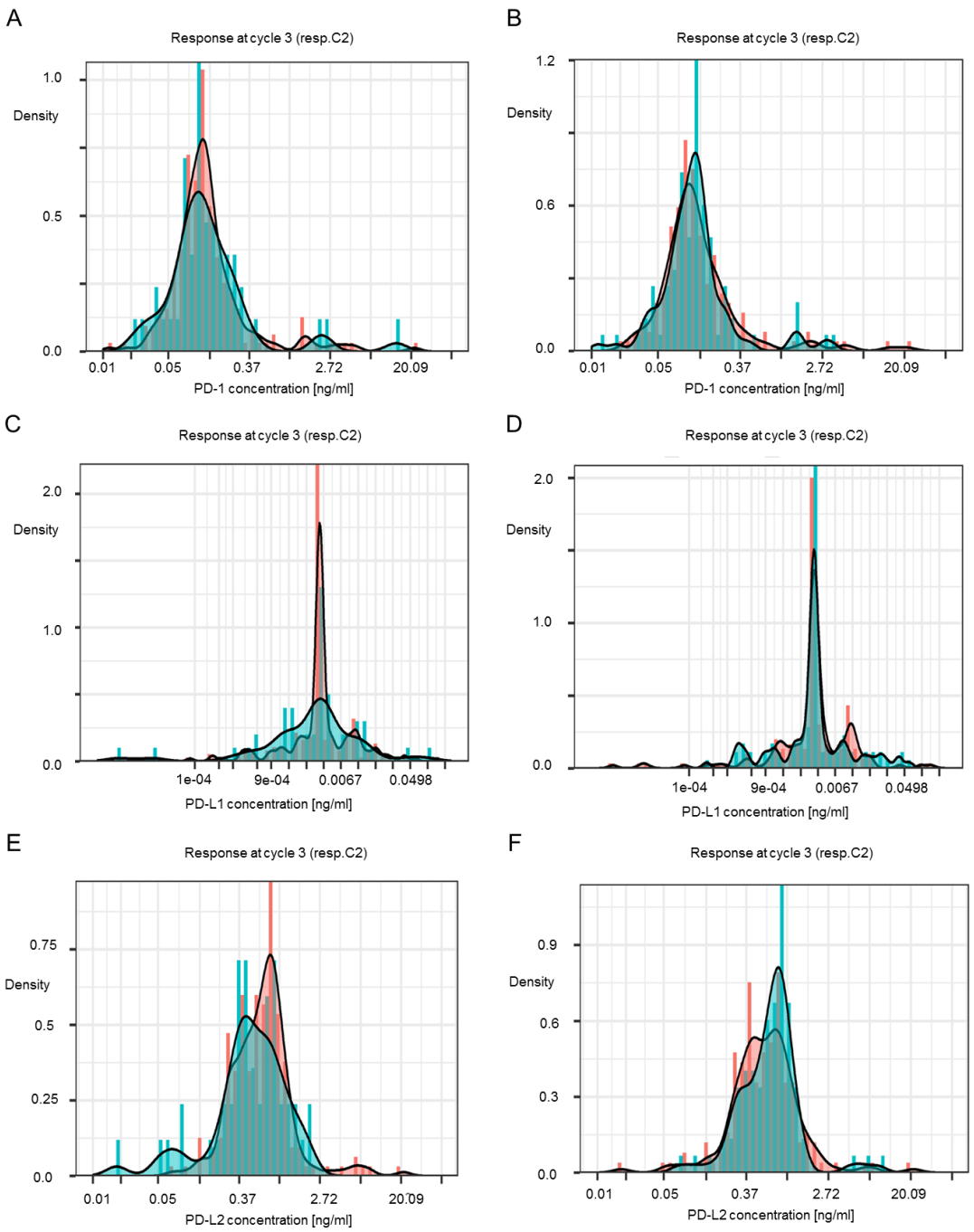

Figure 27: Concentrations at therapy cycle three of responders versus non-responders in PD-1, PD-L1 and PD-L2

Biomarker concentrations at the completion of treatment cycle 2 (=3_1) were plotted separated into responders and non-responders for PD-1 (A, B), PD-L1 (C, D) and PD-L2 (E, F). Stable disease was classified as response in the left column (poor response) and as non-response (good response) in the right column. Non-responders (PD) are shown in turquoise and responders (SD/PR) in orange for poor response to therapy (left). Responders (PR) are shown in turquoise and non-responders (SD/PD) in orange for good response to therapy (right).

The following analysis investigated whether correlations between the three markers at certain time points were detectable. The test on normal distribution (Shapiro-Wilk-test) showed that none of the data groups were normally distributed (Table 25).

Table 25: Test on normal distribution after Shapiro-Wilk for PD-1, PD-L1 and PD-L2 in the cancer cohort

PD-1	**1_1**	**EOT**
p-value	<2.2e-16	<2.2e-16
Result	N.n.d.	N.n.d.
PD-L1	**1_1**	**EOT**
p-value	<2.2e-16	<2.2e-16
Result	N.n.d.	N.n.d.
PD-L2	**1_1**	**EOT**
p-value	<2.2e-16	<2.2e-16
Result	N.n.d.	N.n.d.

N.n.d.: not normally distributed

Consequently, the correlation after Spearman was used to analyze the data. First, the correlation before (1_1) and at the end of treatment (EOT) was looked at. PD-1 concentrations correlated with PD-L1 and PD-L2 concentrations at both time points with correlation coefficients (rho) of 0.337 in cycle one and 0.037 in cycle two. The effect size of the correlation shrinks from medium to weak though. No correlation was detected between the two ligand levels PD-L1 and PD-L2 (Table 26).

Table 26: Calculated correlation of the PD-markers at time points 1_1 and EOT

Correlated values	**Calc. p-value**	**Result**	**rho**	**Effect size**	**CD**
PD-1 1_1 PD-L1 1_1	1.93e-8	Significant	0.337	Medium	11.3
PD-1 1_1 PD-L2 1_1	2.96e-7	Significant	0.309	Medium	9.5
PD-L1 1_1 PD-L2 1_1	0.022	Not significant	0.140	-	-
PD-1 EOT PD-L1 EOT	0.006	Significant	0.210	Weak	4.4
PD-1 EOT PD-L2 EOT	0.0004	Significant	0.263	Weak	6.9
PD-L1 EOT PD-L2 EOT	0.736	Not significant	0.026	-	-

CD: Coefficient of determination r^2 [%]

Obtained by Spearman-correlation, significant: $p<0.05$, effect size rated according to Cohen (4.7)

5.4.4 Healthy cohort

Programmed cell death markers have not been investigated in the blood of study patients according to literature research. Soluble PD-1, PD-L1 and PD-L2 were measured in a cohort of 136 healthy male participants.

The statistics are listed in Table 27., the data was visualized in boxplots (Figure 28).

Mean and Median showed slight differences for the biomarkers PD-1, PD-L1 and PD-L2. In all three markers, the calculated mean was a bit higher than the median. This hinted on some high concentrations in the sample set, which was confirmed by the concentration data. 90% of measured PD-1 concentrations ranged between 0.07 and 6.16 ng/ml. Out of the three biomarkers, PD-1 concentrations presented with the largest variability. . PD-L1 concentrations were very low, with two thirds of participants showing concentrations at the LLOQ. A maximum concentration of 0.14 ng/ml was measured. The majority of measured PD-L2 concentrations ranged between 0.11 and 2.79 ng/ml. A concentration in the quantification range was available for all 136 participants.

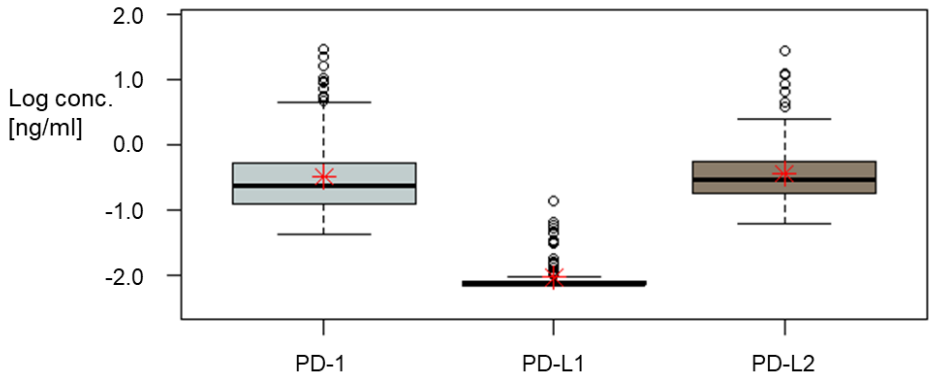

Figure 28: PD-1, PD-L1, PD-L2 concentrations in the healthy cohort

Boxplots indicate the spread of the biomarker values in a healthy cohort. The biomarkers are depicted in the order PD-1, PD-L1, PD-L2. Red starts visualize the mean value.

Table 27: Data summary healthy cohort

	PD-1	PD-L1	PD-L2
N	136	136	136
Median	0.24	0.007	0.29
Mean	1.36	0.012	0.97
5th percentile	0.07	0.007	0.11
95th percentile	6.16	0.038	2.79
Minimum	0.04	0.007	0.06
Maximum	30.0	0.14	29.01
Samples >ULOQ	1	0	0
Samples <LLOQ	0	94	0

ULOQ: Upper limit of quantification, LLOQ: Lower limit of quantification

Units for all markers [ng/ml], except for N

5.4.5 Comparison NSCLC and healthy

The measured concentrations in the cancer cohort were compared with those of the healthy cohort. The time points before treatment (1_1), at the end of treatment cycle 2 (3_1) and end of treatment (EOT) of the cancer study were chosen. PD-1 concentrations resulted into narrow boxes for all three markers. The median and mean of the healthy control samples ranged higher than the both depicted concentrations from the cancer cohort. Even though including the whiskers, a larger overlap of both cohorts was seen. PD-L1 concentrations presented with sharp boxes for both cohorts. Since the majority of data ranged underneath the lower limit of quantification the observation was not surprising. For the marker PD-L2, the boxes for the healthy and the cancer samples looked very alike. A shift of the healthy samples towards lower concentrations was detected (Figure 29).

The significance of the differences between the means of the healthy and the NSCLC patients was calculated applying the Mann-Whitney-U-Test for all three markers. The mean concentration of the control group was significantly higher in all three biomarkers for the three time points pre-treatment, end of cycle 2 and end of treatment (Table 28).

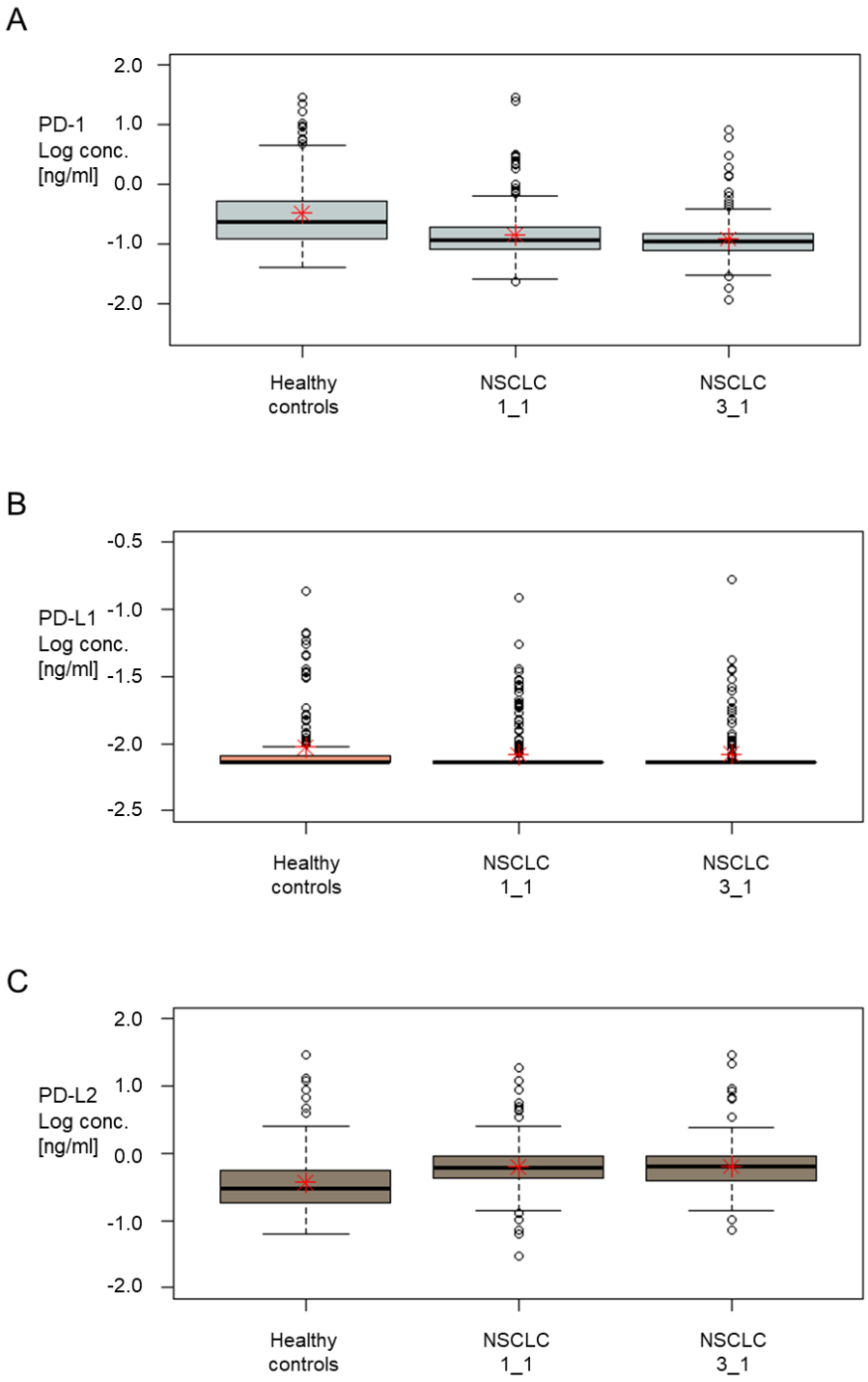

Figure 29: Comparison of the healthy and selected time points in cancer cohort for PD-1, PD-L1 and PD-L2

The concentrations of healthy control samples were related to the concentrations of cancer patients at the beginning and the end of treatment cycle 2 (3_1). Part A shows the PD-1 concentrations, whereas part B the ones of PD-L1 and C the PD-L2 concentrations. Red starts visualize the mean concentration.

Table 28: Significance investigations of PD-1, PD-L1 and PD-L2 in healthy controls versus cancer patients before, at the end of cycle 2 and at the end of treatment

PD-1	**Cycle 1**	**Cycle 3**	**End of treatment**
Description Group	Gr. 1: Controls Gr. 2: Cancer 1_1	Gr. 1: Controls Gr. 2: Cancer 3_1	Gr. 1: Controls Gr. 2: Cancer EOT
Mean group 1	1.36	1.36	1.36
Mean group 2	0.45	0.27	0.63
p-value	5.105e-12	5.547e-14	4.079e-9
Result	Significant	Significant	Significant
PD-L1	**Cycle 1**	**Cycle 3**	**End of treatment**
Description Group	Gr. 1: Controls Gr. 2: Cancer 1_1	Gr. 1: Controls Gr. 2: Cancer 3_1	Gr. 1: Controls Gr. 2: Cancer EOT
Mean group 1	0.012	0.012	0.012
Mean group 2	0.0093	0.0099	0.0099
p-value	0.0010	0.0115	0.0063
Result	Significant	Significant	Significant
PD-L2	**Cycle 1**	**Cycle 3**	**End of treatment**
Description Group	Gr. 1: Controls Gr. 2: Cancer 1_1	Gr. 1: Controls Gr. 2: Cancer 3_1	Gr. 1: Controls Gr. 2: Cancer EOT
Mean group 1	0.97	0.97	0.97
Mean group 2	0.92	1.15	0.84
p-value	8.556e-14	3.04e-11	5.223e-13
Result	Significant	Significant	Significant

Conc. [ng/ml], obtained by Mann-Whitney-U-Test, significance level: 95

6 Discussion

Lung cancer represents the cancer type with one of the greatest incidences in the German population. Although there is currently a large focus on the development and investigation of new therapies, conventional therapy still is and will be an important therapy regimen in the future. There is still a lack of biomarkers that reliably allow prediction of response to therapy and prognosis of progression free survival and overall survival in chemotherapy.

The establishment of informative biomarkers will contribute to the concept of individualized treatment. This idea is publically connected with the preselection of medication on the basis of target identification. Nevertheless also comprehensive biomarker surveillance will contribute to achieve personalized medicine. Some examples for the benefits of informative biomarkers are following. With the identification of biomarkers that early indicate response to therapy, a quicker adaption of the therapy regimen is enabled. This will increase therapy efficacy as well as reduce unnecessary side effects. If a well response to therapy can be reliably identified, it offers the possibility to enlarge distances between radiation-dependent imaging methods.

In this approach eight tumor markers and three newly developed assays were investigated in a NSCLC cohort. The blood sampling in the CESAR Biomarker Substudy was done in the course of the clinical trial CEPAC-TDM. Patients with NSCLC were included and treated with conventional chemotherapy regimen consisting of paclitaxel combined with cisplatin or carboplatin. CEPAC-TDM's objective was to explore the effect of pharmacokinetically(PK)-guided paclitaxel dosing on the occurrence of adverse events. The study compared in two study arms a conventional body surface area dosing approach with a pharmacokinetically-guided approach. Primary end point of the study was the occurrence of grade four neutropenia, secondary end points encompassed neuropathy, radiological response and survival. The study results showed that PK-guided dosing did not reduce the risk for severe neutropenia. Both study arms also reported comparable response and survival data. Nevertheless the drug monitoring allowed reduction of the paclitaxel dose in the PK-guided study arm which resulted in decreased risk to suffer from neuropathy in those patients (Joerger et al., 2016).

The CESAR Biomarker Substudy invests tumor markers and new biomarkers on their potential to predict therapy response and prognosis of survival. Tumor markers have been used in the differential diagnosis, for prognostic, predictive and monitoring purposes in different cancer indications with varying success for years.

CYFRA 21-1, CEA,SCCA, NSE and ProGRP are associated with lung cancer (Tumorzentrum München, 2020). The additionally included tumor markers CA 15-3, CA 125 and HE4 are currently not reported in any guideline to assess response to therapy or predict outcome in lung cancer. But some studies showed utility of these markers particularly in the adenocarcinoma histology in lung cancer (Ghosh et al., 2013; Iwahori et al., 2012; Molina et al., 2003)

Although a number of studies have investigated the potential of different biomarkers before, still few biomarkers entered clinical routine. The main reason for that fact is the heterogeneity of the current biomarker study landscape with a limited number of high quality studies. Conclusively no strong evidence supports the measurement of the abovementioned markers in clinical context. Since no unique study set-up has been defined by now, comparability between different studies is often difficult. Various factors combine to the observed heterogeneity.

Inclusion criteria vary among the studies and as such can already introduce a bias. For example the preselection of certain tumor stages versus the inclusion of all stages. It can change the overall study outcome when stage is not considered as a covariate in the analyses. Studies use different quantification methods, some even within one study, without considering method dependency. The staging by radiation was combined with the drawing of blood samples in the majority of biomarker studies. Nevertheless the time points of response assessment during chemotherapy varied among the studies.

Another problem is the reported variation in tumor response classification. Response is assessed by radiology, for example CT. The interpretation of the obtained results regarding progression and remission can be done in different ways. Differences for example occur in the consideration of newly evolved tumor focuses during therapy. Other circumstances are heterogeneous tumor shrinkage or the inclusion of growth rate and many other. This variety of possibilities leads to different result interpretations in different centers. Additionally the classification of stable disease into response or non-response is still discussed.

The application of biomarker cut-offs is a key element to differentiate response groups. Whereas standardized cut-offs were chosen to evaluate predictive potential of the biomarkers, individualized cut-offs were reported in the monitoring approach (Holdenrieder, 2016; Holdenrieder et al., 2017).

The high variability in radiological response data also stresses the importance of assessing other patient-related end points. Herein, the investigation of progression free and overall survival represent accepted and relevant prognostic factors.

The embedding of the CESAR Biomarker Substudy into a clinical study enabled the thorough investigation of many diagnostic questions under excellent conditions for high quality sample collection and well-defined clinical characterization of patients by homogenous radiological response evaluation by GCP-conform study procedures.

In the current study CYFRA 21-1 was predictive for response to therapy when monitoring the change in concentration between the start of therapy until the end of the second treatment cycle. Though no prognostic value was detected for pre-therapeutic concentrations the concentrations measured after termination of the second treatment cycle were prognostic for progression free and overall survival. CYFRA 21-1 has already been described as a biomarker in monitoring and aftercare. The results confirmed the findings in other studies (Edelman et al., 2012; Holdenrieder et al., 2009, 2017; Okamura et al., 2013). The Manual of the Tumor Center Munich recommends the measurement of CYFRA 21-1 in pre-therapeutic and monitoring samples of unknown histology and in adenocarcinoma, squamous cell carcinoma and large cell carcinoma (Tumorzentrum München, 2020). The current study data confirmed the value of CYFRA 21-1 in monitoring therapy response and was also able to allow prognosis of PFS and OS after termination of two cycles of chemotherapy treatment. Nevertheless CYFRA 21-1 pre-therapy concentrations were not able to reach significance in prediction and prognosis which was not expected in the first place. Referring to the biology of cytokeratins, their presence in squamous cell carcinomas is expected to be higher than in adenocarcinomas. Since three quarters of the patients suffered from adenocarcinoma, this fact provides an adequate explanation why CYFRA 21-1 did not show its full potential in the investigation.

Carcinoembryonic antigen was described to improve the predictive and prognostic value when combined with CYFRA 21-1 in the diagnosis adenocarcinoma in lung cancer (de Jong et al., 2020; Tumorzentrum München, 2020). In the current study CEA was investigated as a single marker and in combination with the other tumor markers. The CEA concentration after the end of the second treatment cycle was prognostic for progression free survival. The combination with CYFRA 21-1 was able to slightly but not significantly increase the predictive value for therapy response by change in concentrations in the first two treatment cycles. CEA is more often elevated in adenocarcinoma which stresses its relevance for differential diagnostic applications. However for prognosis, we were not able to show utility for CEA in our study cohort.

SCCA is recommended in combination with CYFRA 21-1 before treatment and as a single marker assessment in monitoring in the subtype squamous cell carcinoma by the Manual published by the Tumorzentrum Munich (Tumorzentrum München, 2020). Since three quarters of the study cohort suffer from adenocarcinoma, it was not frequently elevated in the patients in our study. Nevertheless SCCA was able to show potential for prognosis of progression free survival after the completion of treatment cycle 2. The analysis proved the value reported by the Tumor Center Munich and its recommendation in monitoring. As it is reported, samples can be contaminated with SCCA from epithelial cells. On this account, extra care has been taken in the sample processing to prevent contamination and ensure highest analytical standards which enables informative results.

NSE and ProGRP are recommended in the analysis of small cell carcinoma as both are expressed mostly by neuroendocrine tissue (Tumorzentrum München, 2020). In consequence it was not expected to find strong correlations in a cohort consisting of NSCLC patients. Pre-therapeutic NSE concentrations were able to predict response to therapy but the observed effect was only poor. There was no significant predictive or prognostic value detectable for the tumor marker ProGRP. The results obtained from the NSCLC cohort confirmed the expected data.

The tumor markers CA 15-3, CA 125 and HE4 have neither been recommended in the support of differential diagnosis nor the prediction, prognosis or monitoring of lung cancer patients. However some studies in literature report on positive results of these markers for differential diagnosis and prognosis in lung cancer. Also some of the markers are currently used in the monitoring of other cancers, particularly in adenocarcinoma histology. The analysis of the data set revealed that the pre-therapeutic concentrations of the tumor marker CA 15-3 offered prognostic potential regarding progression free survival and overall survival. Progression free survival was also predictable by pre-therapeutic CA 125 concentrations. Additionally, the relative change in concentration measured before start of treatment and at the end of cycle 2 was predictive for therapy response. Biologically, CA 15-3 and CA 125 are both mucins. As such they are strongly associated with the adenocarcinoma subtypes of cancers. They are not tissue-specific so patients have to be diagnosed with lung cancer before application of the two markers. If the diagnosis is confirmed, they may offer an earlier estimation of PFS and OS. Currently used CYFRA 21-1 was only able to provide this information at the end of cycle 2 in this study. However, other studies confirmed our positive results regarding CA 125 as they have already hinted at its potential in prognosis (Cedrés et al., 2011; Kimura et al., 1990).

Like CA 125, HE4 is an established biomarker in ovarian cancer. Due to its confirmed expression in lung epithelia tissue, it is suggested to be a potential biomarker in lung cancer. Choi et al. and He et al. found a diagnostic potential in the quantification of HE4 in lung cancer patients (Choi et al., 2017; He et al., 2019). In addition, a small study of Iwahori in 2012 hinted at a potential for prediction and prognosis for the biomarker HE4 in lung cancer, that was reproduced by Lamy et al in 2015 in NSCLC patients (Iwahori et al., 2012; Lamy, Plassot, & Pujol, 2015). HE4 is associated with the adenocarcinoma subtype, too. Even though the majority of patients suffered from adenocarcinoma the analysis did not show predictive or prognostic potential in the investigated NSCLC cohort.

For the quantification of soluble biomarkers PD-1, PD-L1 and PD-L2 in blood we established and optimized novel highly sensitive immunoassays on a chemiluminescent detection platform. By a performing a comprehensive set of analytical and preanalytical experiments a thorough validation process was shown (Krueger et al.,2020a; Krueger et al., 2020b). Validity experiments were according to relevant guidelines in the field (Andreasson et al., 2015; Clinical and Laboratory Standards Institute, 2001; Committee for Medicinal Products for Human Use, 2012; Duffy et al., 2015; Pasella et al., 2013). Successful proof of validity represents a prerequisite for obtaining high quality measurement results. These form the basis for meaningful clinical data analysis.

PD-1, PD-L1 and PD-L2 concentrations were measured in all available time points of the NSCLC cohort. All three markers presented with stable concentrations over the investigation period. For evaluation of predictive value for response to therapy the patients were classified into response groups among the CT-evaluated tumor status after termination of the second treatment cycle. Neither the pre-therapeutic nor the relative change in concentration during the first two treatment cycles was able to predict response to therapy due to a great overlap of the histograms of responder and non-responder concentrations for any of the three biomarkers.

The programmed cell death markers represent important molecules in the regulation of immune response. It is known that some cancer types use the expression of the silencing ligand PD-L1 to evade elimination by the immune system. Stable biomarker concentrations indicate that this regulative mechanism did not play a major role in the presented cohort. If it had, a differentiation between responders and non-responders would have been possible. A correlation of the pre-therapeutic concentrations of the receptor PD-1 with each of its ligands PD-L1 and PD-L2 was seen. It was expected to extract this correlation since receptor and ligand interaction result in downstream signaling. No correlation was detected between the concentrations of the two ligands.

Research showed that although both markers share the PD-1 receptor, both ligands also bind to different proprietary receptors and exhibit different signaling pathways. In this context it was not expected to observe a strong correlation between the two ligands (Butte et al., 2007; Chen et al., 2018).

The findings of the study's investigations were not completely unexpected. The regulation of the activity of the immune system is finely regulated by a plethora of proteins. Cancer and the treatment of cancer induce inflammatory processes. These must be regulated by other proteins than the programmed cell death markers in the presented cohort. The obtained data denied the application of PD-1, PD-L1 and PD-L2 as general markers to assess response to therapy in a chemotherapeutical treated cohort. Since the assays proved validity, the application in a patient cohort treated with immune checkpoint-inhibitors targeting the programmed cell death marker pathways is of interest. Since these drugs directly target the investigated proteins, it is more likely to show an effect. It is hoped, that the biomarkers will uncover prognostic and/or monitoring potential in a checkpoint-treated cohort.

Literature research revealed no comprehensive investigation of the concentrations of the programmed cell death markers PD-1, PD-L1 and PD-L2 in healthy controls so far. Comparisons between the healthy and the cancer cohort showed that the mean and median concentrations of PD-1 and PD-L1 were significantly elevated in the healthy cohort compared to the cancer cohort. The data obtained for PD-L1 has to be handled with caution as the vast majority of patients presented with concentrations below the lower limit of quantification. This made it difficult to draw comparisons and calculate statistics applying this biomarker. Contrary, for PD-L2 median concentrations in the healthy cohort are located significantly below the cancer cohort. Tumor disease creates an inflammatory environment which leads to the activation of the immune system. However the constant stimulation results in the induction of negative feed-back loops which cause regulatory immune depression. Either process might contribute to an explanation for our findings. Regardless, it is important that so far activity was only proven for membrane-bound proteins. The developed assays instead, measure the soluble protein forms. A correlation between surface proteins is likely but has not been investigated yet. The soluble forms are hypothesized to generate by either cleavage from the cell surface by matrixmetaloproteinases or secretion of soluble protein isoforms (Frigola et al., 2011; Keir et al., 2008; Nielsen et al., 2005; Schildberg et al., 2016). A comprehensive explanation for the biology of soluble programmed cell death proteins is currently not possible as many questions remain to be investigated.

Our explorative approach was able to show that the marker concentration between healthy and cancer patients differ significantly. Further investigations, including the biology behind the markers, will hopefully elevate the knowledge about the markers and add to explain the findings.

As mentioned before, the biomarkers are regulators of the immune system. This means that their concentration is hypothesized to be influenced by a variety of factors like immune modulatory molecules and processes. The background of the programmed cell death proteins suggests the application as marker in the context of inflammation-accompanied diseases. This opens up the field for new indications to investigate the newly developed assays, starting but not limited to autoimmune diseases, transplant reactions and infectious diseases. These investigations will help to understand more about the biology and the complex impact of the three markers in the regulation of immune system activity.

The presented biomarker study benefited greatly from its junction to a large, multicentric clinical study that was performed according to GCP-guidelines. The advantages comprise clinical characterization of the patients, defined drug administration, monitoring exams and well-controlled radiologic evaluation of therapy response. The CESAR Biomarker Substudy was planned as a side study when setting up the clinical study (CEPAC-TDM Study). This allowed a comprehensive pre-selection of blood sampling time points. The multi-center study took place at different sites in Germany, Austria and Switzerland. Well clinical characterization of included study patients was performed and reported. Therapy response was monitored by computed tomography and analyzed applying the RECIST-guidelines for good clinical practice. Comprehensive assessment of clinical data is expensive and often not available in biomarker study. In this context the biomarker study benefited from the connection to a clinical study which enabled the access to extensive clinical patient data.

The blood samples were drawn solely for the investigation of biomarkers. Processing and storage was performed according to a standard sample processing protocol. The protocol was written with respect to preserve best pre-analytic sample quality. Central organization and distribution of study materials ensures high comparability within the different study centers.

Sample aliquotation at the biomarker measurement site maintained high sample quality by the reduction of necessary freeze thaw cycles. Approved assays were used for the quantification of the tumor markers. The self-developed assays for the quantification of the soluble programmed cell death protein markers underwent extensive validation to

ensure high data quality. Assays were executed according to a predefined assay protocol. Assay specific quality control samples were included in every performed experiment. Biomarker analysis was executed in cooperation with an independent institution. Data consistency and variation was assessed before analysis. The statistical insecurities of the calculated results were reported in form of significance levels and confidence intervals.

However the study patients were not randomized. Another limitation of the study is the drop-out rate in the analyses. 261 were originally included in the study. Depending on the analysis, 16 to 80 patients could not be included in the analysis due to missing blood drawing time-points. The highest rates of drop-outs were seen the monitoring time-points. The retrospective measurement did not allow for addition of further interesting time points or data. The study findings need to be validated in an independent cohort. However the high quality of execution and analysis applied, allowed for a clear suggestion.

In conclusion it can be stated that pre-therapeutic concentrations offered no predictive and limited prognostic potential in the tumor markers. After termination of the second treatment cycle, the biomarkers CYFRA 21-1, CA 125 and NSE were predictive for poor response, and the biomarkers CYFRA 21-1 and CA 125 were predictive for good response to treatment. Pre-therapeutic concentrations of CA 15-3 and CA 125 were prognostic for progression free survival. After completion of the second therapy cycle the five markers CYFRA 21-1, CEA, SCCA, CA 15-3 and CA125 were prognostic for progression free survival. Pre-therapeutic CA 15-3 concentrations for overall survival, after the end of treatment cycle 2 CYFRA21-1, CA 15-3 and CA 125 were prognostic for OS. CYFRA 21-1 and CA 125 showed most potential in prediction and prognosis when applied after the first treatment cycles, in this case two.

The programmed cell death markers did not show predictive potential for response to therapy in the currently investigated NSCLC cohort. A stronger effect is estimated to be found in a squamous cell cohort what is also more likely to be treated with ICIs that directly target the investigated markers.

7 Conclusion

Tumor markers and soluble programmed cell death markers were measured in a chemotherapy treated cohort of NSCLC patients. Analysis was performed in order to assess prediction of therapy response and prognosis of progression free and overall survival. In the tumor marker measurements, the already known marker CYFRA 21-1 confirmed its potential in predicting therapy response and prognosis of PFS and OS. CEA did not evolve as a significant marker due to the low number of squamous cell cancer patients in the cohort. Cox regression analysis showed potential for SCC in the prognosis of progression free survival. NSE and ProGRP are described markers in small cell lung cancer. As expected neither predictive nor prognostic value was detected in the NSCLC patient group. Formerly not investigated tumor markers CA 15-3 and CA 125 revealed potential in prediction of response and prognosis of survival in the NSCLC cohort. CA 15-3 was able to allow prognosis of progression free and overall survival. CA 125 was able to estimate PFS and also by the change of concentrations during the first two therapy cycles predict response to therapy. HE4 showed no potential regarding prediction of response or prognosis of survival in this investigation.

After extensive experiments to prove analytic and preanalytic validity, qualified EILSA assays for study sample testing on solublePD-1, PD-L1 and PD-L2 were introduced. Examination of the programmed cell death markers in NSCLC cohort treated with chemotherapy revealed no predictive value of the biomarkers in this patient group. A comparison with a healthy cohort detected differences in the mean marker concentrations for all three markers. These findings stress the involvement of the programmed cell death proteins in the tumor microenvironment. It is hypothesized that the PD-marker will uncover their full potential in a patient cohort treated with immune checkpoint inhibitors directly targeting the markers which will be the next step to explore.

8 Outlook

The biomarker measurements on the NSCLC cohort revealed a lot of interesting insights that will lead to a variety of following scientific questions and investigations..

The potential of CA 15-3 and CA 125 in the prediction of response to therapy and prognosis of progression free and overall survival will be further explored.

The researched study cohort is well characterization in terms of clinical data availability. This predestines the remaining samples to be investigated in further biomarker measurements, for example routine markers, the immunogenic cell death markers and inflammation markers. That will be assessed regarding their correspondence with prediction and monitoring of therapy response.

The programmed cell death biomarkers were not able to show predictive or prognostic value. In consequence it will be the next step to measure those markers in a more appropriate target group, for example immune checkpoint inhibitor treated NSCLC patients. For sure, due to a blood based test system and the variety of approved indications it will be interesting to also include other cancer types. Of great interest will be the analysis of melanoma patients treated with immune checkpoint inhibitors as these were the first to be treated with the new anti-cancer drug class and reported impressive response data. Nevertheless the application of the biomarkers will not be limited to the indication of cancer as the underlying target is part of the immune system regulation. Thus the assays will also be interesting in the investigation of inflammatory processes or diseases.

Besides it will also be of great interest to gain a deeper understanding of the biology behind the PD-markers. Cell culture experiments will help to understand whether the detectable proteins in blood are secreted soluble forms or cleaved former transmembrane proteins. They might be attached to transporting proteins or bound on the surface or incorporated in exosomes.

Currently on the verge of grasping the potential of the programmed cell death protein detection, there is a lot more to explore in the field in the next years.

9 References

Andreasson, U., Perret-Liaudet, A., van Waalwijk van Doorn, L. J. C., Blennow, K., Chiasserini, D., Engelborghs, S., … Teunissen, C. E. (2015). A practical guide to immunoassay method validation. *Frontiers in Neurology*, *6:179*(August), 1–8. https://doi.org/10.3389/fneur.2015.00179

Astra Zeneca. (2020). MEDI5725. Retrieved June 18, 2020, from www.astrazeneca.com/our-science/pipeline.html

AstraZeneca GmbH. (2018). *Fachinformation Durvalumab*.

Blank, C., Gajewski, T. F., & Mackensen, A. (2005). Interaction of PD-L1 on tumor cells with PD-1 on tumor-specific T cells as a mechanism of immune evasion : implications for tumor immunotherapy. *Cancer Immunology, Immunotherapy*, (54), 307–314. https://doi.org/10.1007/s00262-004-0593-x

Bodenmüller, H. (1995). The biochemistry of CYFRA 21 - 1 and other cytokeratin-tests. *Scandinavian Journal of Clinical and Laboratory Investigation*, *55*(221), 60–66. https://doi.org/10.3109/00365519509090566

Brahmer, J. R., Drake, C. G., Wollner, I., Powderly, J. D., Picus, J., Sharfman, W. H., … Topalian, S. L. (2010). Phase I study of single-agent anti-programmed death-1 (MDX-1106) in refractory solid tumors: Safety, clinical activity, pharmacodynamics, and immunologic correlates. *Journal of Clinical Oncology*, *28*(19), 3167–3175. https://doi.org/10.1200/JCO.2009.26.7609

Bristol-Myers Squibb GmbH & Co. KGaA. (2020). *Fachinformation Nivolumab*.

Broers, J. L. V., Ramaekers, F. C. S., Klein Rot, M., Oostendorp, T., Huysmans, A., van Muijen, G. N. P., … Vooijs, G. P. (1988). Cytokeratins in Different Types of Human Lung Cancer as Monitored by Chain-specific Monoclonal Antibodies. *Cancer Research*, *48*(11), 3221–3229.

Brown, J. A., Dorfman, D. M., Ma, F.-R., Sullivan, E. L., Munoz, O., Wood, C. R., … Freeman, G. J. (2003). Blockade of Programmed Death-1 Ligands on Dendritic Cells Enhances T Cell Activation and Cytokine Production. *The Journal of Immunology*, *170*(3), 1257–1266. https://doi.org/10.4049/jimmunol.170.3.1257

Butte, M. J., Keir, M. E., Phamduy, T. B., Sharpe, A. H., & Freeman, G. J. (2007). Programmed Death-1 Ligand 1 Interacts Specifically with the B7-1 Costimulatory Molecule to Inhibit T Cell Responses. *Immunity*, *27*(1), 111–122. https://doi.org/10.1016/j.immuni.2007.05.016

Cedrés, S., Nunes, I., Longo, M., Martinez, P., Checa, E., Torrejón, D., & Filip, E. (2011). Serum Tumor markers CEA, CYFRA21-1, and CA-125 are associated with worse prognosis in advanced N-Small-Cell Lung Cancer (NSCLC). *Clinical Lung Cancer*, *12*(3), 172–179. https://doi.org/https://doi.org/10.1016/j.cllc.2011.03.019

Chemnitz, J. M., Parry, R. V, Nichols, K. E., June, C. H., & Riley, J. L. (2004). SHP-1 and SHP-2 Associate with Immunoreceptor Tyrosine-Based Switch Motif of Programmed Death 1 upon Primary Human T Cell Stimulation, but Only Receptor Ligation prevents T Cell Activation. *The Journal of Immunology*, *173*(2), 945–954. https://doi.org/10.4049/jimmunol.173.2.945

Chen, G., Huang, A. C., Zhang, W., Zhang, G., Wu, M., Xu, W., … Guo, W. (2018). Exosomal PD-L1 contributes to immunosuppression and is associated with anti-PD-1 response. *Nature*, *560*, 382–386. https://doi.org/10.1038/s41586-018-0392-8

Choi, S. I., Jang, M.-A., Jeon, B. R., Shin, H. B., Lee, Y. K., & Lee, Y.-W. (2017). Clinical usefulness of Human Epididymis Protein 4 in Lung Cancer. *Annals of Laboratory Medicine*, *37*(6), 526–530. https://doi.org/10.3343/alm.2017.37.6.526

Clinical and Laboratory Standards Institute. (2001). *C31-A2 Ionized Calcium Determinations: Precollection variables, Specimen choice, Collection and Handling: Approved guideline (2nd Edition)*. Wayne. https://doi.org/ISBN 1-56238-436-8

Cohen, J. (1992). Statistical Power Analysis. *American Psychological Society*, *1*(3), 98–101. https://doi.org/https://doi.org/10.1111/1467-8721.ep10768783

Committee for Medicinal Products for Human Use. (2012). *Guideline on bioanalytical method validation* (Vol. EMEA/CHMP/). London. Retrieved from https://www.ema.europa.eu/en/bioanalytical-method-validation

de Jong, C., Deneer, V. H. M., Kelder, J. C., Ruven, H., Egberts, T. C. G., & Herder, G. J. M. (2020). Association between serum biomarkers CEA and LDH and response in advanced non-small cell lung cancer patients treated with platinum-based chemotherapy. *Thoracic Cancer*, 1–11. https://doi.org/10.1111/1759-7714.13449

Deutsche Krebsgesellschaft, Deutsche Krebshilfe, & AWMF. (2018). S3-Leitlinie Prävention, Diagnostik, Therapie und Nachsorge des Lungenkarzinoms. Retrieved from https://www.leitlinienprogramm-onkologie.de/index.php?id=98&type=0

Dong, H., Strome, S. E., Salomao, D. R., Tamura, H., Hirano, F., Flies, D. B., … Chen, L. (2002). Tumor-associated B7-H1 promotes T-cell apoptosis: A potential mechanism of immune evasion. *Nature Medicine*, *8*(8), 793–800. https://doi.org/10.1038/nm730

Dong, H., Zhu, G., Tamada, K., & Chen, L. (1999). B7-H1, a third member of the B7 family, co-stimulates T-cell proliferation and interleukin-10 secretion. *Nature Medicine*, *5*(12), 1365–1369. https://doi.org/10.1038/70932

Drapkin, R., Von Horsten, H. H., Lin, Y., Mok, S. C., Crum, C. P., Welch, W. R., & Hecht, J. L. (2005). Human epididymis protein 4 (HE4) is a secreted glycoprotein that is overexpressed by serous and endometrioid ovarian carcinomas. *Cancer Research*, *65*(6), 2162–2169. https://doi.org/10.1158/0008-5472.CAN-04-3924

Duffy, M. J., Sturgeon, C. M., Sölétormos, G., Barak, V., Molina, R., Hayes, D. F., … Bossuyt, P. M. M. (2015). Validation of new cancer biomarkers: A position statement from the european group on tumor markers. *Clinical Chemistry*, *61*(6), 809–820. https://doi.org/10.1373/clinchem.2015.239863

Dunn, G. P., Bruce, A. T., Sheehan, K. C. F., Shankaran, V., Uppaluri, R., Bui, J. D., … Schreiber, R. D. (2005). A critical function for type I interferons in cancer immunoediting. *Nature Immunology*, *6*(7), 722–729. https://doi.org/10.1038/ni1213

Edelman, M. J., Hodgson, L., Rosenblatt, P. Y., Christenson, R. H., Vokes, E., Wang, X., … Cancer and Leukemia Group B. (2012). CYFRA 21-1 as a prognostic and predictive marker in advanced non-small-cell lung cancer in a prospective trial: CALGB 150304. *Journal of Thoracic Oncology*, *7*(4), 649–654. https://doi.org/10.1097/JTO.0b013e31824a8db0

Escors, D., Gato-Cañas, M., Zuazo, M., Arasanz, H., García-Granda, M. J., Vera, R., & Kochan, G. (2018). The intracellular signalosome of PD-L1 in cancer cells. *Signal Transduction and Targeted Therapy*, *3*(26), 1–9. https://doi.org/10.1038/s41392-018-0022-9

Escudero, J. M., Auge, J. M., Filella, X., Torne, A., Pahisa, J., & Molina, R. (2011). Comparison of serum human epididymis protein 4 with cancer antigen 125 as a tumor marker in patients with malignant and nonmalignant diseases. *Clinical Chemistry*, *57*(11), 1534–1544. https://doi.org/10.1373/clinchem.2010.157073

Ettinger, D. S., Wood, D. E., Aggarwal, C., Aisner, D. L., Akerley, W., Bauman, J. R., … Hughes, M. (2019). Non-small cell lung cancer, version 1.2020: Featured updates to the NCCN guidelines. *JNCCN Journal of the National Comprehensive Cancer Network*, *17*(12), 1464–1472. https://doi.org/10.6004/jnccn.2019.0059

European Medicines Agency. (2019). Biomarker. Retrieved from https://www.ema.europa.eu/en/glossary/biomarker

Food and Drug Administration. (2019). About Biomarkers and Qualification. Retrieved from https://www.cancer.gov/publications/dictionaries/cancer-terms/def/biomarker

Francisco, L. M., Sage, P. T., & Sharpe, A. H. (2010). The PD-1 Pathway in Tolerance and Autoimmunity. *Immunological Reviews*, *236*(1), 291–242. https://doi.org/10.1111/j.1600-065X.2010.00923.x.The

Freeman, G. J., Long, A. J., Iwai, Y., Bourque, K., Chernova, T., Nishimura, H., … Honjo, T. (2000). Engagement of the PD-1 immunoinhibitory receptor by a novel B7 family member leads to negative regulation of lymphocyte activation. *Journal of Experimental Medicine*, *192*(7), 1027–1034. https://doi.org/10.1084/jem.192.7.1027

Frigola, X., Inman, B. A., Lohse, C. M., Krco, C. J., Cheville, J. C., Thompson, R. H., … Kwon, E. D. (2011). Identification of a soluble form of B7-H1 that retains immunosuppressive activity and is associated with aggressive renal cell carcinoma. *Clinical Cancer Research*, *17*(7), 1915–1923. https://doi.org/10.1158/1078-0432.CCR-10-0250

Gendler, S. J., Lancaster, C. A., Taylor-Papadimitriou, J., Duhig, T., Peat, N., Burchell, J., … Wilson, D. (1990). Molecular Cloning and Expression of Human Tumor-associated Polymorphic Epithelial Mucin. *Journal of Biological Chemistry*, *265*(25), 15286–15293.

Ghosh, I., Bhattacharjee, D., Das, A. K., Chakrabarti, G., Dasgupta, A., & Dey, S. K. (2013). Diagnostic role of tumour markers CEA, CA15-3, CA19-9 and CA125 in lung cancer. *Indian Journal of Clinical Biochemistry*, *28*(1), 24–29. https://doi.org/10.1007/s12291-012-0257-0

Gold, P., & Freedman, S. O. (1964). Demonstration of tumor-specific antigens in human colonic carcinomata by immunological tolerance and absorption techniques. *The Journal of Experimental Medicine*, *121*(3), 439–462. https://doi.org/10.1084/jem.121.3.439

Goldstraw, P., Chansky, K., Crowley, J., Rami-Porta, R., Asamura, H., Eberhardt, W. E. E., … Bolejack, V. (2016). The IASLC Lung Cancer Staging Project: Proposals for Revision of the TNM Stage Groupings in the Forthcoming (Eighth) Edition of the TNM Classification for Lung Cancer. *Journal of Thoracic Oncology*, *11*(1), 39–51. https://doi.org/10.1016/j.jtho.2015.09.009

Griesinger, F., Heigener, D. F., Tiemann, M., & Wiewrodt, R. (2018). Behandlungsmethoden bei Lungenkrebs im Einzelnen. Retrieved May 23, 2020, from https://www.krebsgesellschaft.de/onko-internetportal/basis-informationen-krebs/krebsarten/definition/behandlungsmethoden-bei-lungenkrebs.html

Hammarström, S. (1999). The carcinoembryonic antigen (CEA) family: Structures, suggested functions and expression in normal and malignant tissues. *Seminars in Cancer Biology*, *9*(2), 67–81. https://doi.org/10.1006/scbi.1998.0119

Hatzfeld, M., & Franke, W. W. (1985). Pair Formation and Promiscuity of Cytokeratins: Formation in vitro of Heterotypic Complexes and Intermediate-Sized Filaments by Homologous and Heterologous Recombinations of Purified Polypeptides. *Journal of Cell Biology*, *101*(5), 1826–1841. https://doi.org/10.1083/jcb.101.5.1826

He, Y.-P., Li, L.-X., Tang, J.-X., Yi, L., Zhao, Y., Zhang, H.-W., … Gan, L. (2019). HE4 as a biomarker for diagnosis of lung cancer: A meta-Analysis. *Medicine (Baltimore)*, *98*(39), 1–10. https://doi.org/10.1097/MD.0000000000017198

Herbst, R. S., Soria, J.-C., Kowanetz, M., Fine, G. D., Hamid, O., Gordon, M. S., … Hodi, S. F. (2016). Predictive correlates of response to the anti-PD-L1 antibody MPDL3280A. *Nature*, *515*(7528), 563–567. https://doi.org/10.1038/nature14011.Predictive

Herold, G. und M. (2018). *Innere Medizin*. Köln: Dr. med. Gerd Herold.

Hilkens, J., Wesseling, J., Vos, H. L., Litvinov, S. L., Boer, M., van der Valk, S., … Figdor, C. (1995). Cell surface associated mucins: Structure and effects on cell adhesion. In S. Papa & J. M. Tager (Eds.), *Biochemistry of Cell Membranes* (pp. 259–260). Basel: Birkhäuser Basel. https://doi.org/10.1007/978-3-0348-9057-1_18

Hirsch, F. R., Suda, K., Wiens, J., & Bunn Jr, P. A. (2016). New and emerging targeted treatments in advanced non-small-cell lung cancer. *The Lancet*, *388*(10048), 1012–1024. https://doi.org/10.1016/S0140-6736(16)31473-8

Holdenrieder, S. (2016). Biomarkers along the continuum of care in lung cancer. *Scandinavian Journal of Clinical and Laboratory Investigation*, *76*(S245), S40–S45. https://doi.org/10.1080/00365513.2016.1208446

Holdenrieder, S., Krueger, K., Hettwer, K., Simon, K., Rössler, M., Joerger, M., & Uhlig, S. (2020). Unpublished manuscript. *Tumor marker-based therapy monitoring in lung cancer patients*.

Holdenrieder, S., & von Pawel, J. (2013). ProGRP beim SCLC. *Diagnostik Im Dialog*, (42), 13–16.

Holdenrieder, S., von Pawel, J., Dankelmann, E., Duell, T., Faderl, B., Markus, A., … Stieber, P. (2009). Nucleosomes and CYFRA 21-1 indicate tumor response after one cycle of chemotherapy in recurrent non-small cell lung cancer. *Lung Cancer*, *63*(1), 128–135. https://doi.org/10.1016/j.lungcan.2008.05.001

Holdenrieder, S., Wehnl, B., Hettwer, K., Simon, K., Uhlig, S., & Dayyani, F. (2017). Carcinoembryonic antigen and cytokeratin-19 fragments for assessment of therapy response in non-small cell lung cancer: a systematic review and meta-Analysis. *British Journal of Cancer*, *116*(8), 1037–1045. https://doi.org/10.1038/bjc.2017.45

Hutarew, G. (2016). PD-L1 testing, fit for routine evaluation? From a pathologist's point of view. *Memo - Magazine of European Medical Oncology*, *9*(4), 201–206. https://doi.org/10.1007/s12254-016-0292-2

Ishida, Y., Agata, Y., Shibahara, K., & Honjo, T. (1992). Induced expression of PD-1, a novel member of the immunoglobulin gene superfamily, upon programmed cell death. *The EMBO Journal*, *11*(11), 3887–3895. https://doi.org/10.1002/j.1460-2075.1992.tb05481.x

Iwahori, K., Suzuki, H., Kishi, Y., Fujii, Y., Uehara, R., Okamoto, N., … Naka, T. (2012). Serum HE4 as a diagnostic and prognostic marker for lung cancer. *Tumor Biology*, *33*(4), 1141–1149. https://doi.org/10.1007/s13277-012-0356-9

Joerger, M., von Pawel, J., Kraff, S., Fischer, J. R., Eberhardt, W., Gauler, T. C., … Jaehde, U. (2016). Open-label, randomized study of individualized, pharmacokinetically (PK)-guided dosing of paclitaxel combined with carboplatin or cisplatin in patients with advanced non-small-cell lung cancer (NSCLC). *Annals of Oncology*, *27*(10), 1895–1902. https://doi.org/10.1093/annonc/mdw290

Kagohashi, K., Satoh, H., Kurishima, K., Kadono, K., Ishikawa, H., Ohtsuka, M., & Sekizawa, K. (2008). Squamous cell carcinoma antigen in lung cancer and nonmalignant respiratory diseases. *Lung*, *186*(5), 323–326. https://doi.org/10.1007/s00408-008-9108-4

Kaneko, O., Gong, L., Zhang, J., Hansen, J. K., Hassan, R., Lee, B., & Ho, M. (2009). A binding domain on mesothelin for CA125/MUC16. *Journal of Biological Chemistry*, *284*(6), 3739–3749. https://doi.org/10.1074/jbc.M806776200

Keir, M. E., Butte, M. J., Freeman, G. J., & Sharpe, A. H. (2008). PD-1 and Its Ligands in Tolerance and Immunity. *Annual Review of Immunology*, *26*, 677–704. https://doi.org/10.1146/annurev.immunol.26.021607.090331

Kerr, K. M., Tsao, M.-S., Nicholson, A. G., Yatabe, Y., Wistuba, I. I., & Hirsch, F. R. (2015). Programmed death-ligand 1 immunohistochemistry in lung cancer: In what state is this art? *Journal of Thoracic Oncology*, *10*(7), 985–989. https://doi.org/10.1097/JTO.0000000000000526

Kimura, Y., Fujii, T., Hamamoto, K., Miyagawa, N., Kataoka, M., & Iio, A. (1990). Serum CA125 level is a good prognostic indicator in lung cancer. *British Journal of Cancer*, *62*(4), 676–678. https://doi.org/10.1038/bjc.1990.355

Kirchhoff, C. (1998). Molecular characterization of epididymal proteins. *Reviews of Reproduction*, *3*(2), 86–95. https://doi.org/10.1530/ror.0.0030086

Krueger, K., Mayer, Z., Gerckens, M., Kruger, S., Luppa, P., Zehn, D., & Holdenrieder, S. (2020). Manuscript submitted for publication. Development and analytical validation of three novel ELISAs for the sensitive quantification of soluble PD-1, PD-L1 and PD-L2 in blood. *Clinical Chemistry and Laboratory Medicine*.

Krueger, K., Mayer, Z., Kottmaier, M., Gerckens, M., Luppa, P., Zehn, D., & Holdenrieder, S. (2020). Manuscript submitted for publication. Impact of preanalytical factors on novel ELISAs for soluble PD-1, PD-L1 and PD-L2 in blood. *Clinical Chemistry and Laboratory Medicine*.

Kufe, D. W. (2009). Mucins in cancer: function, prognosis and therapy. *Nature Reviews Cancer*, *9*(12), 874–885. https://doi.org/10.1038/nrc2761

Lamy, P. J., Plassot, C., & Pujol, J. L. (2015). Serum HE4: An independent prognostic factor in non-small cell lung cancer. *PLOS ONE*, *10*(6). https://doi.org/10.1371/journal.pone.0128836

Latchman, Y., Wood, C. R., Chernova, T., Chaudhary, D., Borde, M., Chernova, I., … Freeman, G. J. (2001). PD-L2 is a second ligand for PD-1 and inhibits T cell activation. *Nature Immunology*, *2*(3), 261–268. https://doi.org/10.1038/85330

Marzec, M., Zhang, Q., Goradia, A., Raghunath, P. N., Liu, X., Paessler, M., … Wasik, M. A. (2008). Oncogenic kinase NPM/ALK induces through STAT3 expression of immunosuppressive protein CD274 (PD-L1, B7-H1). *Proceedings of the National Academy of Sciences of the United States of America*, *105*(52), 20852–20857. https://doi.org/10.1073/pnas.0810958105

Merck Europe B.V. (2019a). *Fachinformation Avelumab*.

Merck Europe B.V. (2019b). M7824. Retrieved June 18, 2020, from https://www.merckgroup.com/de/news/m7824-2019-02-05.html

Meso Scale Discovery. (2020). Electrochemiluminescence. Retrieved June 5, 2020, from https://www.mesoscale.com/en/technical_resources/our_technology/ecl

Miralles, C., Orea, M., España, P., Provencio, M., Sánchez, A., Cantos, B., … Gea, T. (2003). Cancer antigen 125 associated with multiple benign and malignant pathologies. *Annals of Surgical Oncology*, *10*(2), 150–154. https://doi.org/10.1245/ASO.2003.05.015

Molina, R., Filella, X., Augé, J. M., Fuentes, R., Bover, I., Rifa, J., … Viladiu, P. (2003). Tumor markers (CEA, CA 125, CYFRA 21-1, SCC and NSE) in patients with non-small cell lung cancer as an aid in histological diagnosis and prognosis. *Tumor Biology*, *24*(4), 209–218. https://doi.org/10.1159/000074432

MSD SHARP & DOHME GMBH. (2019). *Fachinformation Pembrolizumab*.

Mu, R.-Z., Liu, S., Liang, K.-G., Jiang, D., & Huang, Y.-J. (2020). A Meta-Analysis of Neuron-Specific Enolase Levels in Cerebrospinal Fluid and Serum in Children With Epilepsy. *Frontiers in Molecular Neuroscience*, *13*(24), 1–13. https://doi.org/10.3389/fnmol.2020.00024

Muley, T., Ebert, W., Stieber, P., Raith, H., Holdenrieder, S., Nagel, D., … Drings, P. (2003). Technical performance and diagnostic utility of the new elecsys® neuron-specific enolase enzyme immunoassay. *Clinical Chemistry and Laboratory Medicine*, *41*(1), 95–103. https://doi.org/10.1515/CCLM.2003.017

Mutschler, E., Geisslinger, G., Kroemer, H. K., Menzel, S., & Ruth, P. (2013). *Arzneimittelwirkungen: Lehrbuch der Pharmakologie, der klinischen Pharmakologie und Toxikologie*. (E. Mutschler, Ed.) (10th ed.). Stuttgart: Wissenschaftliche Verlagsgesellschaft.

Nath, S., & Mukherjee, P. (2014). MUC1: a multifaceted oncoprotein with a key role in cancer progression. *Trends in Molecular Medicine*, *20*(6), 332–342. https://doi.org/10.1016/j.molmed.2014.02.007

National Cancer Institute. (2020a). MK-1308. Retrieved June 18, 2020, from https://www.cancer.gov/publications/dictionaries/cancer-drug/def/793094

National Cancer Institute. (2020b). MK-4280. Retrieved June 18, 2020, from https://www.cancer.gov/publications/dictionaries/cancer-drug/def/anti-lag3-monoclonal-antibody-mk-4280

Nielsen, C., Ohm-Laursen, L., Barington, T., Husby, S., & Lillevang, S. T. (2005). Alternative splice variants of the human PD-1 gene. *Cellular Immunology*, *235*(2), 109–116. https://doi.org/10.1016/j.cellimm.2005.07.007

O'Brien, T. J., Beard, J. B., Underwood, L. J., & Shigemasa, K. (2002). The CA 125 gene: A newly discovered extension of the glycosylated N-terminal domain doubles the size of this extracellular superstructure. *Tumor Biology*, *23*(3), 154–169. https://doi.org/10.1159/000064032

Okamura, K., Takayama, K., Izumi, M., Harada, T., Furuyama, K., & Nakanishi, Y. (2013). Diagnostic value of CEA and CYFRA 21-1 tumor markers in primary lung cancer. *Lung Cancer*, *80*(1), 45–49. https://doi.org/10.1016/j.lungcan.2013.01.002

Okazaki, T., Maeda, A., Nishimura, H., Kurosaki, T., & Honjo, T. (2001). PD-1 immunoreceptor inhibits B cell receptor-mediated signaling by recruiting src homology 2-domain-containing tyrosine phosphatase 2 to phosphotyrosine. *Proceedings of the National Academy of Sciences of the United States of America*, *98*(24), 13866–13871. https://doi.org/10.1073/pnas.231486598

Pardoll, D. M. (2012). The blockade of immune checkpoints in cancer immunotherapy. *Nature Reviews Cancer*, *12*(4), 252–264. https://doi.org/10.1038/nrc3239

Parsa, A. T., Waldron, J. S., Panner, A., Crane, C. A., Parney, I. F., Barry, J. J., … Pieper, R. O. (2007). Loss of tumor suppressor PTEN function increases B7-H1 expression and immunoresistance in glioma. *Nature Medicine*, *13*(1), 84–88. https://doi.org/10.1038/nm1517

Pasella, S., Baralla, A., Canu, E., Pinna, S., Vaupel, J., Deiana, M., … Deiana, L. (2013). Pre-analytical stability of the plasma proteomes based on the storage temperature. *Proteome Science*, *11*, 1–10. https://doi.org/10.1186/1477-5956-11-10

Patsoukis, N., Brown, J., Petkova, V., Liu, F., Li, L., & Boussiotis, V. A. (2012). Selective effects of PD-1 on Akt and Ras pathways regulate molecular components of the cell cycle and inhibit T cell proliferation. *Science Signaling*, *5*(230), 1–30. https://doi.org/10.1126/scisignal.2002796

Polak, J. M., Hamid, Q., Springall, D. R., Cuttitta, F., Spindel, E., Ghatei, M. A., & Bloom, S. R. (1988). Localization of Bombesin-like Peptides in Tumors. *Annals of the New York Academy of Sciences*, *547*(1), 322–335. https://doi.org/10.1111/j.1749-6632.1988.tb23900.x

R&D Systems. (2018). *DuoSet ® ELISA Human PD-L1*. Minneapolis.

R&D Systems Inc. (2016a). *DuoSet ® ELISA Human PD-1*. Minneapolis.

R&D Systems Inc. (2016b). *DuoSet ® ELISA Human PD-L2*. Minneapolis.

Reck, M., & Rabe, K. F. (2017). Precision Diagnosis and Treatment for Advanced Non-Small-Cell Lung Cancer. *New England Journal of Medicine*, *377*(9), 849–861. https://doi.org/10.1056/NEJMra1703413

Rober Koch-Institut. (2019). Neu Zahlen zu Krebs in Deutschland. https://doi.org/1

Roche Diagnostics GmbH. (2011). *Factsheet HE4*. Basel.

Roche Diagnostics GmbH. (2012). *Factsheet CYFRA 21-1*. Basel.

Roche Diagnostics GmbH. (2013). *Elecsys CA 15-3 Manual*. Basel.

Roche Diagnostics GmbH. (2017). *Elecsys NSE Manual*. Basel.

Roche Diagnostics GmbH. (2018a). *Elecsys CEA Manual*. Basel.

Roche Diagnostics GmbH. (2018b). *Elecsys HE4 Manual*. Basel.

Roche Diagnostics GmbH. (2019). *Elecsys CA 125 II Manual*. Basel. Retrieved from http://www.cobas.be/home/product/overview-swa/elecsys-ca-125.html

Roche Diagnostics GmbH. (2020a). *Elecsys CYFRA 21-1 Manual*. Basel.

Roche Diagnostics GmbH. (2020b). *Elecsys ProGRP Manual*. Basel. Retrieved from http://www.cobas.com/home/product/clinical-and-immunochemistry-testing/elecsys-progrp-assay.html

Roche Diagnostics GmbH. (2020c). *Elecsys SCC Manual*. Basel.

Roche Pharma AG. (2019a). *Fachinformation Atezolizumab 1200mg*.

Roche Pharma AG. (2019b). *Fachinformation Atezolizumab 840 mg*.

Roche Pharma AG. (2020). Drug Pipeline.

Rozali, E. N., Hato, S. V., Robinson, B. W., Lake, R. A., & Lesterhuis, W. J. (2012). Programmed death ligand 2 in cancer-induced immune suppression. *Clinical and Developmental Immunology*, 1–8. https://doi.org/10.1155/2012/656340

Rump, A., Morikawa, Y., Tanaka, M., Minami, S., Umesaki, N., Takeuchi, M., & Miyajima, A. (2004). Binding of Ovarian Cancer Antigen CA125/MUC16 to Mesothelin Mediates Cell Adhesion. *Journal of Biological Chemistry*, *279*(10), 9190–9198. https://doi.org/10.1074/jbc.M312372200

Sanofi-Aventis Deutschland GmbH. (2019). *Fachinformation Cemiplimab*.

Scatena, R. (Ed.). (2015). *Advances in cancer biomarkers From biochemistry to clinic for a critical revision* (Vol. 867). Springer Dordrecht Heildberg New York London. https://doi.org/10.41007/978-94-017-7215-0

Scheel, A. H., Dietel, M., Heukamp, L. C., Jöhrens, K., Kirchner, T., Reu, S., … Buettner, R. (2016). Harmonized PD-L1 immunohistochemistry for pulmonary squamous-cell and adenocarcinomas. *Modern Pathology*, *29*(10), 1165–1172. https://doi.org/10.1038/modpathol.2016.117

Schick, C., Brömme, D., Bartuski, A. J., Uemura, Y., Schechter, N. M., & Silverman, G. A. (1998). The reactive site loop of the serpin SCCA1 is essential for cysteine proteinase inhibition. *Proceedings of the National Academy of Sciences of the United States of America*, *95*(23), 13465–13470. https://doi.org/10.1073/pnas.95.23.13465

Schildberg, F. A., Klein, S. R., Freeman, G. J., & Sharpe, A. H. (2016). Coinhibitory Pathways in the B7-CD28 Ligand-Receptor Family. *Immunity*, *44*(5), 955–972. https://doi.org/10.1016/j.immuni.2016.05.002

Sheppard, K.-A., Fitz, L. J., Lee, J. M., Benander, C., George, J. A., Wooters, J., … Chaudhary, D. (2004). PD-1 inhibits T-cell receptor induced phosphorylation of the ZAP70/CD3ζ signalosome and downstream signaling to PKCθ. *FEBS Letters*, *574*(1–3), 37–41. https://doi.org/10.1016/j.febslet.2004.07.083

Smyth, M. J. (2005). Type I interferon and cancer immunoediting. *Nature Immunology*, *6*(7), 646–648. https://doi.org/10.1038/ni0705-646

Solinas, C., Aiello, M., Rozali, E., Lambertini, M., Willard-Gallo, K., & Migliori, E. (2020). Programmed Cell Death-Ligand 2: A Neglected But Important Target in the Immune Response to Cancer? *Translational Oncology*, *13*(10), 1–12. https://doi.org/10.1016/j.tranon.2020.100811

Spranger, S., Spaapen, R. M., Zha, Y., Williams, J., Meng, Y., Ha, T. T., & Gajewski, T. F. (2013). Up-Regulation of PD-L1, IDO and Tregs in the Melanoma Tumor Microenvironment Is Driven by CD8+ T Cells. *Science Translational Medicine*, *5*(200), 1–21. https://doi.org/10.1126/scitranslmed.3006504.Up-Regulation

Steinhilber, D., Schubert-Zsilavecz, M., & Roth, H. J. (2010). *Medizinische Chemie* (2nd ed.). Stuttgart: Deutscher Apotheker Verlag (DAV).

Stieber, P., Hasholzer, U., Bodenmüller, H., Nagel, D., Sunder-Plassmann, L., Dienemann, H., … Fateh-Moghadam, A. (1993). CYFRA 21-1 A new marker in lung cancer. *Cancer*, *72*(3), 707–713. https://doi.org/10.1515/labm.1993.17.7-8.328

Taube, J. M., Anders, R. A., Young, G. D., Xu, H., Sharma, R., McMiller, T. L., … Chen, L. (2012). Colocalization of Inflammatory Response with B7-H1 Expression in Human Melanocytic Lesions Supports an Adaptive Resistance Mechanism of Immune Escape. *Science Translational Medicine*, *4*(127), 1–22. https://doi.org/10.1126/scitranslmed.3003689.Colocalization

Topalian, S. L., Drake, C. G., & Pardoll, D. M. (2015). Immune checkpoint blockade: A common denominator approach to cancer therapy. *Cancer Cell*, *27*(4), 450–461. https://doi.org/10.1016/j.ccell.2015.03.001

Travis, W. D., Brambilla, E., Nicholson, A. G., Yatabe, Y., Austin, J. H. M., Beasley, M. B., … Wistuba, I. (2015). The 2015 World Health Organization Classification of Lung Tumors: Impact of Genetic, Clinical and Radiologic Advances since the 2004 Classification. *Journal of Thoracic Oncology*, *10*(9), 1243–1260. https://doi.org/10.1097/JTO.0000000000000630

Tseng, S.-Y., Otsuji, M., Gorski, K., Huang, X., Slansky, J. E., Pai, S. I., … Tsuchiya, H. (2001). B7-DC, a new dendritic cell molecule with potent costimulatory properties for T cells. *Journal of Experimental Medicine*, *193*(7), 839–845. https://doi.org/10.1084/jem.193.7.839

Tumorzentrum München. (2020). *Manual Tumoren der Lunge und des Mediastinums*. (R. M. Huber & Tumorzentrum München, Eds.) (12. Auflag). München: Zuckschwerdt Verlag München. Retrieved from http://www.tumorzentrum-muenchen.de

U.S. National Library of Medicine, U.S. National Institutes of Health, & U.S. Department of Health and Human Services. (2020a). CEPAC-TDM Clinical Trials. Retrieved May 28, 2020, from https://clinicaltrials.gov/ct2/show/NCT01326767

U.S. National Library of Medicine, U.S. National Institutes of Health, & U.S. Department of Health and Human Services. (2020b). ClinicalTrials. Retrieved June 18, 2020, from https://clinicaltrials.gov/

Union for International Cancer Control (UICC). (2020). *TNM Klassifikation maligner Tumoren*. (Christian Wittekind, Ed.) (8th ed.). Weinheim: Wiley-VCH.

Vivier, E., & Daëron, M. (1997). Immunoreceptor tyrosine-based inhibition motifs. *Immunology Today*, *18*(6), 286–291. https://doi.org/10.1016/S0167-5699(97)80025-4

Wan, B., Nie, H., Liu, A., Feng, G., He, D., Xu, R., … Zhang, J. Z. (2006). Aberrant Regulation of Synovial T Cell Activation by Soluble Costimulatory Molecules in Rheumatoid Arthritis. *The Journal of Immunology*, *177*(12), 8844–8850. https://doi.org/10.4049/jimmunol.177.12.8844

Xiao, Y., Yu, S., Zhu, B., Bedoret, D., Bu, X., Francisco, L. M., … Freeman, G. J. (2014). RGMb is a novel binding partner for PD-L2 and its engagement with PD-L2 promotes respiratory tolerance. *Journal of Experimental Medicine*, *211*(5), 943–959. https://doi.org/10.1084/jem.20130790

Xu, Y., Wu, Y., Zhang, S., Ma, P., Jin, X., Wang, Z., … Fan, Y. (2019). A Tumor-Specific Super-Enhancer Drives Immune Evasion by Guiding Synchronous Expression of PD-L1 and PD-L2. *Cell Reports*, *29*(11), 3435–3447.e4. https://doi.org/10.1016/j.celrep.2019.10.093

Youngnak, P., Kozono, Y., Kozono, H., Iwai, H., Otsuki, N., Jin, H., … Azuma, M. (2003). Differential binding properties of B7-H1 and B7-DC to programmed death-1. *Biochemical and Biophysical Research Communications*, *307*(3), 672–677. https://doi.org/10.1016/S0006-291X(03)01257-9

Zhang, X., Schwartz, J.-C. D., Guo, X., Bhatia, S., Cao, E., Chen, L., … Almo, S. C. (2004). Structural and functional analysis of the costimulatory receptor programmed death-1. *Immunity*, *20*(3), 337–347. https://doi.org/10.1016/S1074-7613(04)00114-1

10 Table index

Table 1: Differentiation of lung cancer subtypes 4
Table 2: Staging and TNM classification of lung cancers (NSCLC and SCLC) 8
Table 3: EMA-approved PD-1 and PD-L1 immune checkpoint inhibitors 14
Table 4: Recommended tumor markers to assist in lung cancer diagnosis and monitoring 21
Table 5: Tumor markers and their corresponding cut-off values 23
Table 6: Patient characteristics in the CESAR Biomarker Substudy 27
Table 7: Tumor marker reagents 30
Table 8: Tumor marker additional reagents 30
Table 9: Tumor markers consumables 31
Table 10: Specification of PD-1, PD-L1 and PD-L2 antibodies 31
Table 11: Applied chemicals and their corresponding suppliers 37
Table 12: Solutions and their composition 37
Table 13: Consumables and their corresponding suppliers 38
Table 14: Instruments and their corresponding suppliers 39
Table 15: Specification of centrifugation programs 40
Table 16: Hazard ratios for the single markers investigating progression free survival of pre-therapeutic concentrations 67
Table 17: Hazard ratios resulting from Cox regression analysis of covariates on progression free survival in pre-therapeutic concentrations 68
Table 18: Hazard ratios for the single markers investigating progression free survival of end of treatment cycle 2 concentrations 71
Table 19: Hazard ratios resulting from Cox regression analysis of covariates on progression free survival in end of treatment cycle 2 concentrations 72
Table 20: Hazard ratios for the single markers investigating overall survival of pre-therapeutic concentrations 75
Table 21: Hazard ratios resulting from Cox regression analysis of covariates on overall survival in pre-therapeutic concentrations 76
Table 22: Hazard ratios for the single markers investigating overall survival of end of treatment cycle 2 concentrations 79
Table 23: Hazard ratios resulting from Cox regression analysis of covariates on overall survival in end of treatment cycle 2 concentrations 80
Table 24: Data summary of PD-1, PD-L1 and PD-L2 values for the cancer cohort 83
Table 25: Test on normal distribution after Shapiro-Wilk for PD-1, PD-L1 and PD-L2 in the cancer cohort 88
Table 26: Calculated correlation of the PD-markers at time points 1_1 and EOT 89
Table 27: Data summary healthy cohort 91
Table 28: Significance investigations of PD-1, PD-L1 and PD-L2 in healthy controls versus cancer patients before, at the end of cycle 2 and at the end of treatment 93

11 Figure index

Figure 1: Lung carcinoma subtypes 3
Figure 2: Signaling pathways of the programmed-cell death markers 11
Figure 3: Blood collection scheme of the biomarker substudy 26
Figure 4: ELISA processing scheme 33
Figure 5: Template assay protocol PD-1, PD-L1 and PD-L2 DHM assays 34
Figure 6: Detection based on electrochemiluminescence 35
Figure 7: Tumor marker concentrations development during cancer therapy 44
Figure 8: Decision tree outlining included samples in the analysis for prediction of response 47
Figure 9: Comparison of the pre-therapeutic concentrations in the response groups based on poor response to therapy 49
Figure 10: Predictive value of pre-therapeutic marker levels on therapy response 50
Figure 11: Comparison of the relative change in concentrations in the response groups based on poor response to therapy 53
Figure 12: Predictive value of relative change in marker levels between cycle 1 and end of cycle 2 on therapy response 54
Figure 13: Comparison of the pre-therapeutic concentrations in the response groups based on good response to therapy 56
Figure 14: Predictive value of pre-therapeutic marker levels on well response to therapy 57
Figure 15: Comparison of the relative change in concentrations in the response groups based on good response to therapy 59
Figure 16: Predictive value of relative change in marker levels between cycle 1 and end of cycle 2 on well response to therapy 60
Figure 17: Decision tree outlining included samples in the analysis for prognosis of survival 62
Figure 18: Kaplan-Meier curves on progression free survival and overall survival 63
Figure 19: Kaplan-Meier curves analyzing the influence of different covariates on PFS 64
Figure 20: Kaplan-Meier curves showing progression free survival distributed among the quartiles of the measured pre-therapeutic concentration range 66
Figure 21: Kaplan-Meier curves showing progression free survival distributed among the quartiles of the measured concentration range at the end of treatment cycle 2 70
Figure 22: Kaplan-Meier curves showing overall survival distributed among the quartiles of the measured pre-therapeutic concentration range 74
Figure 23: Kaplan-Meier curves showing overall survival distributed among the quartiles of the measured concentration range at the end of treatment cycle 2 78
Figure 24: PD-1, PD-L1 and PD-L2 biomarker concentrations at the six different time points during treatment 84
Figure 25: Decision tree outlining included samples in the analysis for prediction of response in the programmed cell death markers 85
Figure 26: Pre-therapeutic concentrations of responders versus non-responders in PD-1, PD-L1 and PD-L2 86
Figure 27: Concentrations at therapy cycle three of responders versus non-responders in PD-1, PD-L1 and PD-L2 87
Figure 28: PD-1, PD-L1, PD-L2 concentrations in the healthy cohort 90
Figure 29: Comparison of the healthy and selected time points in cancer cohort for PD-1, PD-L1 and PD-L2 92